

AD-A211 717

13

Final Report

RADAR TARGET DISCRIMINATION AND IDENTIFICATION USING
EXTINCTION-PULSES AND SINGLE-MODE EXTRACTION SIGNALS

Naval Air Systems Command
Contract No. N00019-85-C-0411

DTIC FILE COPY

DTIC
ELECTE
AUG 28 1989
S D
D CS

Reporting Period

September 11, 1985 to March 30, 1987

Prepared by

Kun-Mu Chen, Principal Investigator

Division of Engineering Research
College of Engineering
Michigan State University
East Lansing, Michigan 48824

DISTRIBUTION STATEMENT A
Approved for public release
Dissemination Unlimited

89 8 28 009

REPORT DOCUMENTATION PAGE

1a. REPORT SECURITY CLASSIFICATION UNCLASSIFIED		1b. RESTRICTIVE MARKINGS N/A	
2a. SECURITY CLASSIFICATION AUTHORITY N/A		3. DISTRIBUTION/AVAILABILITY OF REPORT Approved for public release; distribution unlimited.	
2b. DECLASSIFICATION/DOWNGRADING SCHEDULE N/A		5. MONITORING ORGANIZATION REPORT NUMBER(S)	
4. PERFORMING ORGANIZATION REPORT NUMBER(S) N/A		7a. NAME OF MONITORING ORGANIZATION Naval Air Systems Command	
6a. NAME OF PERFORMING ORGANIZATION Division of Engineering Res. Michigan State University	6b. OFFICE SYMBOL (if applicable)	7b. ADDRESS (City, State, and ZIP Code) Naval Air Systems Command, AIR-340J Department of the Navy Washington, D.C. 20361	
6c. ADDRESS (City, State, and ZIP Code) East Lansing, Michigan 48824		9. PROCUREMENT INSTRUMENT IDENTIFICATION NUMBER N00019-85-C-0411	
8a. NAME OF FUNDING/SPONSORING ORGANIZATION Naval Air Systems Command	8b. OFFICE SYMBOL (if applicable) NAVAIR	10. SOURCE OF FUNDING NUMBERS	
8c. ADDRESS (City, State, and ZIP Code) Naval Air Systems Command, AIR-340J Department of the Navy Washington, D.C. 20361		PROGRAM ELEMENT NO.	PROJECT NO.
11. TITLE (Include Security Classification) Radar Target Discrimination and Identification Using Extinction-pulses and Single-Mode Extraction Signals		TASK NO.	WORK UNIT ACCESSION NO.
12. PERSONAL AUTHOR(S) Chen, Kun-Mu		14. DATE OF REPORT (Year, Month, Day) 4/8/87	
13a. TYPE OF REPORT Final	13b. TIME COVERED FROM 9/11/85 TO 3/30/87	15. PAGE COUNT 120	
16. SUPPLEMENTARY NOTATION			
17. COSATI CODES			18. SUBJECT TERMS (Continue on reverse if necessary and identify by block number) Radar target discrimination and identification, natural frequencies, E-pulses, single-mode extraction signals, discriminant signals
FIELD	GROUP	SUB-GROUP	
19. ABSTRACT (Continue on reverse if necessary and identify by block number) <p>The purpose of this research is to develop a new scheme of radar discrimination and identification. The new scheme is based on the natural frequencies of the target. It consists of synthesizing <u>aspect-independent</u> discriminant signals, called Extinction-pulses (E-pulses) and single-mode extraction signals which, when convolved numerically with the late-time transient response of an expected target, lead to zero or single-mode responses. When the synthesized, discriminant signals for an expected target are convolved with the radar return from a different target, the resulting signal will be significantly different from the expected zero or single-mode responses, thus, the differing targets can be discriminated.</p> <p>The basic principle of our scheme based on <u>aspect-independent</u>, E-pulses and single-mode extraction signals is described based on the time-domain and frequency-domain analysis. The <u>noise-insensitivity</u> of our scheme is also reported. Extraction of the natural frequencies of a radar target from a measured response using E-pulse technique, and determination of the <u>impulse response</u> of a complex target through a deconvolution method are also presented.</p>			
20. DISTRIBUTION/AVAILABILITY OF ABSTRACT <input checked="" type="checkbox"/> UNCLASSIFIED/UNLIMITED <input type="checkbox"/> SAME AS RPT. <input type="checkbox"/> DTIC USERS		21. ABSTRACT SECURITY CLASSIFICATION UNCLASSIFIED	
22a. NAME OF RESPONSIBLE INDIVIDUAL Dr. Richard Whiting		22b. TELEPHONE (Include Area Code) (202) 696-4713	22c. OFFICE SYMBOL ONR (Code 01221)

Table of Contents

		Page
1.	Introduction	1
2.	Research Achievements	2
2.1.	Radar target discrimination by convolution of radar return with extinction - pulses and single-mode extraction signals	4
2.2.	Radar target discrimination using the extinction-pulse technique	29
2.3.	Frequency domain E-pulse synthesis and target discrimination	56
2.4.	Extraction of the natural frequencies of a radar target from a measured response using E-pulse technique	79
2.5.	Noise-insensitivity of E-pulse technique for target discrimination	102
2.6.	Determination of the impulse response of a complex target through a deconvolution	112
3.	Publication	119
4.	Personnel	120



Accession For	
NTIS	✓
DTIC	✓
Unannounced	✓
Justification	
By	
Distribution	
Availability	
Dist	
A1	

I. INTRODUCTION

This is the final report on the research program on "Radar Target Discrimination and Identification using Extinction-Pulses and Single-Mode Extraction Signals" supported by the Naval Air Systems Command under Contract N00019-85-C-0411, covering the period of September 11, 1985 to March 30, 1987. The original contract was for the period of September 11, 1985 to September 10, 1986, but it was extended on no-cost basis from September 11, 1986 to March 30, 1987 in order to complete some additional new research topics.

The purpose of this research is to develop a new scheme of radar target discrimination and identification. This scheme consists of synthesizing aspect-independent discriminant signals, called extinction-pulses (E-pulses) and single-mode extraction signals, which can be used to produce zero response or single-mode responses of the target in the late-time period when the discriminant signals are convolved, using a computer, with radar returns of the target. When the synthesized discriminant signals for a preselected target are convolved with the radar return from a wrong target, the convolved outputs will be significantly different from the expected zero response or single-mode response, thus, the wrong target can be discriminated.

Under this research program, the investigation included both theoretical analysis and experimental studies conducted in a time-domain scattering range. Scale models of various aircrafts with complex geometries have been used in the experiment. Over the past few years, we have largely accomplished our research goals. We have proved the feasibility of our scheme and developed it into a workable and practical scheme. We feel that the phase of basic research has been completed and it is ready for us to move into the phase of applied research and development.

2. RESEARCH ACHIEVEMENTS

Since this research program under the sponsorship of the Naval Air Systems Command terminates at this point, it seems appropriate to review our overall achievements of this research program. They are described in the following sections:

- 2.1 Radar target discrimination by convolution of radar return with extinction-pulses and single-mode extraction signals: This section describes the basic principle of our scheme. This information has been published in IEEE Trans. on Antennas and Propagation, Vol. AP-34, No. 7, pp. 896-904, July 1986.
- 2.2 Radar target discrimination using the extinction-pulse technique: This section describes the extinction-pulse technique in depth. A paper on this subject has been published in IEEE Tran. on Antennas and Propagation, Vol. AP-33, No. 9, pp. 929-937, September 1985.
- 2.3 Frequency domain E-pulse synthesis and target discrimination: This section presents the frequency domain approach of our scheme. The results of this section will be published in the April 1987 issue of IEEE Trans. on Antennas and Propagation.
- 2.4 Extraction of the natural frequencies of a radar target from a measured response using E-pulse technique: This section describes a new method of natural frequency extraction. This new method will be published in a future issue of IEEE Trans. on Antennas and Propagation.
- 2.5 Noise-insensitivity of E-pulse technique for target discrimination: This section proves our scheme to be quite noise insensitive. The results of this section have been presented at 1986 National Radio Science Meeting, Philadelphia, Pennsylvania, June 9-13, 1986.

2.6 Determination of the impulse response of a complex target through a deconvolution: This section presents a new method of deconvolution for obtaining the impulse response of a target from its measured data. Some results of this section have been presented at 1986 National Radio Science Meeting, Philadelphia, Pennsylvania, June 9-13, 1986.

2.1 RADAR TARGET DISCRIMINATION BY CONVOLUTION OF RADAR RETURN WITH
EXTINCTION-PULSES AND SINGLE-MODE EXTRACTION SIGNALS

ABSTRACT

A new method of radar target discrimination and identification is presented. This new method is based on the natural frequencies of the target. It consists of synthesizing aspect-independent discriminant signals, called Extinction-pulses (E-pulses) and single-mode extraction signals which, when convolved numerically with the late-time transient response of an expected target, lead to zero or single-mode responses. When the synthesized, discriminant signals for an expected target are convolved with the radar return from a different target, the resulting signal will be significantly different from the expected zero or single-mode responses, thus, the differing targets can be discriminated. Theoretical synthesis of discriminant signals from known target natural frequencies and experimental synthesis of them for a complex target from its measured pulse response are presented. The scheme has been tested with measured responses of various targets in the laboratory.

I. INTRODUCTION

A new radar discrimination scheme has been investigated by our group over the past few years and this paper describes the basic principle of the scheme and reports some recent results. The present scheme is based on the finding [1-5] that for a specific target there exist aspect-independent discriminant signals, called the extinction-pulses (E-pulses*) and single-mode extraction signals, which can be used to excite the target to produce desirable late-time radar returns. When these aspect-independent discriminant signals with particular waveforms are used to excite the target they will produce zero response or single-mode responses in the late-time period. On the other hand, if the late-time response of the target radar return, which is excited by a convenient radar pulse and is the sum of target's natural modes, is convolved with the discriminant signals, the convolved output will yield zero response or single-mode responses. The former scheme is a transmitting scheme and the latter a receiving scheme. Since it is difficult to physically synthesize and radiate the discriminant signals with particular waveforms without suffering distortion, the latter receiving scheme is preferred. The synthesized signals with particular waveforms are now stored in the computer; they are convolved with the received radar return inside the computer. Thus, we can sidestep the difficulty of synthesizing and radiating the discriminant signals.

The synthesized discriminant signals can be used to discriminate targets because when the radar return of a wrong target is convolved with the synthesized discriminant signals of the expected target, the convolved outputs will be significantly different from the

*The E-pulse is similar to the K-pulse studied by other workers [5,10].

expected zero response or single-mode responses. Thus the wrong target can be discriminated.

The complex natural resonant frequencies of a radar target are aspect independent features of its transient electromagnetic response. A number of researchers have recently attempted to discriminate among various targets by extracting those natural frequencies from late-time transient radar returns. Since extraction of natural frequencies from late-time target responses is an inherently ill-conditioned numerical procedure, very large S-N ratios are required in the transient return. It has therefore been concluded that this method for the direct discrimination of differing targets is impractical. Our discrimination scheme differs significantly. Synthesis of the discriminant signals requires only knowledge of the natural frequencies of various expected targets. The latter natural frequencies are measured in the laboratory where they are extracted from the late-time pulse responses of target scale models. The numerically ill-conditioned natural frequency extraction procedure need therefore be applied only to target responses measured in a controlled S-N environment. Synthesized discriminant signals based upon those laboratory measurements are stored as computer data files, and subsequently convolved numerically with actual transient target radar returns. Since the latter convolution operation is numerically well conditioned (a smoothing integral operator), the S-N requirements for the actual radar return are significantly relaxed.

Another observation made in the course of our study is worth noting. It is common thinking among many researchers that radar detection utilizing the late-time transient radar return may not be practical because it contains little energy; most energy is associated with the early-time part of that return. This thinking may be true for very low-Q targets. Fortunately, for most space vehicles, such as rockets and aircrafts, these targets are not exactly low-Q structures. There is sufficient energy contained in the late-time returns of such targets, as can be evidenced from our measured responses of complex targets as discussed in this paper.

In Sections 2 and 3, we will demonstrate how to synthesize theoretically and experimentally E-0, E-1, —, E-n pulse or the zero-mode, the first-mode, —, the nth-mode excitation signal. E-0 pulse (extinguishing all the modes) or the zero-mode extraction signal can be used to produce a zero-response in the convolved output while E-n pulse (extinguishing all but the nth-mode) or the nth-mode extraction signal will produce a nth-mode response in the convolved output.

In Section 4, examples are given to show the convolution of the synthesized discriminant signals with the measured radar returns of various targets. The effectiveness of target discrimination by the present method is also discussed.

Finally, a potential radar detection system based on the present scheme is suggested in Section 5.

II. SYNTHESIS OF DISCRIMINANT SIGNALS BASED ON KNOWN NATURAL FREQUENCIES

The zero-mode and other single-mode extraction signals or E-0 pulse and E-n pulses of a given target can be synthesized theoretically based on the prior knowledge of natural frequencies of the target.

The late-time radar return of a target is the sum of natural modes, assuming the absence of noise, and it can be expressed as

$$h(t) = \sum_{n=1}^N a_n(\theta, \phi) e^{\sigma_n t} \cos(\omega_n t + \phi_n(\theta, \phi)) \quad (1)$$

where σ_n is the damping coefficient and ω_n is the angular frequency of the nth natural mode, and $a_n(\theta, \phi)$ and $\phi_n(\theta, \phi)$ are the amplitude and the phase angle of the nth natural mode. It is noted that σ_n and ω_n are independent of the aspect-angle (θ and ϕ), but $a_n(\theta, \phi)$ and $\phi_n(\theta, \phi)$ are usually strong functions of the aspect angle. N is the total number of natural modes which have significant amplitudes to be considered. In practice, N can be estimated based on the frequency spectrum of the interrogating radar pulse.

We aim to synthesize an extraction signal of duration T_e which can be convolved with the radar return $h(t)$ to produce a single-mode or zero-mode output in the late-time period ($t > T_e$):

$$E^0(t) = \int_0^{T_e} E^e(t') h(t - t') dt', \text{ for } t > T_e \quad (2)$$

where $E^0(t)$ is the convolved output signal, $E^e(t)$ is the extraction signal to be synthesized. The substitution of (1) in (2) leads to

$$E^0(t) = \sum_{n=1}^N a_n(\theta, \phi) e^{\sigma_n t} [A_n \cos(\omega_n t + \phi_n(\theta, \phi)) + B_n \sin(\omega_n t + \phi_n(\theta, \phi))], \text{ for } t > T_e \quad (3)$$

where

$$A_n = \int_0^{T_e} E^e(t') e^{-\sigma_n t'} \cos \omega_n t' dt' \quad (4)$$

$$B_n = \int_0^{T_e} E^e(t') e^{-\sigma_n t'} \sin \omega_n t' dt' \quad (5)$$

The coefficients A_n and B_n which determine the amplitudes of the natural modes of the convolved output are independent of the aspect angle (θ and ϕ). This makes it possible to synthesize the aspect-independent $E^e(t)$ for producing single-mode or zero-mode $E^0(t)$. It is noted that A_n and B_n are numerically stable because they are finite integrals over a short period of time T_e , even though there is a time growing factor of $e^{-\sigma_n t}$ in them.

Now for example, if we synthesize $E^e(t)$ in such a way that $A_1 = 1$ and all other A_n and B_n go to zero, then the output signal will be a cosine first natural mode as

$$r'(t) = a_1(\theta, \rho) e^{\sigma_1 t} \cos(\omega_1 t + \phi_1(\theta, \rho)), \text{ for } t > T_e.$$

If we choose $E^e(t)$ in such a way that $B_3 = 1$ and all other A_n and B_n go to zero, then the output signal will be a sine third natural mode such as

$$E^o(t) = a_3(\theta, \rho) e^{\sigma_3 t} \sin(\omega_3 t + \phi_3(\theta, \rho)), \text{ for } t > T_e.$$

If we synthesize $E^e(t)$ in such a way that all A_n and B_n vanish, then the zero-mode output is obtained:

$$E^o(t) = 0, \text{ for } t > T_e.$$

This $E^e(t)$ is the E-0 pulse or the zero-mode extraction signal because it extinguishes the late-time response completely.

The next task is to synthesize $E^e(t)$. Construct $E^e(t)$ with a set of basis function $f_m(t)$ as

$$E^e(t) = \sum_{m=1}^{2N} d_m f_m(t) \quad (6)$$

where $\{f_m(t)\}$ can be pulse functions, impulse functions or Fourier cosine functions, etc. and $\{d_m\}$ are the unknown coefficients to be determined. We need $2N$ of $f_m(t)$ because there are $2N$ of A_n and B_n to be specified,

$$A_n = \sum_{m=1}^{2N} M_{nm}^c d_m \quad (7)$$

$$B_n = \sum_{m=1}^{2N} M_{nm}^s d_m \quad (8)$$

where

$$M_{nm}^c = \int_0^{T_e} f_m(t') e^{-\alpha_n t'} \cos \omega_n t' dt' \quad (9)$$

$$M_{nm}^s = \int_0^{T_e} f_m(t') e^{-\alpha_n t'} \sin \omega_n t' dt' \quad (10)$$

Equations (7) and (8) can be expressed in a matrix form as

$$\begin{bmatrix} A_n \\ B_n \end{bmatrix} = \begin{bmatrix} M_{nm}^C \\ M_{nm}^S \end{bmatrix} \begin{bmatrix} d_m \end{bmatrix} \quad \begin{array}{l} n = 1, 2, \dots, N \\ m = 1, 2, \dots, 2N \end{array} \quad (11)$$

The coefficient d_m for constructing $E^e(t)$ can then be obtained from

$$\begin{bmatrix} d_m \end{bmatrix} = \begin{bmatrix} M_{nm}^C \\ M_{nm}^S \end{bmatrix}^{-1} \begin{bmatrix} A_n \\ B_n \end{bmatrix} \quad (12)$$

To synthesize $E^e(t)$ for the j th-mode extraction, we can assign $A_j = 1$ or $B_j = 1$ and let all other A_n and B_n go to zero, and then calculate $[d_m]$ from (12) accordingly. Using this approach, we select an appropriate value for the signal duration T_e which is short and also leads to a well behaved waveform for $E^e(t)$.

To synthesize the E-0 pulse or the extraction signal for zero response, all A_n and B_n are set to be zero. For this case $[d_m]$ will have non-trivial solutions only when the determinant of $\begin{bmatrix} M_{nm}^C \\ M_{nm}^S \end{bmatrix}$ vanishes. That is

$$\det \begin{bmatrix} M_{nm}^C \\ M_{nm}^S \end{bmatrix} = 0 \quad (13)$$

This condition can be met because all the elements of M_{nm}^C and M_{nm}^S are functions of the signal duration T_e , and it is possible to numerically search for the optimum value of T_e which makes (13) valid. Usually we use the Newton method for this purpose. Once the optimum T_e is determined, $[d_m]$ can be easily determined from a set of homogeneous equations generated from (11) by setting A_n and B_n to be zero.

Single-mode extraction signals or E-n pulses can also be synthesized in a similar way as that for the E-0 pulse. For example, if we aim to synthesize the cosine first mode extraction signal, we drop the first equation involving A_1 in (11). We then have a new set of $(2N-1)$ simultaneous equations as

$$\begin{bmatrix} A_2 \\ \vdots \\ A_N \\ B_1 \\ \vdots \\ B_N \end{bmatrix} = \begin{bmatrix} M_{nm}^C \\ \vdots \\ M_{nm}^S \end{bmatrix}' \begin{bmatrix} d_m \end{bmatrix} \quad \begin{array}{l} n = 2, 3, \dots, N \text{ for } M_{nm}^C \\ n = 1, 2, \dots, N \text{ for } M_{nm}^S \\ m = 1, 2, \dots, 2N-1 \end{array} \quad (14)$$

where $\begin{bmatrix} M_{nm}^C \\ \vdots \\ M_{nm}^S \end{bmatrix}'$ is a $(2N-1) \times (2N-1)$ matrix and it is the original $\begin{bmatrix} M_{nm}^C \\ \vdots \\ M_{nm}^S \end{bmatrix}$ matrix with its first row and its last column removed. We now force $A_2, \dots, A_N, B_1, \dots, B_N$ to be zero. This requires that

$$\det \begin{bmatrix} M_{nm}^C \\ \vdots \\ M_{nm}^S \end{bmatrix}' = 0 \quad (15)$$

Equation (15) can be solved numerically to determine the optimum T_e for the cosine first mode extraction signal. After that $[d_m]$ can be determined from a corresponding set of homogeneous equations from (14).

It has been found that the signal duration T_e for various discriminant signals is not unique but there exists an optimum value of T_e for which the waveform of the discriminant signal is best behaved and it possesses a maximal sensitivity in discriminating the target [6]. This optimum value of T_e is numerically found to be slightly longer than twice the transit time of the target or $2L/C$ where L is the longest dimension of the target and C is the speed of light.

III. SYNTHESIS OF DISCRIMINANT SIGNALS BASED ON EXPERIMENTAL PULSE RESPONSE

In the preceding section, discriminant signals for zero response or single-mode responses were synthesized based on the prior knowledge of target's natural frequencies. In the case of complex targets, this information is difficult to obtain, and the synthesis of the discriminant signals will be based on an experimental measurement of the pulse response or the late-time response of the scale model of the target combined with some theoretical techniques described below.

A. Application of Continuation Method to a Measured Pulse Response

The first method we have employed to synthesize the discriminant signals for a target is to apply a recently developed, continuation method [7] to extract major natural frequencies of the target from its measured pulse response.

This method is to regularize the ill-conditioned problem. After the natural frequencies are determined, the theoretical technique of the preceding section is used to synthesize the discriminant signals. The following steps are used in the process:

- (1) Measure the pulse response of the scale model of the target at various aspect angles.
- (2) Use the Fast Fourier Transform to obtain approximate values of natural frequencies from the measured pulse response.
- (3) Employ the continuation method and the natural frequencies obtained from FFT as the initial guesses to calculate accurate values of natural frequencies of the target. At each step of the algorithm, the condition number of the regularized problem is checked.
- (4) The theoretical technique of the preceding section is then applied to synthesize the discriminant signals for the target.

B. Application of Fast Prony's Method to a Measured Pulse Response

The second method we have used to synthesize the discriminant signals for a target is mainly based on the fast Prony's method [3,8] and a measured pulse response. This method in discrete-time basis consists of the following steps:

- (1) The fast Prony's method is applied to the sampled data of the measured pulse response of the target. The coefficients of Prony polynomial are obtained. The time-ordered sequence of these coefficients can be shown to become the E-0 pulse [E-0] of the target [8], which eliminates the natural modes of the target and other noise.

- (2) Find roots of the Z-transform of the sequence which represents $[E-0]$. From those roots in the proper locations of the complex plane, the complex natural frequencies $[S_m]$ of the target can be calculated.
- (3) At this step, E-0 pulse $[E-0]$ which extinguishes N natural modes of the target can be constructed by convolving N couplets $(1, -z_m)$ for $m = 1, 2, \dots, N$ where $z_m = \exp(S_m \Delta T)$ and ΔT is the sampling interval:

$$[E-0] = (1, -z_1) * (1, -z_2) * \dots * (1, -z_N)$$

- (4) The jth-mode extraction signal $[E_j^e]$ can be obtained by removing the couplet $(1, -z_j)$ from $[E-0]$ as

$$[E_j^e] = (1, -z_1) * \dots * (1, -z_i) * (1, -z_k) * \dots * (1, -z_N)$$

4. CONVOLUTION OF SYNTHESIZED DISCRIMINANT SIGNALS WITH EXPERIMENTAL RADAR RETURNS

To demonstrate the applicability of the present target discrimination method in practice, we have convolved the measured radar returns of various targets with the corresponding synthesized signals for extracting zero-response and single-mode responses. We have tested many targets and produced many interesting results but only a few examples will be given here for brevity.

Experimental pulse responses of various radar targets used in the present study were either measured recently in the time-domain scattering range at Michigan State University or have been published previously [3]. The MSU scattering range uses a biconical transmitting antenna (2.5 m long, 16° cone angle) and as a receiving probe it uses a short monopole field probe on the ground plane (6 m x 5 m), a current probe or a charge probe on the target surface. The transmitting antenna is excited either by a mercury-switched nanosecond pulser (Tektronix-109), which produces pulses of about 100ps risetime and variable duration $1 \text{ ns} < t_p < 1 \text{ } \mu\text{s}$ with amplitude as great as 500 volts at a 1 kHz rate, or by another picosecond pulser (Picosecond Lab-1000B) which produces

a narrower but a lower amplitude pulse. The signal from the receiving probe is measured by a sampling scope and the signal processing, including averaging and clutter subtraction, is performed by a computer controlled system.

Figure 1 shows the measured impulse response of a thin cylinder target, having length $l = 12.5$ in $= 31.75$ cm and length-to-radius ratio $l/a = 400$, illuminated obliquely by a nanosecond plane-wave pulse at $\theta = 60^\circ$ aspect and the synthesized E-0 pulse. This E-0 pulse was synthesized in terms of pulse functions with the first three natural modes, indicated in the figure, extracted by the continuation method as described in Section 3.A. The band-limited frequency spectrum of the l-nS incident pulse precluded the identification of higher natural frequencies. Figure 2 shows the convolved result of the E-0 pulse of Fig. 1 with the pulse response of the correct cylinder along with the similar convolved results with the pulse responses of cylinders 5% and 25% longer. The correct cylinder yields a low-amplitude late-time response which approximates the expected zero response; failure to achieve a perfect zero response is the result of imperfect experimental data having content other than the assumed sum of pure natural modes (the latter may be artifacts introduced by the measurement system). Longer targets lead to responses which can be discriminated from an expected zero response. Discrimination of the 5% longer cylinder is marginal while that of the 25% longer target is clear.

Next example was given to show the convolution of single-mode extraction signals with the measured radar return of a target. Figure 3 shows the results of the convolution of the measured pulse response of a wire target with $18.6''$ length and $.0465''$ radius with the synthesized signal for the third mode extraction. Figure 3(a) shows the synthesized signal for extracting the cosine third mode, constructed in terms of impulse basis functions using the fast Prony's method described in Section 3.B, and the convolved output. It is observed that a cosine third mode is produced in the late-time period of the

convolved output. Figure 3(b) shows the synthesized signal for extracting the sine third mode (in terms of impulse basis functions) and convolved output. A sine third mode is produced in the late-time period. To demonstrate that these late-time responses are indeed that of the third mode, a complex convolved output is constructed as

$$C(t) = A(t) - j B(t)$$

where $A(t)$ is the convolved output of Fig. 3(a) and $B(t)$ is the convolved output of Fig. 3(b). If the late-time response of $A(t)$ is a pure cosine third mode, it can be expressed as

$$[A(t)]_{\text{late}} = a_3 e^{\sigma_3 t} \cos(\omega_3 t + \phi_3).$$

Similarly, if the late-time response of $B(t)$ is a pure sine third mode, it can be expressed as

$$[B(t)]_{\text{late}} = a_3 e^{\sigma_3 t} \sin(\omega_3 t + \phi_3).$$

Thus, the late-time response of the complex convolved output should be

$$[C(t)]_{\text{late}} = a_3 e^{\sigma_3 t} e^{-j(\omega_3 t + \phi_3)}$$

The logarithm of the late-time response of $C(t)$ yields

$$\ln[C(t)]_{\text{late}} = \ln a_3 + \sigma_3 t - j(\omega_3 t + \phi_3)$$

and

$$\text{real part of } \ln[C(t)]_{\text{late}} = \sigma_3 t + \ln a_3$$

$$\text{imaginary part of } \ln[C(t)]_{\text{late}} = -\omega_3 t - \phi_3$$

Figure 3(c) shows the real part of $\ln[C(t)]$ in comparison with the line of $(\sigma_3 t)$. It is observed that the late-time response of $\text{Re}\{\ln[C(t)]\}$ is nearly in parallel with the line of $(\sigma_3 t)$ for the late-time period of $t/(L/C) > 3$ where $t/(L/C)$ is the normalized time with L as the wire length and C as the speed of light. Figure 3(d) shows the imaginary part of $\ln[C(t)]$ in comparison with the line of $(-\omega_3 t)$. It is again observed that the late-time response of $\text{Im}\{\ln[C(t)]\}$ is in parallel with the line of $(-\omega_3 t)$ for the late-time period

of $t/(L/C) > 3$. Figures 3(c) and 3(d) give a positive indication that the late-time response of the convolved outputs of Figs. 3(a) and 3(b) contain only (or predominantly) the third mode of the target.

An example is also given to show the capability of target discrimination provided by the present method. Figure 4 shows the results of the convolution of the radar return of a wrong target, a 16.74" wire, with the synthesized signal for extracting the third mode of the right target, a 18.6" wire. In Figs. 4(a) and 4(b), the convolved outputs are significantly different from the expected third mode of the right target. Furthermore, the late time response of $\text{Re} \{ \ln[C(t)] \}$ deviates greatly from the line of $(\sigma_3 t)$ and the late-time response of $\text{Im} \{ \ln[C(t)] \}$ also differs significantly from the line of $(-\omega_3 t)$ as shown in Figs. 4(c) and 4(d). The results given in Fig. 4 give a positive discrimination of the wrong target, implying that the radar return does not belong to the right target of 18.6" wire.

We have also applied the present method to discriminate between complex radar targets. Two targets, experimental models of the F-18 plane and the 707 plane which have similar sizes but different geometrics, were used for this purpose. In the experiment, the half of each model was placed on the ground plane (image effect), and was illuminated by a pulsed electric field polarized perpendicularly to the ground plane. Results on these two targets are depicted in the following figures.

Figure 5(a) shows the convolution of the E-0 pulse for the F-18 plane with the measured radar response of the F-18 plane. The convolved outputs shows a strong early-time response followed by a "extinguished" (almost zero) late-time response as expected. Figure 5(b) shows the convolved output of the E-0 pulse for the 707 plane with the measured radar response of the F-18 plane. This convolved output shows a significant, "unextinguished" late-time response implying that the 707 E-0 pulse was convolved with the radar response of a wrong target other than the 707 plane.

Figure 6 shows the convolved results of the measured radar response of the 707 plane with the fourth-mode extraction signal for the 707 plane. In this figure, the extracted angular frequency line is almost parallel to the $\omega_4 t$ line (of the 707) and the extracted damping coefficient line closely parallel to the $\sigma_4 t$ line (of the 707) in the late-time period. This implies that the radar response belongs to the right target of the 707 plane.

Figure 7 shows the convolved results of the measured radar response of the F-18 plane with the fourth-mode extraction signal for the 707 plane. The extracted angular frequency line deviates from the $(\omega_4 t)$ line of the 707 plane and the extracted damping coefficient line also differs from the $(\sigma_4 t)$ line of the 707 plane. These results imply that the radar response belongs to a wrong target other than the 707 plane.

It is noted that the synthesized E-0 pulses and single-mode extraction signals for these targets are available elsewhere [9].

5. A POTENTIAL RADAR DETECTION SYSTEM BASED ON THE PRESENT CONVOLUTION METHOD

Figure 8 depicts a potential radar detection system based on the present scheme of convolving the target radar return with the synthesized discriminant signals. The system consists of a network of computers and each of them is assigned to store the synthesized signals for extracting various single-mode or zero-mode response for a particular friendly target. All the relevant friendly targets are assumed to be covered in the network of computers. When an approaching target is illuminated by an interrogating radar signal, the radar return is divided and fed to each computer after amplification and signal processing. Inside each computer the stored discriminant signals are convolved with the radar return. In principle, only one of the computers will produce various single-mode and zero-mode outputs in the late-time period; the rest of the computers should produce irregular outputs. The computer producing the single-mode and zero-mode outputs will then be identified with

the target. If none of the computers produces single-mode and zero outputs in the late-time period, the approaching targets will not be a friendly target.

6. Discussion

The present radar discrimination scheme is not a conventional correlation method because the measured radar return is convolved with synthesized discriminant signals which possess particular waveforms. The present scheme is basically different from the matched filtering scheme. A fundamental difference between the E-pulse scheme and the matched filtering scheme is as follows: The E-pulse scheme is to nullify a selected natural mode set, and does not deal with maximizing a specific modal content. For example, the E-0 pulse eliminates all the modes in the late time. The single-mode extraction signal eliminates all but one mode. We do not consider maximization of responses in the presence of noise at specific times as in the matched filtering scheme. A further difference between these two schemes is the following: The natural modes are not, in general, orthogonal. Maximizing the response of a particular mode will not nullify the other modes. Also note that the E-pulse scheme is aspect-independent, whereas the matched filtering is not.

We have not attempted to compare the performance of the E-pulse scheme with that of a matched filtering scheme.

REFERENCES

1. K.M. Chen, D.P. Nyquist, D. Westmoreland, C.I. Chuang, and B. Drachman, "Radar waveform synthesis for single-mode scattering by a thin cylinder and application for target discrimination," *IEEE Trans. on Antennas and Propagation*, Vol. AP-30, No. 5, 867-880, Sept., 1982.
2. K.M. Chen and D. Westmoreland, "Radar waveform synthesis for exciting single-mode backscatters from a sphere and application for target discrimination," *Radio Science*, Vol. 17, No. 3, 574-588, June, 1982.
3. Lance Webb, K.M. Chen, D.P. Nyquist, and B. Hollmann, "Extraction of single-mode backscatters by convolving synthesized radar signal with a radar return," presented at 1983 International IEEE/AP-S Symposium, University of Houston, Houston, Texas, May 23-26, 1983, Symposium Digest, 676-679.
4. Edward Rothwell, D.P. Nyquist, and K.M. Chen, "Synthesis of Kill-pulse using time-domain SEM," presented at 1983 International IEEE/AP-S Symposium, University of Houston, Houston, Texas, May 23-26, 1983 Symposium Digest, 672-675.
5. E.M. Kennaugh, "The K-pulse concept," *IEEE Trans. on Ant. and Prop.*, AP-20, No. 2, pp. 327-331, March, 1981.
6. E. Rothwell, D.P. Nyquist, and K.M. Chen, "Synthesis of Kill-pulse to excite selected target models," presented at 1984 International IEEE/AP-S Symposium, Boston, June 25-29, 1984, Symposium Digest, 15-18.
7. B. Drachman and E. Rothwell, "A continuation method for identification of the natural frequencies of an object using a measured response," *IEEE Trans. on Antennas and Propagation*, AP-33, No. 4, April 1985, pp. 445-450.

8. Lance Webb, "Radar target discrimination using K-pulse from a "fast" Prony's method," Ph.D thesis, Department of Electrical Engineering and Systems Science, Michigan State University, 1984.
9. K.M. Chen, "Radar waveform synthesis for target identification," Final report for Naval Air Systems Command, Division of Engineering Research, Michigan State University, 1983.
10. I. Gerst and J. Diamond, "The elimination of intersymbol interference by input signal shaping," Proceedings of the IRE, July 1961, pp. 1195-1203.

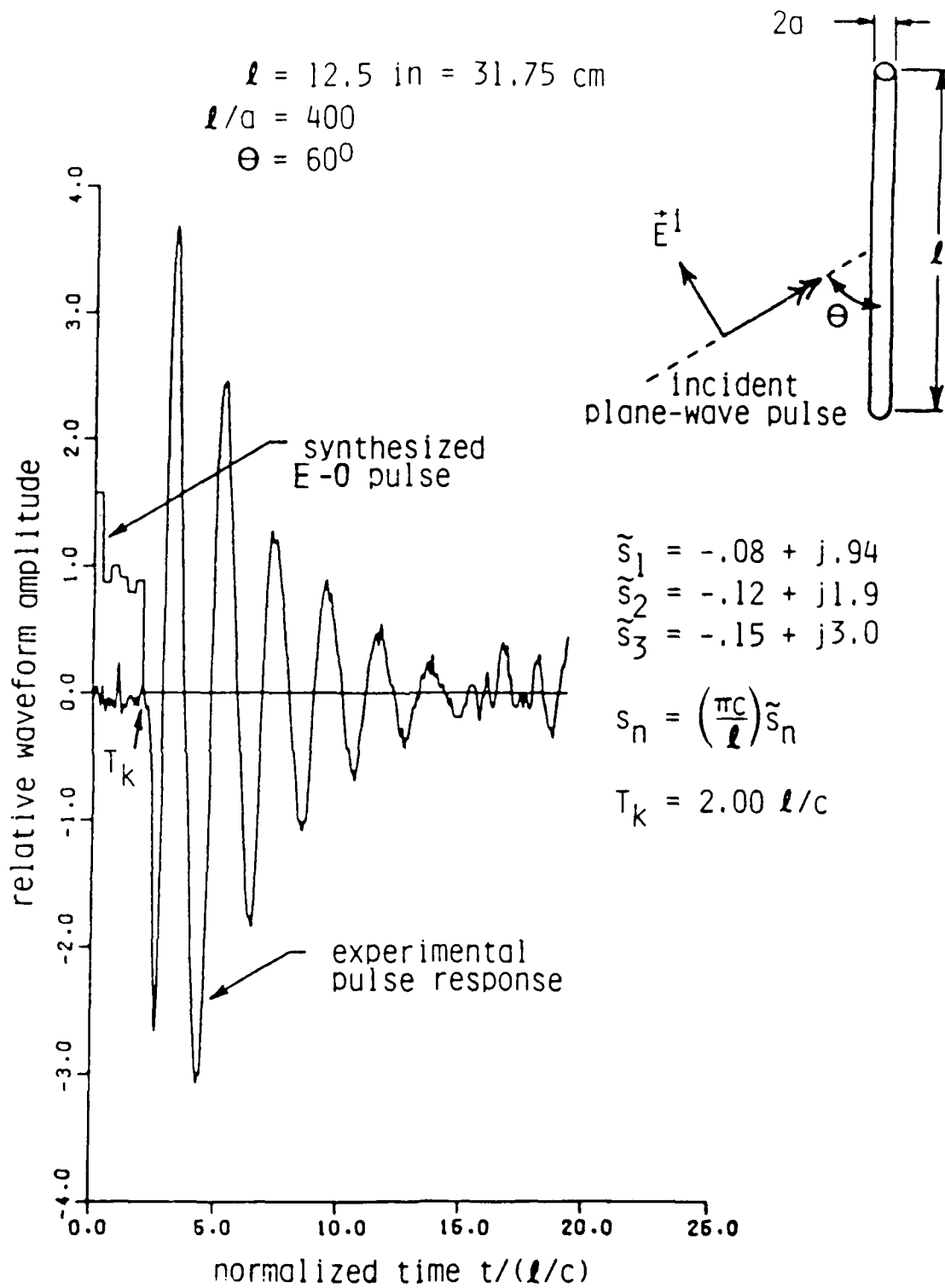


Figure 1. Synthesis of Thin-Cylinder E-0 Pulse from Experimentally Measured Pulse Response; Dominant Natural Frequencies Extracted by the Continuation Method.

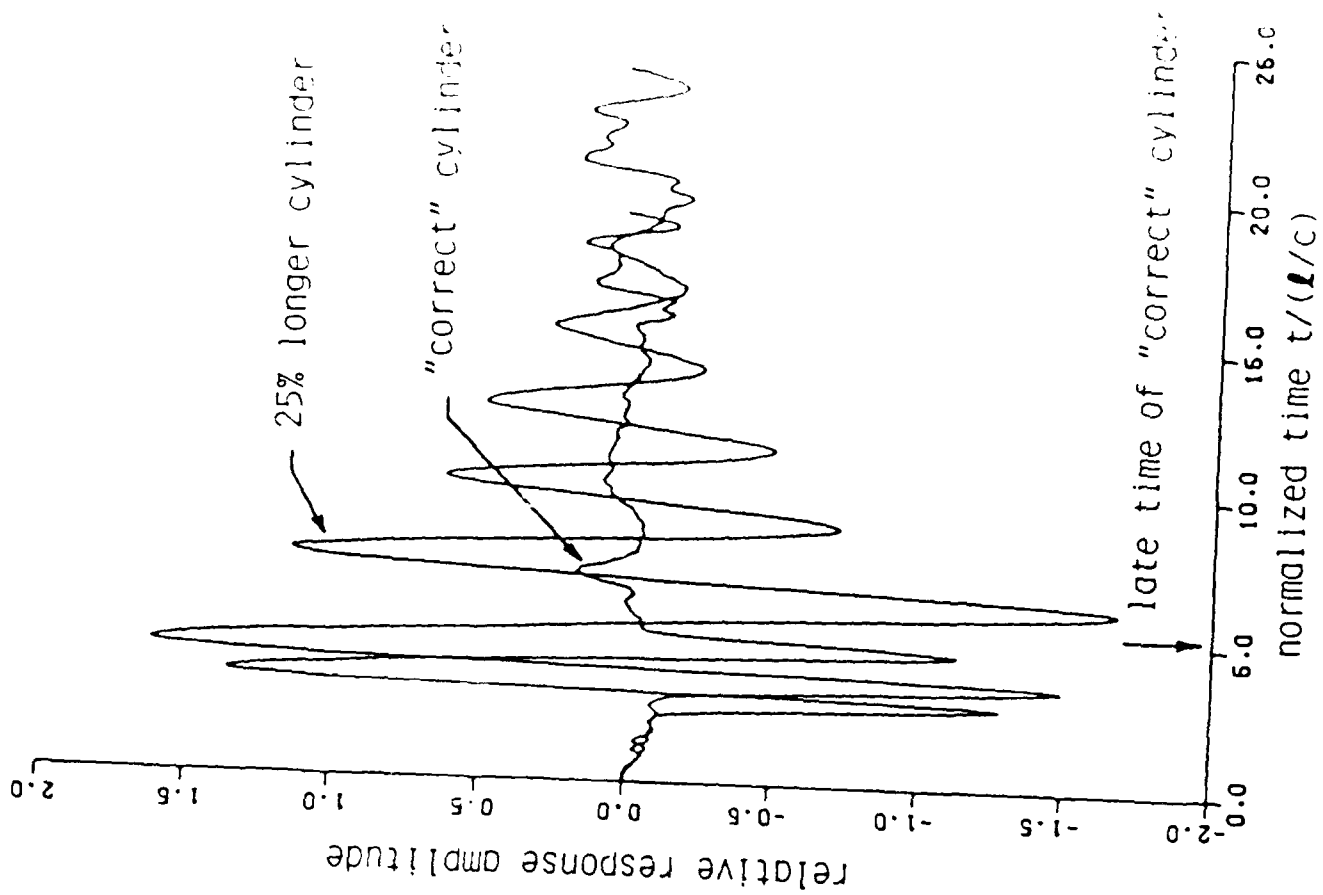
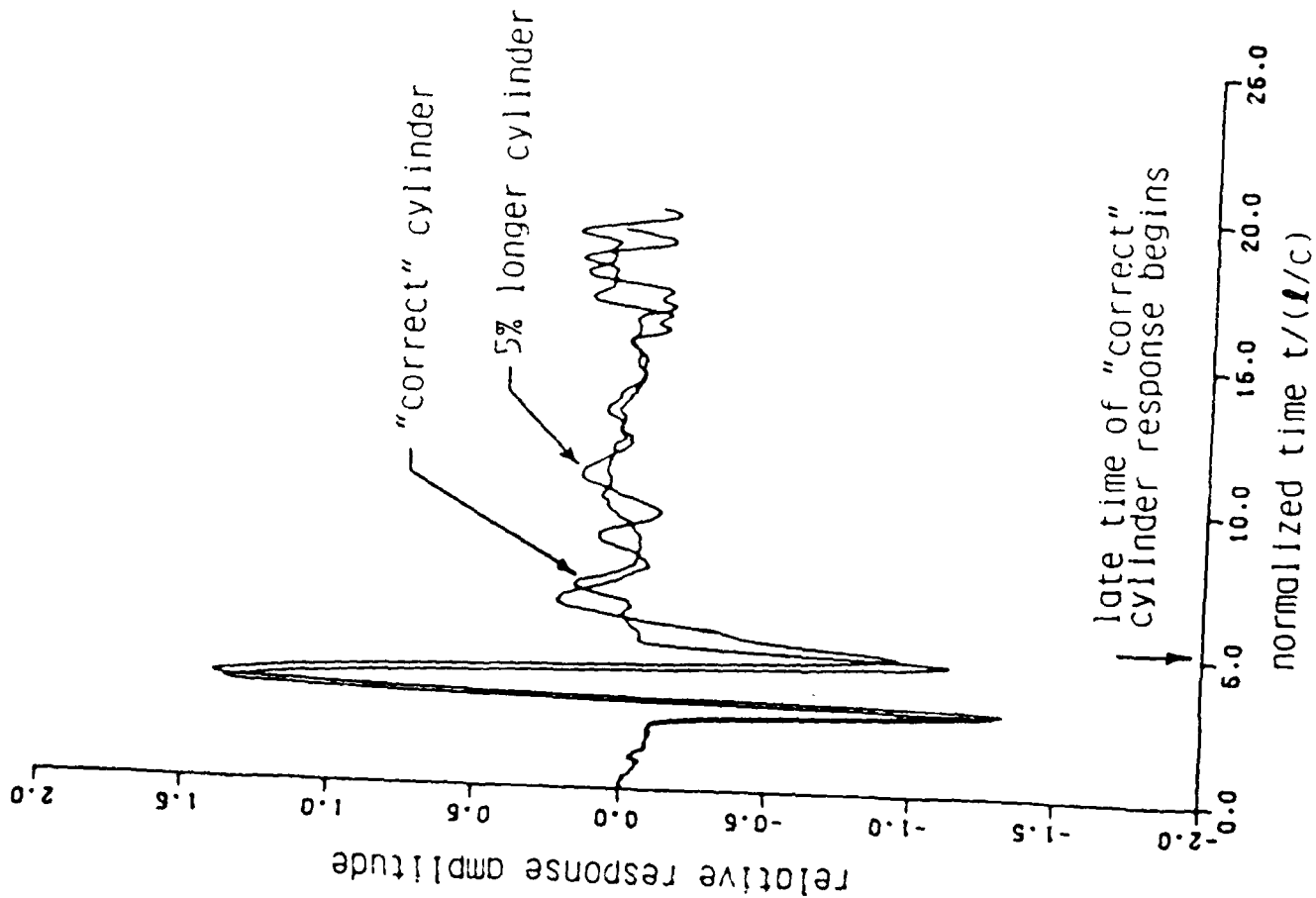


Figure 2 Convolution (Target Response) of Thin-Cylinder E-U Pulse Synthesized from Measured Pulse Response with the Responses of the Same "Correct" Cylinder and Those of 5% and 25% Greater Length.

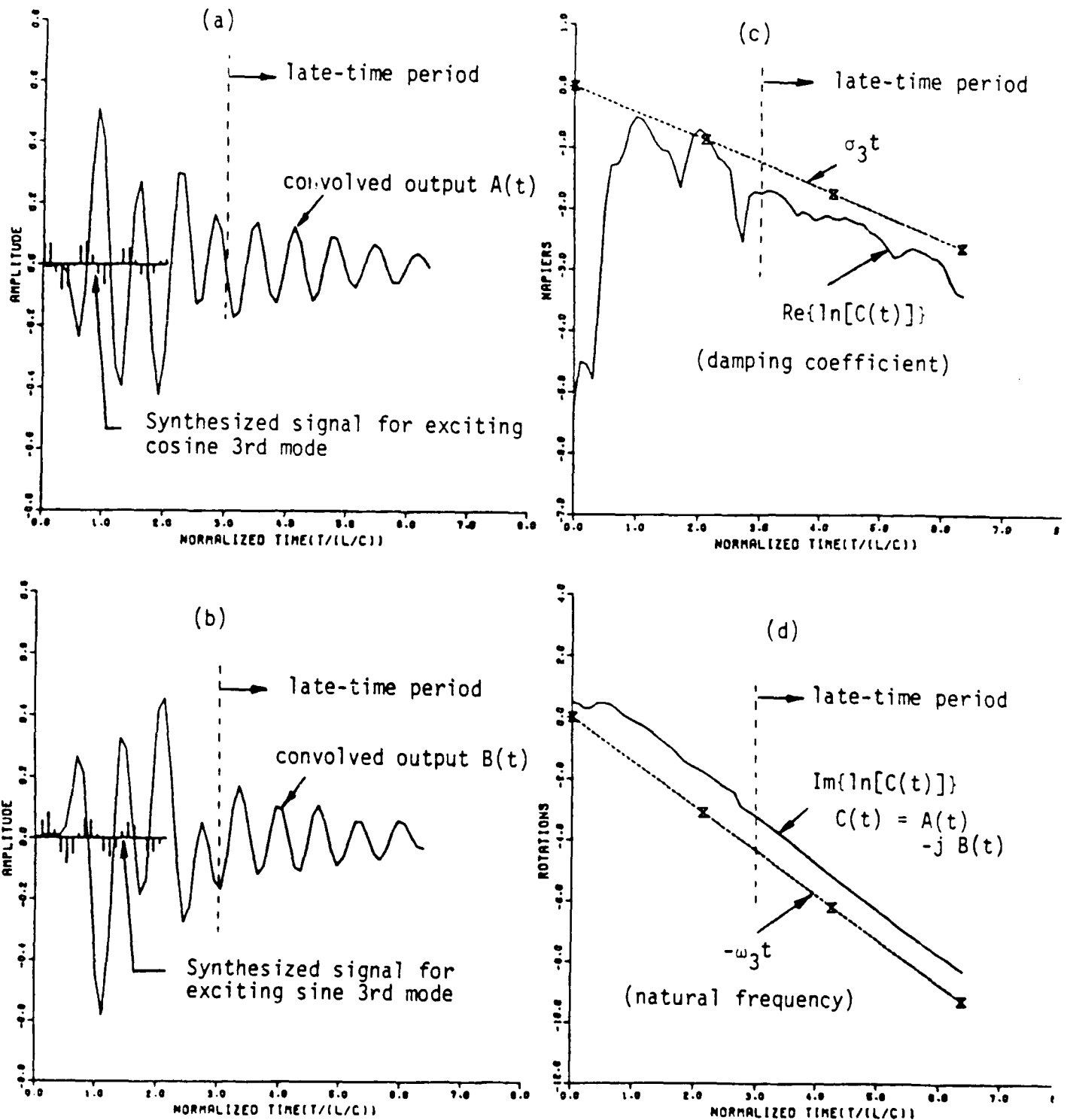


Fig. 3. Convolution of the impulse response of a 18.6" (length) wire with the synthesized signal for the third mode excitation of the 18.6" wire.

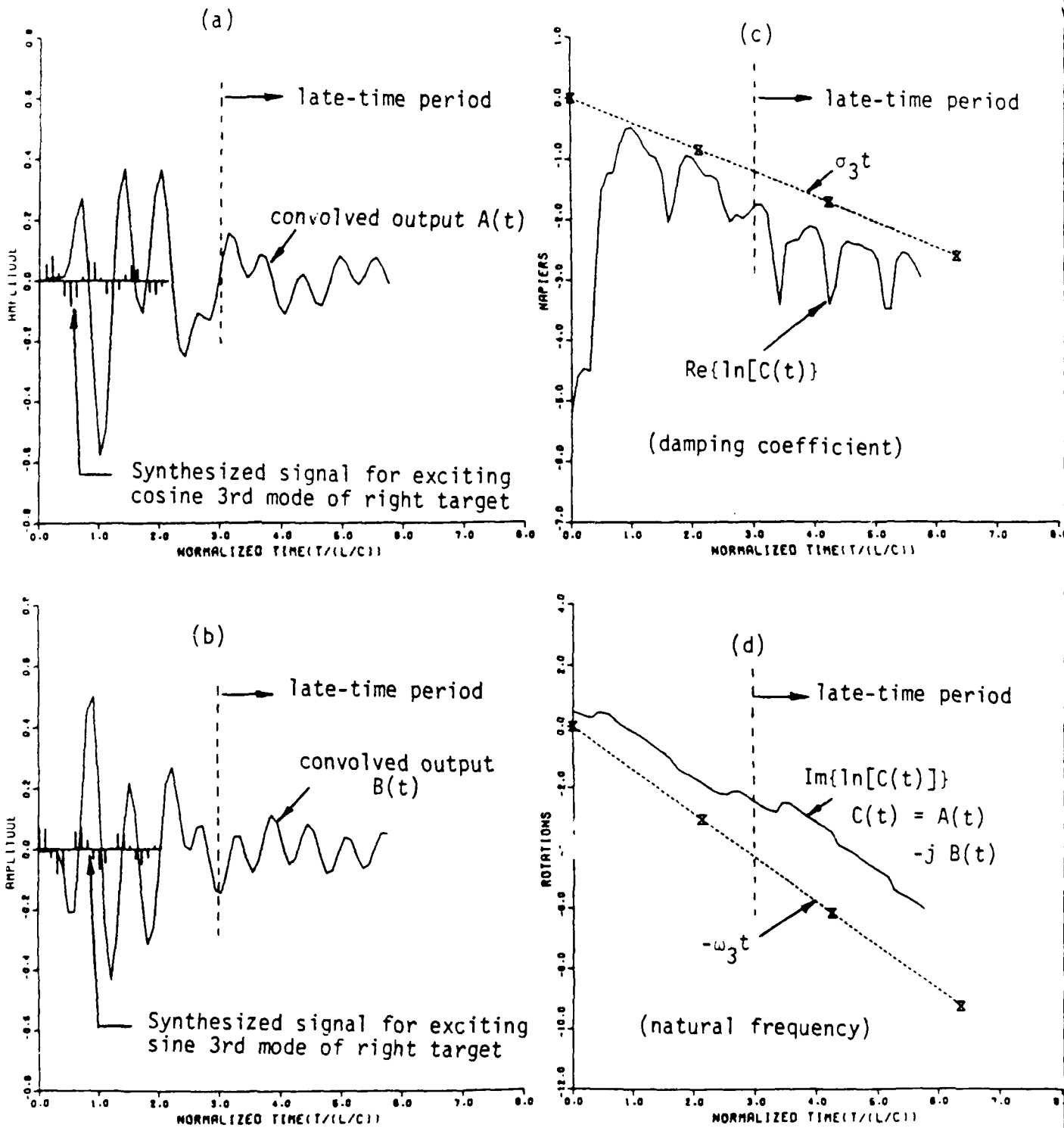


Fig. 4. Convolution of the impulse response of a wrong target, a 16.74" wire, with the synthesized signal for exciting the third mode of the right target, a 18.6" wire.

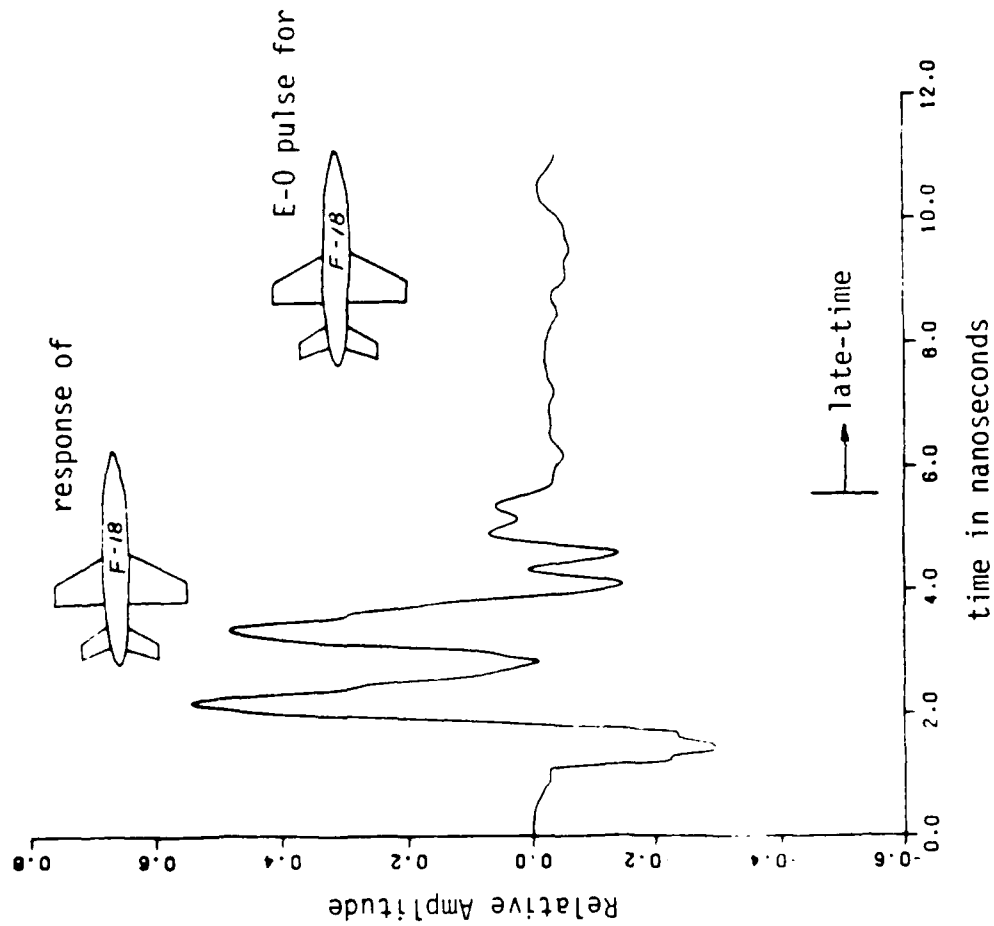


Fig. 5(a) Convolution of the F-18 E-0 pulse with the F-18 measured response showing "extinguished" late-time region.

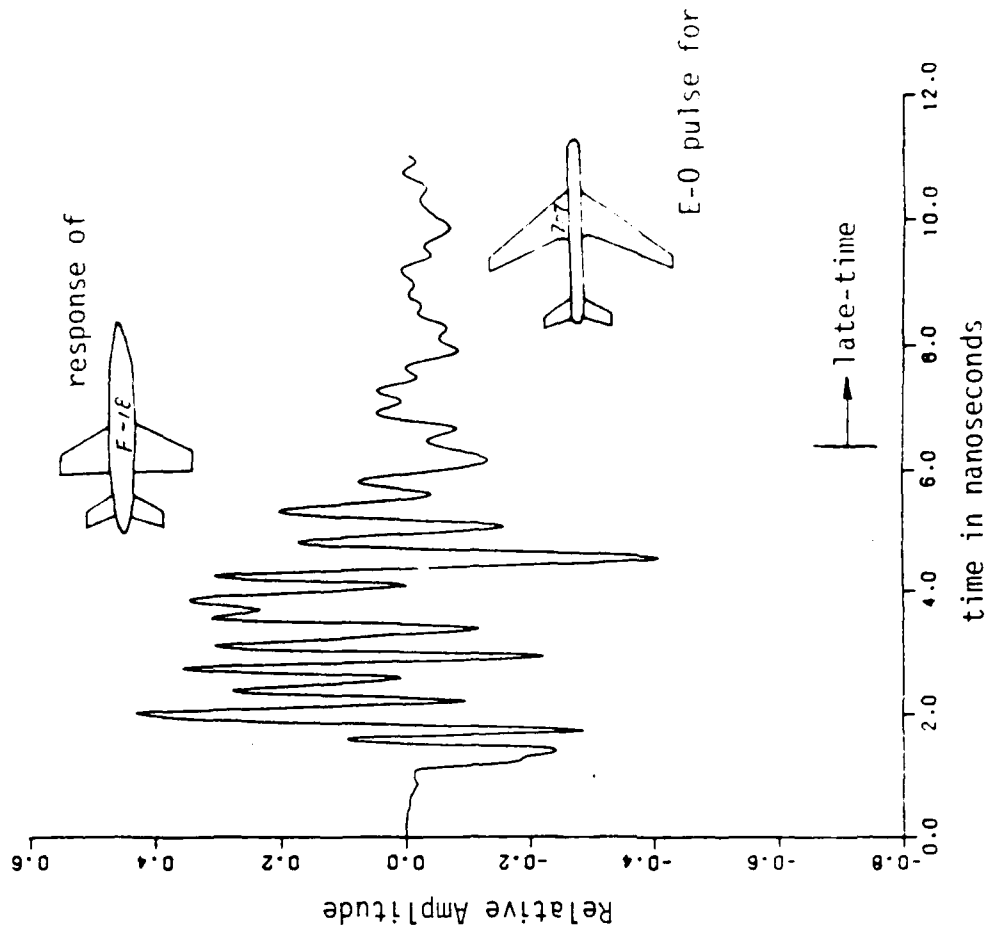


Fig. 5(b). Convolution of the 707 E-0 pulse with the F-18 response showing a significant late-time response.

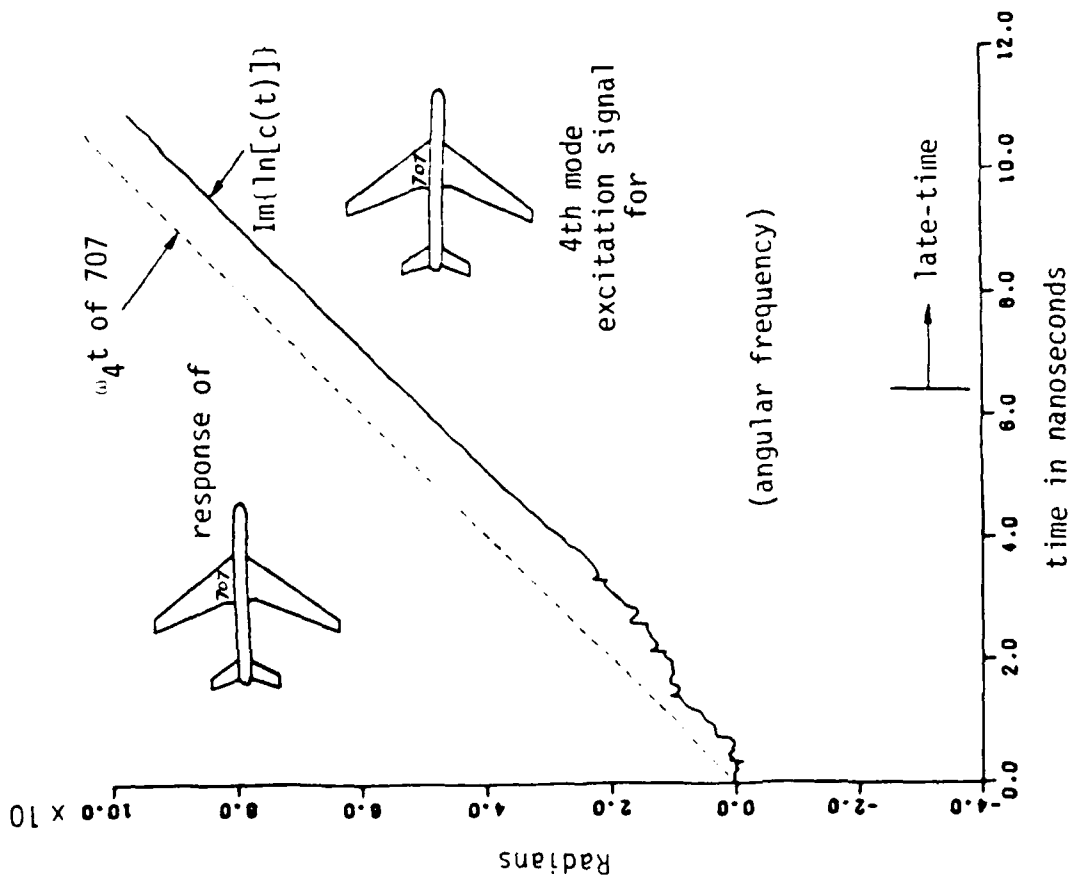
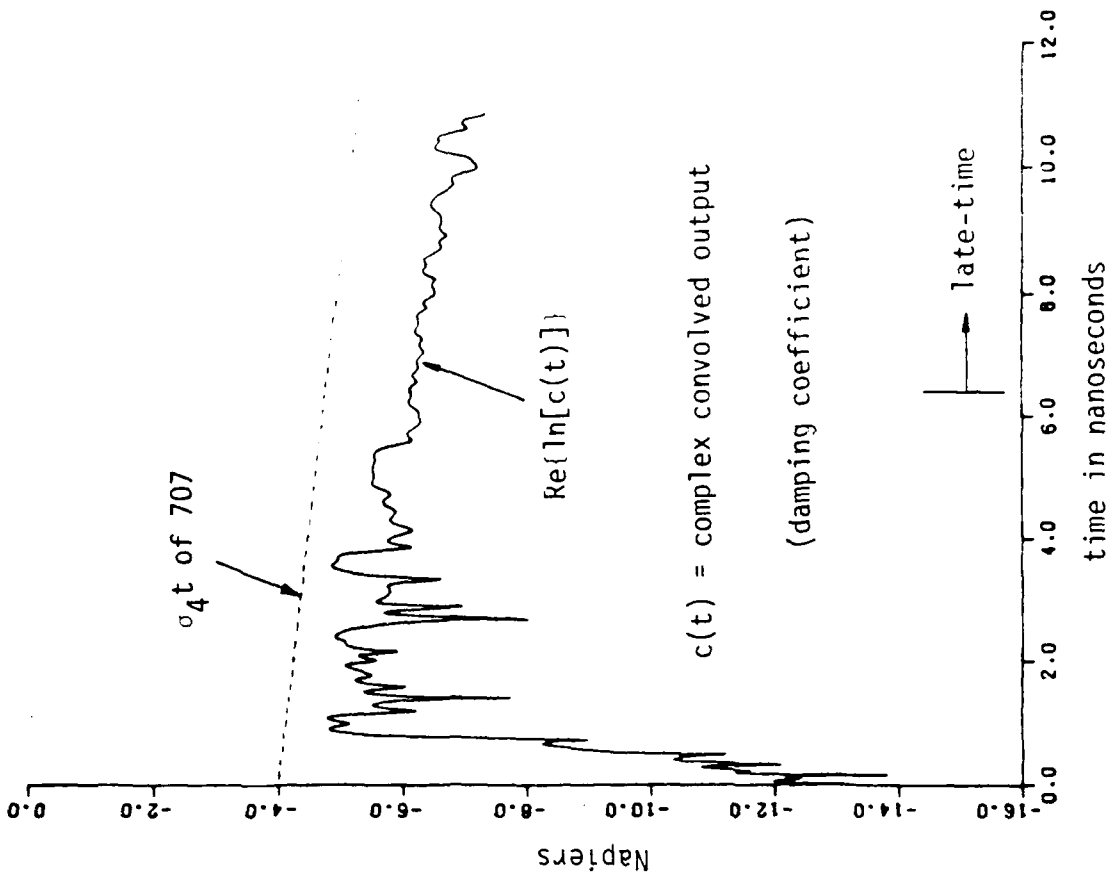


Fig. 6. Angular frequency and damping coefficient extracted from the complex convolved output of the fourth mode excitation signal for the 707 target and the 707 measured response.

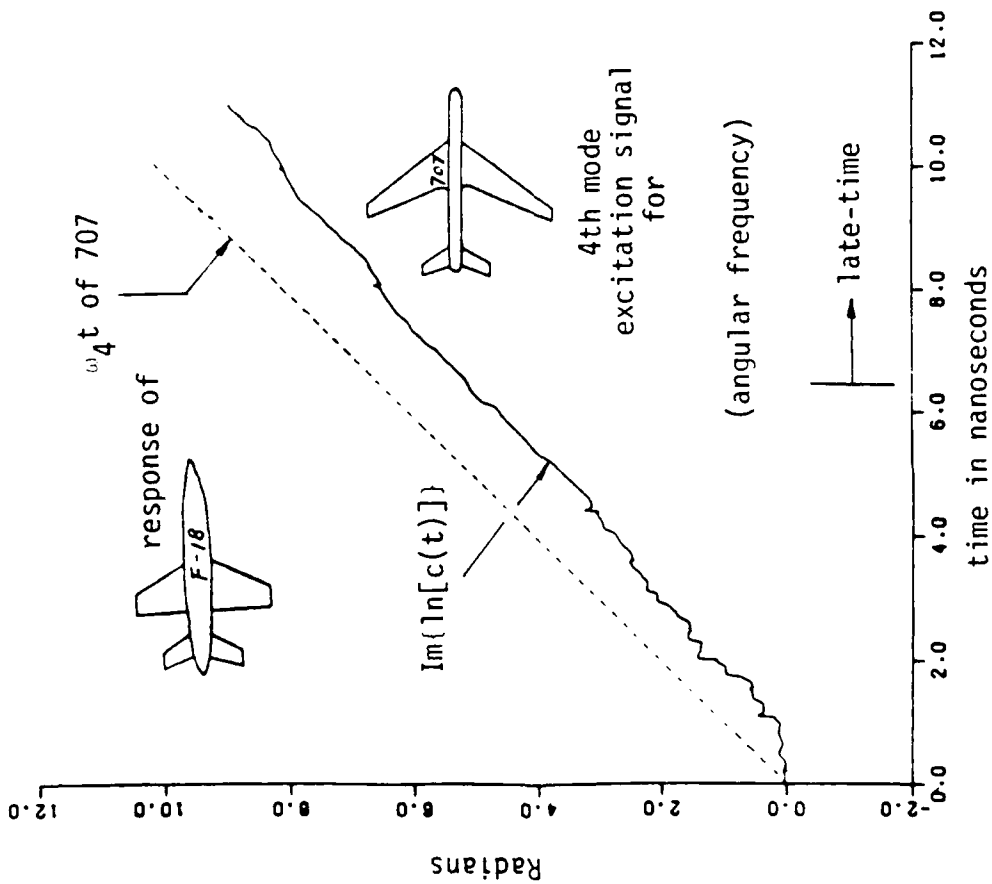
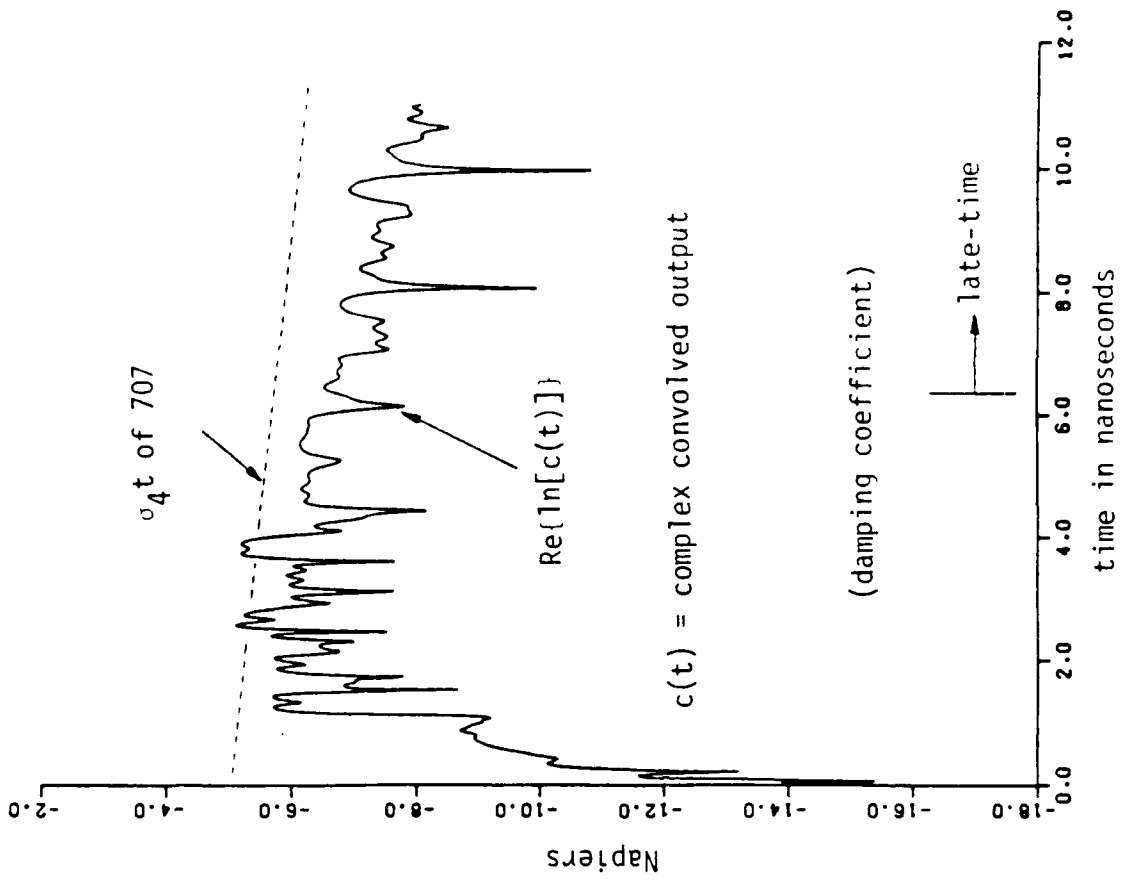


Fig. 7. Angular frequency and damping coefficient extracted from the complex convolved output of the fourth mode excitation signal for the 707 target and the F-18 measured response.

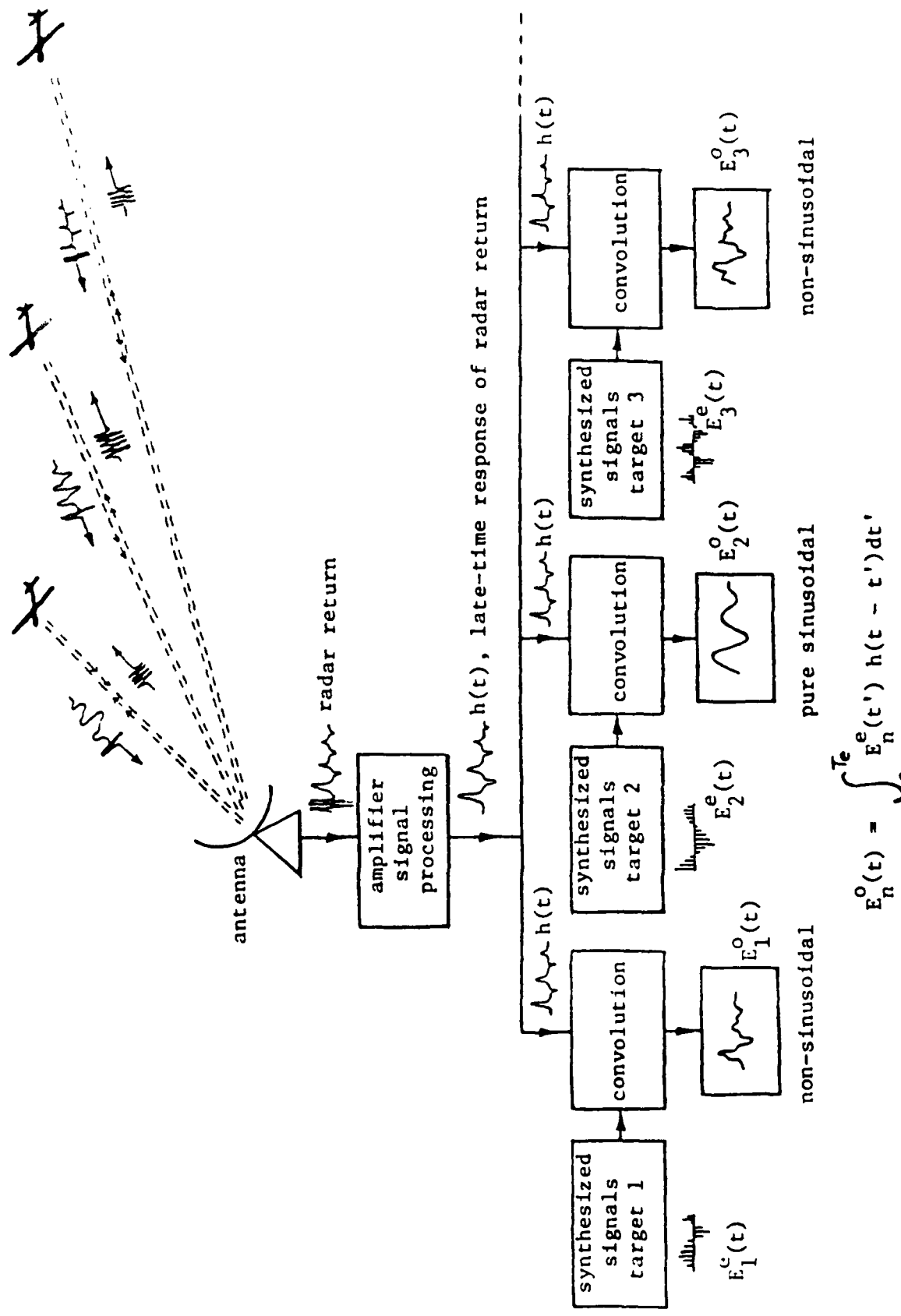


Fig. 8. A proposed target identification and discrimination system.

2.2 RADAR TARGET DISCRIMINATION USING THE EXTINCTION-PULSE TECHNIQUE

ABSTRACT

An aspect independent radar target discrimination scheme based on the natural frequencies of the target is considered. An extinction-pulse waveform upon excitation of a particular conducting target results in the elimination of specified natural modal content of the scattered field. Excitation of a dissimilar target produces a noticeably different late-time response. Construction of appropriate extinction-pulse waveforms is discussed, as well as the effects of random noise on their application to thin cylinder targets. Also presented is experimental verification of this discrimination concept using simplified aircraft models.

I. Introduction

Radar target identification methods using the time-domain response of a target to a transient incident waveform have gained considerable interest recently [1-4]. One of the most intriguing schemes involves the so-called "Kill-pulse" technique as first described by Kennaugh [5]. A Kill-pulse (K-pulse) is an excitation waveform synthesized in such a way as to minimize a transient scattered field response. Target discrimination results from the unique correspondence of a K-pulse to a particular target; excitation of a dissimilar target yields a "larger" response.

This paper describes a related "extinction-pulse" (E-pulse) concept, based on the natural resonance of a conducting radar target via the singularity expansion method (SEM) [6]. The time domain electric field scattered by the target is divided into an early-time, forced response period when the excitation waveform is traversing the target, and a late-time, free oscillation period that exists after the excitation waveform has passed [7,8]. The early-time response is not utilized due to its complicated nature. The late-time response can be decomposed into a sum of damped sinusoids oscillating at frequencies determined entirely by the geometry of the target. An E-pulse is then viewed as a transient, finite duration waveform which annihilates the contribution of a select number of these natural resonances to the late-time response. A related target identification scheme based on natural target resonances has been examined by Chen [9].

Target discrimination using this SEM viewpoint is easily visualized. Each target can be described by a set of natural frequencies. An E-pulse designed to annul certain natural resonances of one target will excite those of a target with different natural frequencies, resulting in a different scattered field. Also made apparent is the aspect-independent nature of the E-pulse. Since the values of the target resonance frequencies are independent

of the excitation waveform, the E-pulse will eliminate the desired natural modal content of the late-time scattered field regardless of the orientation of the target with respect to the transmitting and receiving antennas.

It is important to note that the E-pulse waveform need not be transmitted to employ this concept. It is assumed that an excitation waveform with finite usable bandwidth will be used to excite the target, resulting in a measured scattered field with the desired (finite) modal content. The E-pulse can then be convolved numerically with the measured target response, yielding results analogous to E-pulse transmission. If the maximum modal content of the target scattered field can be estimated from the frequency content of the excitation pulse, then the E-pulse waveform can be constructed to yield a null late-time convolved response.

After an initial presentation of the SEM representation of the backscattered field excited by a transient incident wave and calculation of the corresponding impulse response, two types of E-pulses, forced and natural, will be discussed. The results are then specialized to a thin cylinder target, which has an impulse response amenable to analytic calculation. Target discrimination using the natural thin cylinder E-pulse, as well as the effects of random noise are also investigated. Lastly, experimental verification of the E-pulse concept is presented.

II. Backscattered Field Excited by Transient Incident Wave

A perfectly conducting radar target is illuminated by a plane electromagnetic wave as shown in Figure 1. The electric field associated with this transient wave can be written in the Laplace transform domain as

$$\vec{E}^i(\vec{r}, s) = \hat{\zeta} e(s) e^{-\frac{s}{c} \hat{k} \cdot \vec{r}} \quad (1)$$

where \vec{r} is a position vector in a coordinate system local to the target, $\hat{\zeta}$ is a constant unit vector specifying the polarization of the wave, \hat{k} is a unit vector in the direction of propagation, and $e(t)$ represents the time dependence of the incident field. The current \vec{K} induced on the surface of the target is given by the solution to the transform domain E-field integral equation

$$\int_S \left[\hat{r}' \cdot \vec{K}(\vec{r}', s) (\hat{t} \cdot \nabla) - \frac{s^2}{c^2} \hat{t} \cdot \vec{K}(\vec{r}', s) \right] \frac{e^{-\frac{s}{c} R}}{4\pi R} ds' = -s \epsilon_0 \hat{t} \cdot \vec{E}^i(\vec{r}, s) \quad (2)$$

where \hat{t} is a unit vector tangent to the surface of the target at the point \vec{r} on S , and $R = |\vec{r} - \vec{r}'|$. The surface current can also be expanded using the SEM representation

$$\vec{K}(\vec{r}, s) = \sum_{\alpha=1}^N a_{\alpha} \vec{K}_{\alpha}(\vec{r}) (s - s_{\alpha})^{-1} + \vec{W}(\vec{r}, s) \quad (3)$$

where $\vec{W}(\vec{r}, s)$ represents any entire function contribution to the current, and it is assumed that only a finite number of natural modes are substantially excited by the incident field. It is further assumed that the only singularities of $\vec{K}(\vec{r}, s)$ in the finite complex s -plane are simple poles at natural frequencies $s_{\alpha} = \sigma_{\alpha} + j\omega_{\alpha}$. Then, $\vec{K}_{\alpha}(\vec{r})$ represents the current distribution of the α th natural mode, and a_{α} is the "class-1" coupling coefficient given by Baum [10].

The far-zone backscattered electric field can be computed by integrating the current distribution over the surface of the target. The ζ component of backscattered field can then be written as

$$E_{\zeta}^S(r, s, \hat{k}) = \frac{e^{-\frac{s}{c} r}}{r} e(s) H(s, \hat{k}, \hat{\zeta}) \quad (4)$$

where $r = |\vec{r}|$ and $H(s, \hat{k}, \hat{\zeta})$ is the aspect dependent transfer function of the target. Using (3) to represent the surface current, the transfer function can be inverse transformed to determine the backscatter impulse response of the target.

Because of the entire function contribution to the current, the impulse response will exhibit two distinct regions. The early-time, forced component represents the backscattered field excited by currents during the time when the impulse is traversing the target; it has a duration equal to twice the one-way maximal transit time of the target, T . The late-time free oscillation component is composed purely of a sum of constant amplitude natural modes and exists for all time $t > 2T$ as

$$h(t, \hat{k}, \hat{\zeta}) = \sum_{n=1}^N a_n(\hat{k}, \hat{\zeta}) e^{\sigma_n t} \cos(\omega_n t + \phi(\hat{k}, \hat{\zeta})) \quad t > 2T \quad (5)$$

where it has been assumed that the entire function makes no contribution to the late-time component [6]. Thus, the ζ component of the far-zone backscattered field is given simply by the convolution of the time domain incident field and the impulse response, and is also composed of forced and freely oscillating portions.

III. Incident E-pulse Waveform Synthesis

To synthesize an E-pulse for a particular target, the convolutional representation of the backscattered field is written in integral form using the impulse response of (5) as

$$\begin{aligned} E_{\zeta}^S(t, \hat{k}) &= \int_0^T e(t') h(t-t', \hat{k}, \hat{\zeta}) dt' \\ &= \int_0^T e(t') \sum_{n=1}^N a_n(\hat{k}, \hat{\zeta}) e^{\sigma_n(t-t')} \cos[\omega_n(t-t') + \phi_n(\hat{k}, \hat{\zeta})] dt' \end{aligned} \quad (6)$$

This response is valid for the late-time portion of the scattered field, $t > T_L = T_e + 2T$, where T_e is the duration of $e(t)$. The excitation waveform becomes an E-pulse when the scattered field is forced to vanish identically in the late-time. Rewriting equation (6) and employing this condition yields a defining equation for the E-pulse

$$\sum_{n=1}^N a_n(\hat{k}, \hat{z}) e^{\sigma_n t} [A_n(T_e) \cos(\omega_n t + \phi_n(\hat{k}, \hat{z})) + B_n(T_e) \sin(\omega_n t + \phi_n(\hat{k}, \hat{z}))] = 0$$

$$t > T_L = T_e + 2T \quad (7)$$

where the coefficients $A_n(T_e)$ and $B_n(T_e)$ are given by

$$\begin{Bmatrix} A_n(T_e) \\ B_n(T_e) \end{Bmatrix} = \int_0^{T_e} e(t') e^{-\sigma_n t'} \begin{Bmatrix} \cos \omega_n t' \\ \sin \omega_n t' \end{Bmatrix} dt' \quad (8)$$

The linear independence of the damped sinusoids in equation (7) requires $A_n(T_e) = B_n(T_e) = 0$ for all $1 \leq n \leq N$.

It is important to note that $A_n(T_e)$ and $B_n(T_e)$ are independent of the aspect parameters \hat{k} and \hat{z} , verifying the aspect independence of the E-pulse. This is a direct consequence of the separability of the terms of the impulse response.

A physical interpretation of the E-pulse can be facilitated by decomposing the excitation waveform as shown in Figure 2 as

$$e(t) = e^f(t) + e^e(t) \quad (9)$$

where $e^f(t)$ is an excitatory component, nonvanishing during $0 \leq t < T_f$, the response to which is subsequently extinguished by $e^e(t)$ which follows during $T_f \leq t \leq T_e$. Substituting equation (9) into equation (8) and using $A_n(T_e) = B_n(T_e) = 0$ yields

$$\int_{T_f}^{T_e} e^e(t') e^{-\sigma_n t'} \begin{Bmatrix} \cos \omega_n t' \\ \sin \omega_n t' \end{Bmatrix} dt' = - \int_0^{T_f} e^f(t') e^{-\sigma_n t'} \begin{Bmatrix} \cos \omega_n t' \\ \sin \omega_n t' \end{Bmatrix} dt' \quad (10)$$

The extinction component of the E-pulse necessary to eradicate the response due to a preselected excitatory component can be constructed as an expansion over an appropriately chosen set of linearly independent basis functions as

$$e^e(t) = \sum_{m=1}^{2N} c_m g_m(t) \quad (11)$$

Equation (10) then becomes

$$\sum_{m=1}^{2N} M_{\lambda,m}^{C,S}(T_e) C_m = - F_{\lambda}^{C,S} \quad 1 \leq \lambda \leq N \quad (12)$$

where

$$M_{\lambda,m}^{C,S}(T_e) = \int_{T_f}^{T_e} g_m(t') e^{-\sigma_{\lambda} t'} \begin{Bmatrix} \cos \omega_{\lambda} t' \\ \sin \omega_{\lambda} t' \end{Bmatrix} dt' \quad (13a)$$

$$F_{\lambda}^{C,S} = \int_0^{T_f} e^f(t') e^{-\sigma_{\lambda} t'} \begin{Bmatrix} \cos \omega_{\lambda} t' \\ \sin \omega_{\lambda} t' \end{Bmatrix} dt' \quad (13b)$$

This can be written using matrix notation as

$$\begin{bmatrix} M_{\lambda,m}^C(T_e) \\ \text{-----} \\ M_{\lambda,m}^S(T_e) \end{bmatrix} \begin{bmatrix} C_1 \\ \vdots \\ C_{2N} \end{bmatrix} = - \begin{bmatrix} F_1 \\ \vdots \\ F_{2N} \end{bmatrix} \quad (14)$$

Solving this equation for C_1, \dots, C_{2N} determines the extinction component via equation (11) and thus the E-pulse.

It is convenient at this point to identify two fundamental types of E-pulses. When $T_f > 0$ the forcing vector on the right hand side of equation (14) is non-zero and a solution for $e^e(t)$ exists for almost all choices of T_e . This type of E-pulse has a non-zero excitatory component and is termed a "forced" E-pulse. In contrast, when $T_f = 0$ the forcing vector vanishes and solutions for $e^e(t)$ exist only when the determinant of the coefficient matrix vanishes, i.e., when $\det[M(T_e)] = 0$. These solutions correspond to discrete eigenvalues for the E-pulse duration T_e , which are determined by rooting the

determinantal characteristic equation. Since there is no excitatory component, this type of E-pulse is viewed as extinguishing its own excited field and is called a "natural" E-pulse.

IV. Thin Cylinder E-pulse Analysis

A theoretical analysis of a thin wire target has been undertaken by various authors [11,12]. Target natural frequencies are determined from the homogeneous solutions to the integral equation (2). The geometry of the target and its orientation with respect to the excitation field are given in Figure 3 along with the first ten natural frequencies. The frequencies are normalized by $\pi c/L$ where L is the length of the wire and c is the speed of light, and correspond to a wire of radius given by $L/a = 200$.

The thin cylinder impulse response can be calculated by inverting equation (4) [12] and becomes a pure sum of natural modes in the late-time. Figure 4 shows the impulse responses of thin cylinders oriented at $\theta = 30^\circ$ and $\theta = 60^\circ$, generated by using the first ten modes of the target. Note the distinct early and late-time regions. An E-pulse to extinguish the first ten modes of the target is created by solving equation (14) using the corresponding frequencies.

Figure 5 shows a natural E-pulse synthesized to kill the first ten natural modes of the thin wire target, using a pulse function basis set. The duration of the waveform, $T_e = 2.0408 L/c$, corresponds to the first root of the resulting determinantal equation. Superimposed with this is Kennaugh's original K-pulse. The similarity is striking, with the major difference being the finite duration of the E-pulse. Also shown in Figure 5 is a forced pulse function E-pulse constructed to extinguish the first ten modes of the target. The duration has been chosen as $T_e = 2.3$ and the excitation component

has been chosen as a pulse function of width equal to that of the basis functions.

Numerical verification of the thin wire E-pulse is given in Figure 6. The natural E-pulse waveform of Figure 5 is convolved with the 30° and 60° impulse responses of Figure 4 and the resulting backscattered field representations are observed to be zero in the late-time. Note also the expected non-zero early-time response. This portion is useful since it provides a comparative benchmark assessing the quality of the annulled component of the response; this is important when imperfect "extinction" is evident (due to noise, errors in the natural frequencies, etc.).

The question of E-pulse waveform uniqueness as the number of natural frequencies extinguished, N , is taken to infinity has not been resolved. For the thin cylinder target there appears to be such a unique waveform. Evidence is provided by Figure 7 which shows natural E-pulses of minimum duration designed to extinguish various numbers of natural modes, using both Fourier cosine and pulse function basis sets. It is apparent that these waveforms are nearly identical and they appear to be converging to a particular shape.

The most critical parameter necessary for E-pulse uniqueness is the finite E-pulse duration, T_e . This must converge to a distinct value as $N \rightarrow \infty$. For the pulse function basis set it can be shown that the natural E-pulse durations are given by

$$T_e = 2\pi N \frac{p}{\omega_\lambda} \quad p = 1, 2, \dots \quad 1 \leq \lambda \leq N \quad (15)$$

where ω_λ is the imaginary part of the λ th natural frequency. If this is written for the thin cylinder as

$$\omega_\lambda = \pi[\lambda - s(\lambda)] \frac{c}{L} \quad (16)$$

where $\varepsilon(z)/z$ decreases asymptotically to zero with increasing z , then the minimum E-pulse duration converges to

$$\begin{aligned} (T_e)_{\min} &= \lim_{N \rightarrow \infty} \frac{2-N}{\pi[N-\varepsilon(N)]} \frac{L}{c} \\ &= 2 \frac{L}{c} \end{aligned} \quad (17)$$

V. Target Discrimination with E-pulse Waveforms

Discrimination between different thin cylinder targets is demonstrated by convolving the natural E-pulse of Figure 5, which has been constructed to extinguish the first ten modes of a target of length L , with the impulse response of the expected target and a target 5% longer. The result is shown in Figure 8. The late-time response of the expected target has been successfully annulled, while the response of the differing target is non-zero over the same period. The difference in target natural frequencies provides the basis for discrimination based on the comparison of adequately dissimilar late-time responses of differing targets.

Sensitivity of E-pulse performance to the presence of uncorrelated random noise is investigated by perturbing each point of the thin cylinder impulse response of Figure 4 by a random amount not exceeding 10% of the maximum waveform amplitude. The result is shown in Figure 9. An attempt is then made to extinguish this noisy response by convolving it with the natural E-pulse of Figure 5. As expected, the convolution, shown in Figure 10, does not exhibit a null late-time response, but results in a distribution of noise about the zero line. Also plotted in this figure is the convolution of the E-pulse with a noisy waveform representing a target 5% longer. It is quite easy to separate the effects of noise and target length sensitivity, suggesting that random noise will not interfere with target discrimination.

VI. Experimental Verification of the E-pulse Concept

Time domain measurements of complex conducting target responses provide the means for a practical test of the E-pulse concept. The present experiment involves measuring the near scattered field response of a simplified aircraft model to transient pulse excitation. A Tektronix 109 pulse generator is used to provide a quasi-rectangular 400 V incident pulse of nanosecond duration. Transmission of the pulse over a 5 x 6 m conducting ground screen is accomplished by using an (imaged) biconical antenna of axial height 2.5 m, half angle of 8° and characteristic impedance of 160Ω , while reception is implemented using a short monopole E-field probe of length 1.6 cm. Although the receiving probe is not positioned in the far field region of the scatterer, the resulting measurements have the desired modal content in the late-time period, provided the small probe purely differentiates the waveform. Lastly, discrete sampling of the time domain waveform is accomplished by using a Tektronix sampling oscilloscope (S2 sampling heads, 75 psec risetime) coupled to a Radio Shack model III microcomputer.

In this experiment, an attempt is made to discriminate between two aircraft models by employing the E-pulse technique. Figures 11 and 12 show the measured pulse responses of simplified Boeing 707 and McDonnell Douglas F-18 aircraft models, respectively. Each model is constructed of aluminum and has a geometry as indicated in the figures. Also shown in the figures are the dominant natural frequencies extracted from the late-time portion of the response using a nonlinear least-squares curve fitting technique [13]. E-pulse waveforms can then be constructed to annul these frequencies.

Pulse function based natural E-pulses constructed to annul each of the two target responses are shown in Figures 13 and 14. Discrimination between the targets is accomplished by convolving these waveforms with the measured responses of Figures 11 and 12. Figure 15 shows the convolution of the F-18 E-

pulse with the F-18 measured response. Compared to early-time, the late-time region has been effectively annulled. In contrast, Figure 16 shows the convolution of the 707 E-pulse with the F-18 measured response. The result is a relatively larger late-time amplitude. Similarly, Figure 17 displays the convolution of the 707 E-pulse with the 707 measured response. Again, the late-time region of the convolution exhibits small amplitude. Lastly, Figure 18 shows the convolution of the F-18 E-pulse and the measured response of the 707 model. As before, the "wrong" target is exposed by its larger late-time convolution response.

VII. Summary and Conclusion

Radar target discrimination based on the natural frequencies of a conducting target has been investigated. The response of targets to a particular class of waveforms known as "E-pulses" has been demonstrated to provide an effective means for implementing a discrimination process in the presence of random noise.

Two types of E-pulses have been identified, natural and forced. Discrimination based on natural E-pulses and the response of a thin cylinder target has been demonstrated theoretically.

Most encouraging are the experimental results which reveal that two quite complicated, similar sized targets can be adequately and convincingly discriminated using natural E-pulse waveforms. Further experimentation using more accurate aircraft models is currently being undertaken.

References

1. K.M. Chen, "Radar waveform synthesis method -- a new radar detection scheme," IEEE Trans. Antennas Propagat., AP-29, No. 4, 553-566, July, 1981.

2. D.L. Moffatt and R.K. Mains, "Detection and discrimination of radar targets," IEEE Trans. Antennas Propagat., AP-23, No. 3, 358-367, May, 1975.
3. A.J. Berni, "Target identification by natural resonance estimation," IEEE Trans. Aerospace and Electronic Systems, AES-11, No. 2, 147-154, March, 1975.
4. C.W. Chuang and D.L. Moffatt, "Natural resonances of radar targets via Prony's method and target discrimination," IEEE Trans. Aerospace and Electronic Systems, AES-12, No. 5, 583-589, September, 1976.
5. E.M. Kennaugh, "The K-pulse concept," IEEE Trans. Antennas Propagat., AP-29, No. 2, 327-331, March, 1981.
6. C.E. Baum, "The singularity expansion method," Transient Electromagnetic Fields, Edited by L.B. Felson, Springer-Verlag, 1976, Chap. 3, pp. 129-179.
7. M.A. Morgan, "Singularity expansion representation of fields and currents in transient scattering," IEEE Trans. Antennas and Propagat., AP-32, No. 5, 466-473, May, 1984.
8. L.W. Pearson, "A note on the representation of scattered fields as a singularity expansion," IEEE Trans. Antennas and Propagat., AP-32, No. 5, 520-524, May, 1984.

9. K.M. Chen and D. Westmoreland, "Radar waveform synthesis for exciting single-mode backscatter from a sphere and application for target discrimination," Radio Sci., Vol. 17, No. 3, pp. 574-588, May-June, 1982.
10. C.E. Baum, "Emerging technology for transient and broad-band analysis of antennas and scatterers," Proc. IEEE, Vol. 64, No. 11, 1598-1616, November, 1982.
11. K.M. Chen, et al., "Radar waveform synthesis for single-mode scattering by a thin cylinder and application for target discrimination," IEEE Trans. Antennas Propagat., AP-30, No. 5, 867-880, September, 1982.
12. F.M. Tesche, "On the analysis of scattering and antenna problems using the singularity expansion technique," IEEE Trans. Antennas Propagat., AP-21, No. 1, 53-62, January, 1973.
13. B. Drachman and E. Rothwell, "A continuation method for identification of the natural frequencies of an object using a measured response," IEEE Trans. Antennas Propagat., to appear, 1985.

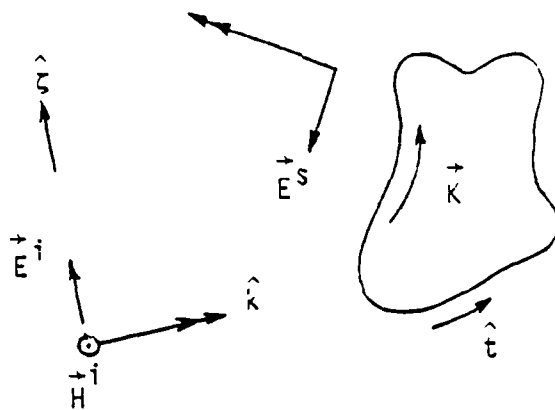


Figure 1 Illumination of a conducting target by an incident electromagnetic wave.

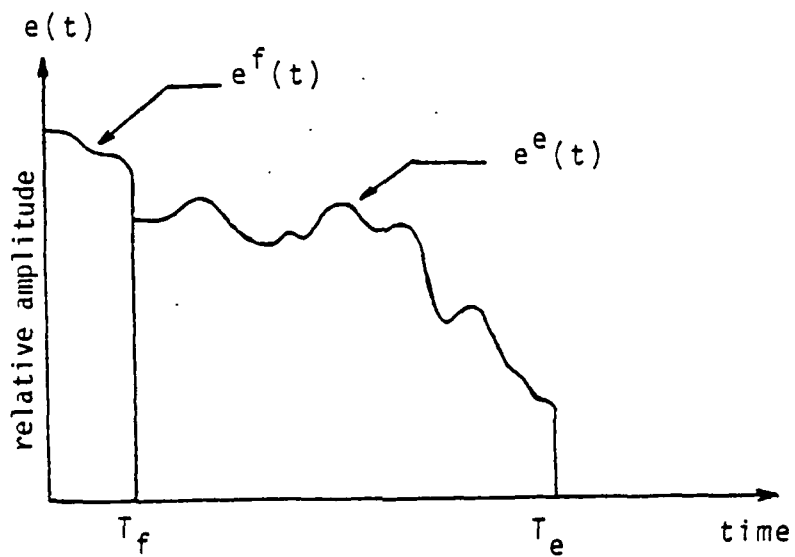
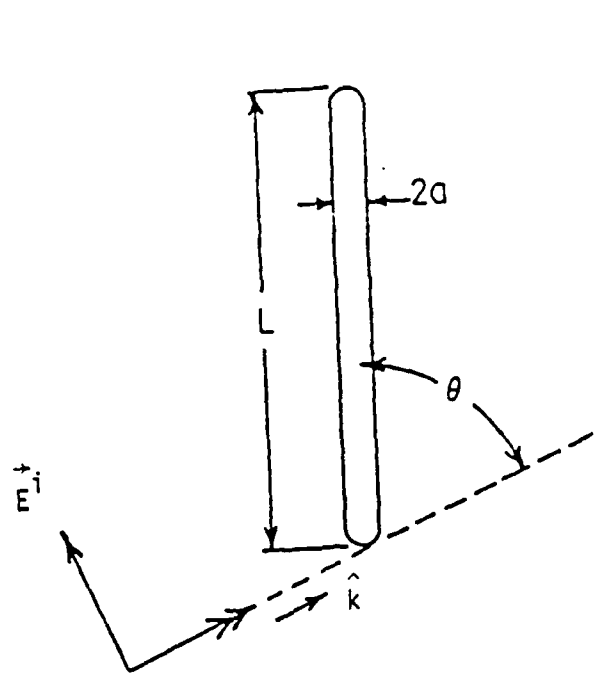


Figure 2 Decomposition of E-pulse into forcing and extinction components.



$$L/a = 200$$

\underline{n}	\underline{S}_n
1	$-0.0828 + j0.9251$
2	$-0.1212 + j1.912$
3	$-0.1491 + j2.884$
4	$-0.1713 + j3.874$
5	$-0.1909 + j4.854$
6	$-0.2080 + j5.845$
7	$-0.2240 + j6.829$
8	$-0.2383 + j7.821$
9	$-0.2522 + j8.807$
10	$-0.2648 + j9.800$

Figure 3 Orientation for thin cylinder excitation and first ten natural frequencies.

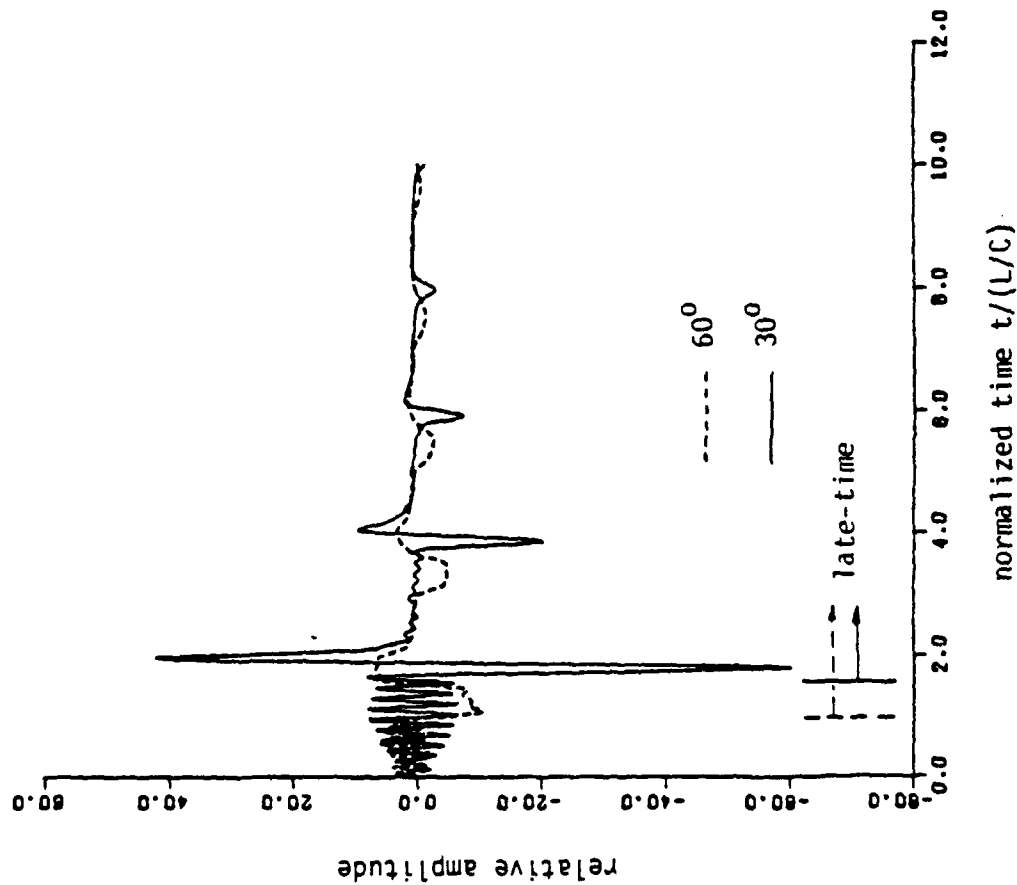


Figure 4 Thin cylinder impulse responses for $\theta=30^\circ$ and $\theta=60^\circ$ generated using the first ten natural modes.

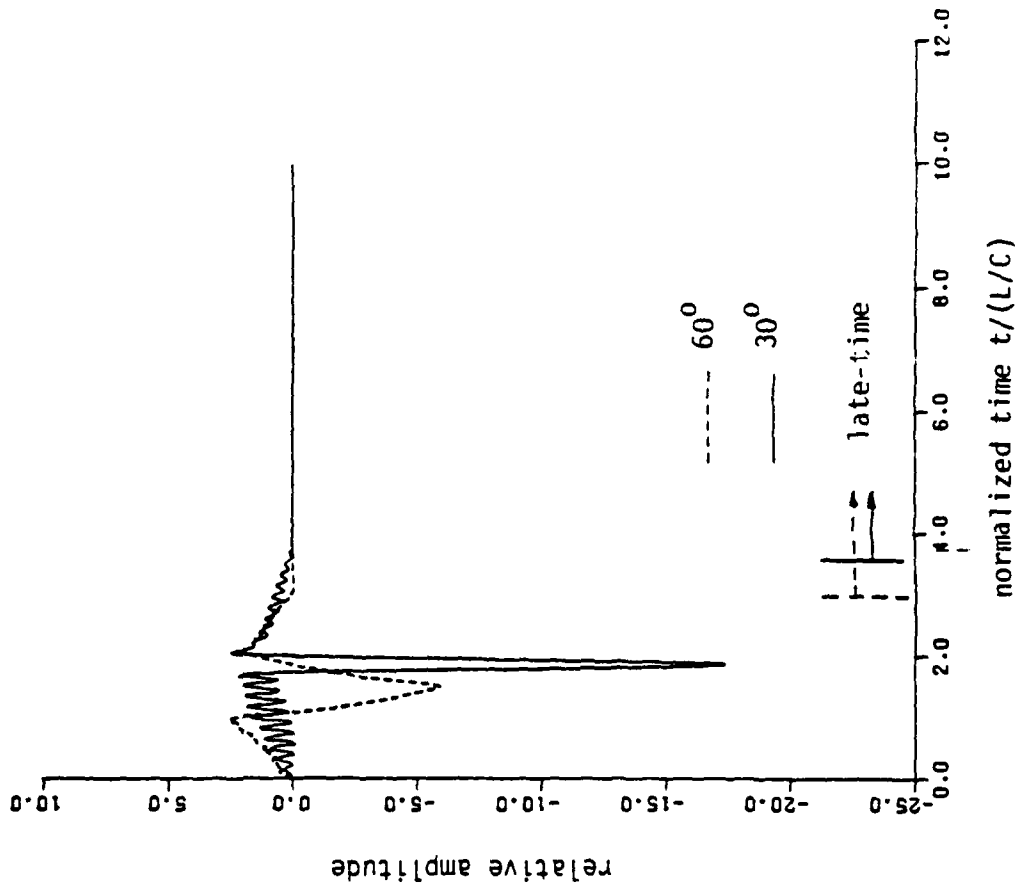
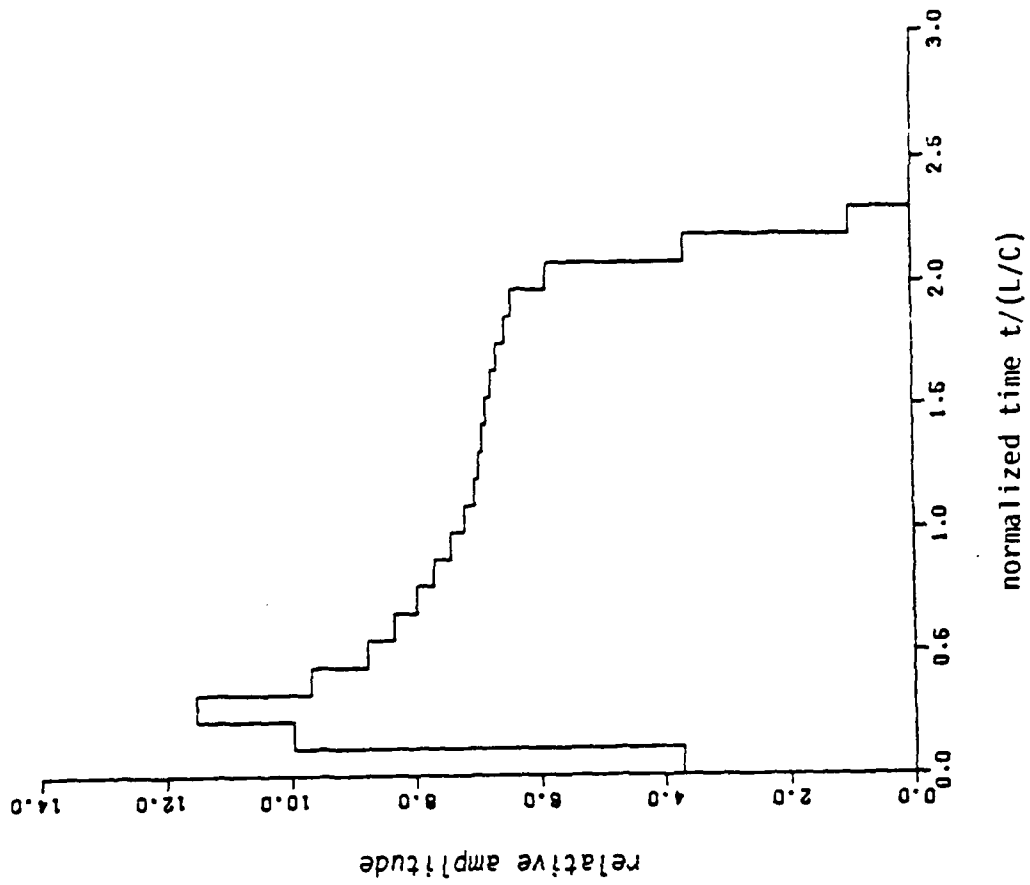
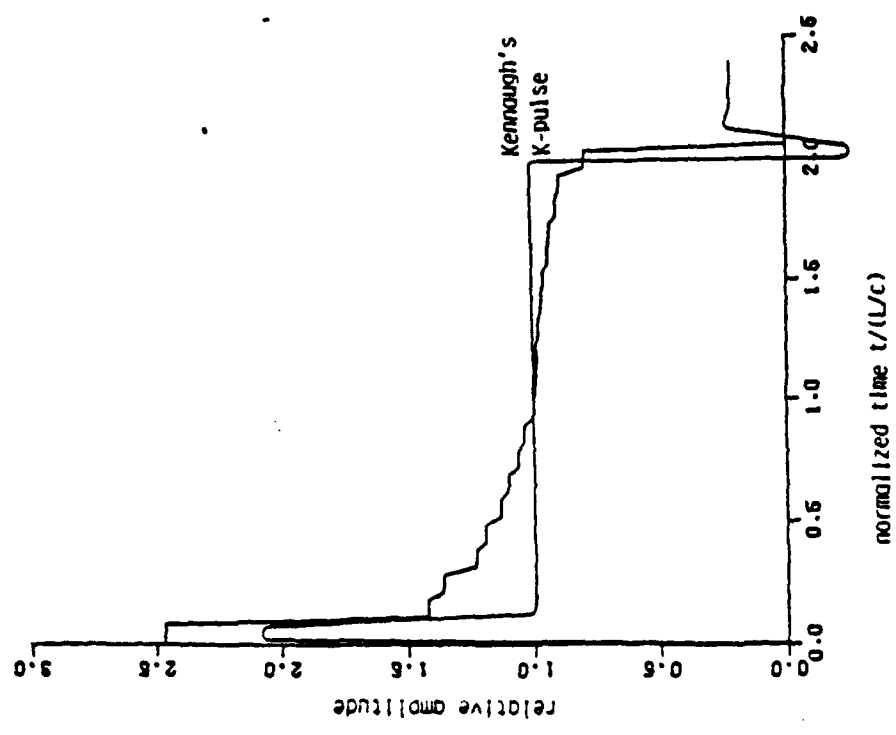


Figure 6 Convolution of ten mode natural E-pulse with 30° and 60° ten mode impulse responses showing null late-time response.

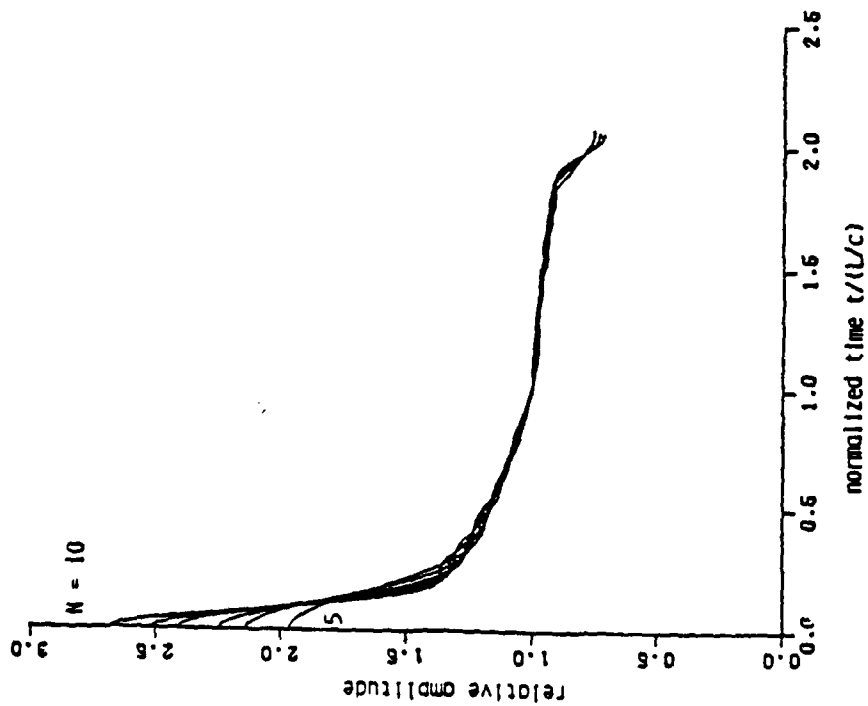


(a)

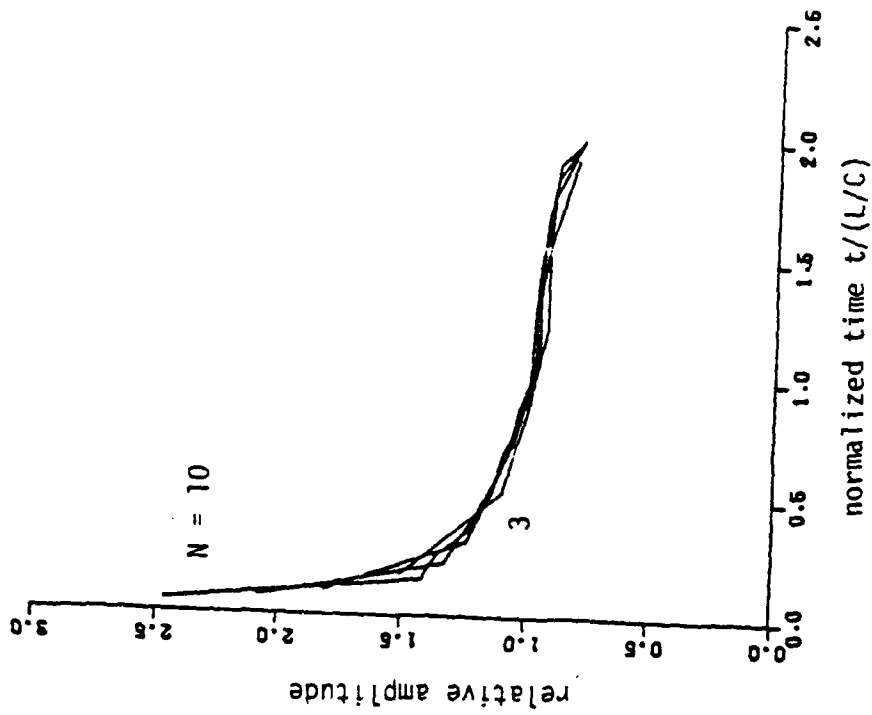


(b)

Figure 5 Pulse function based E-pulse synthesized to eliminate first ten modes of thin cylinder target.
 (a) Natural E-pulse compared to Kennough's K-pulse;
 (b) Forced E-pulse of duration $T_e = 2.3 L/c$.



(a)



(b)

Figure 7 Natural E-pulse constructed using (a) Fourier cosine basis functions to eliminate 5, 6, 7, 8, 9, and 10 modes; (b) pulse function basis functions to eliminate 3, 5, 7, and 10 modes.

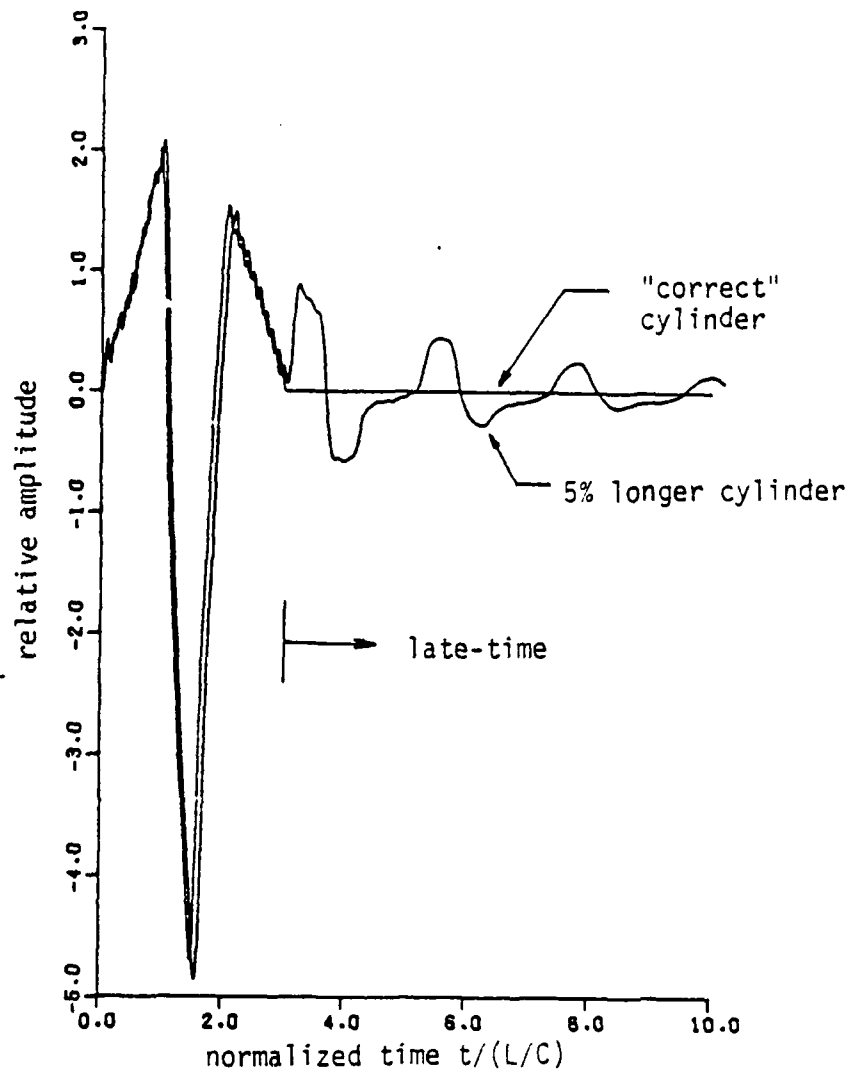


Figure 8 Convolution of 10 mode natural thin cylinder E-pulse with 60° thin cylinder impulse response and 60° response of a cylinder 5% longer.

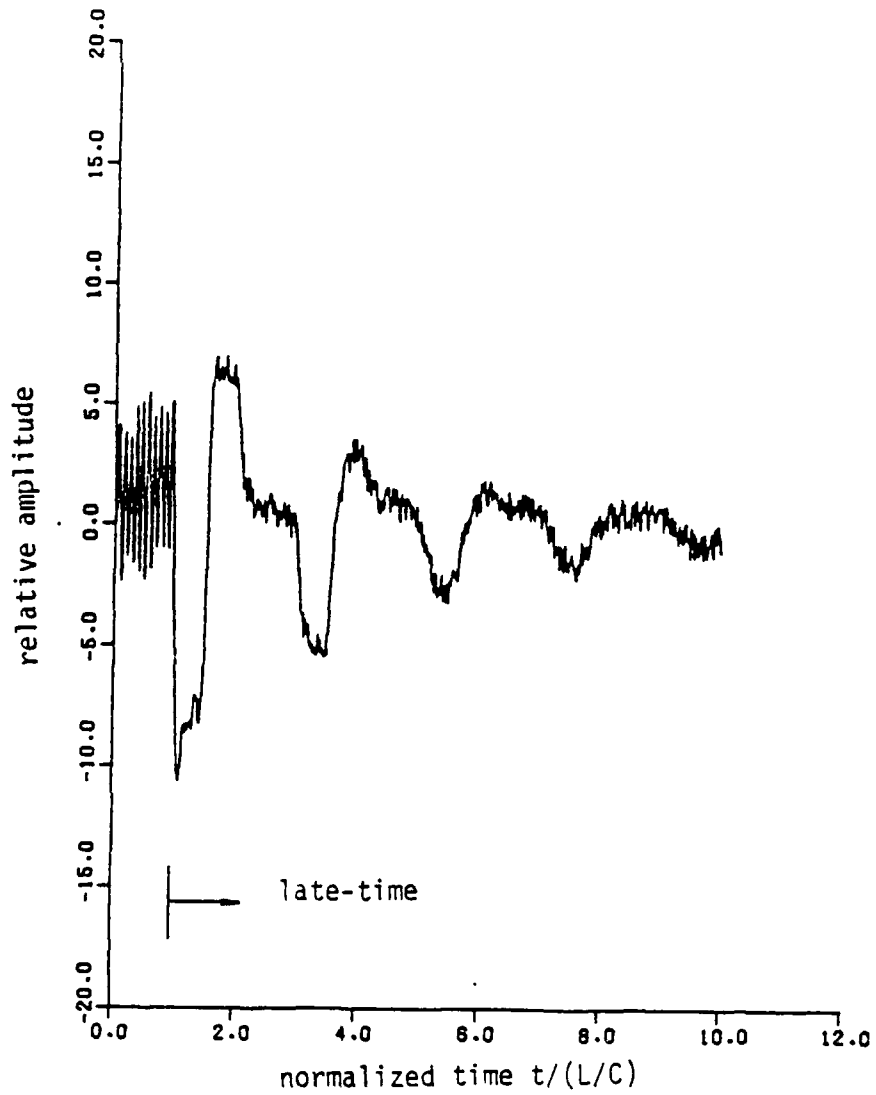


Figure 9 Thin cylinder 60° impulse response generated from first ten natural modes, with 10% random noise added.

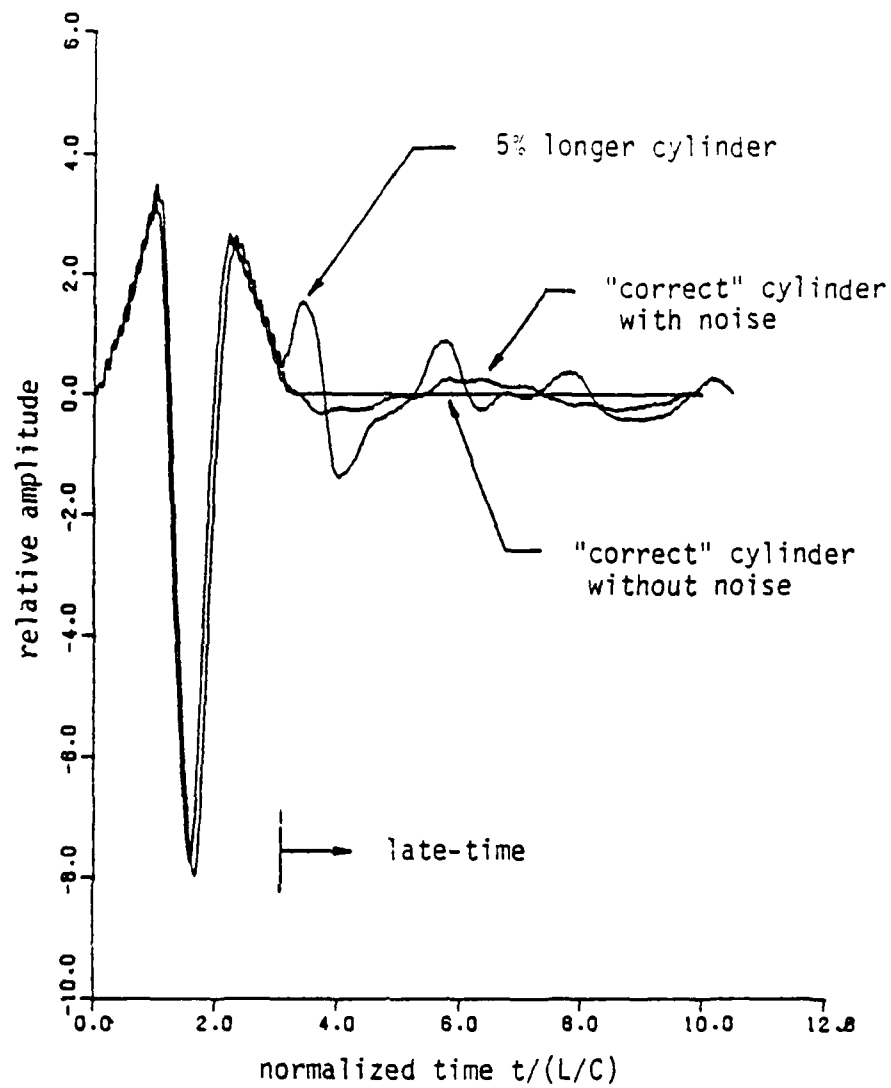


Figure 10 Convolution of natural ten mode E-pulse with noisy ten mode 60° impulse response.

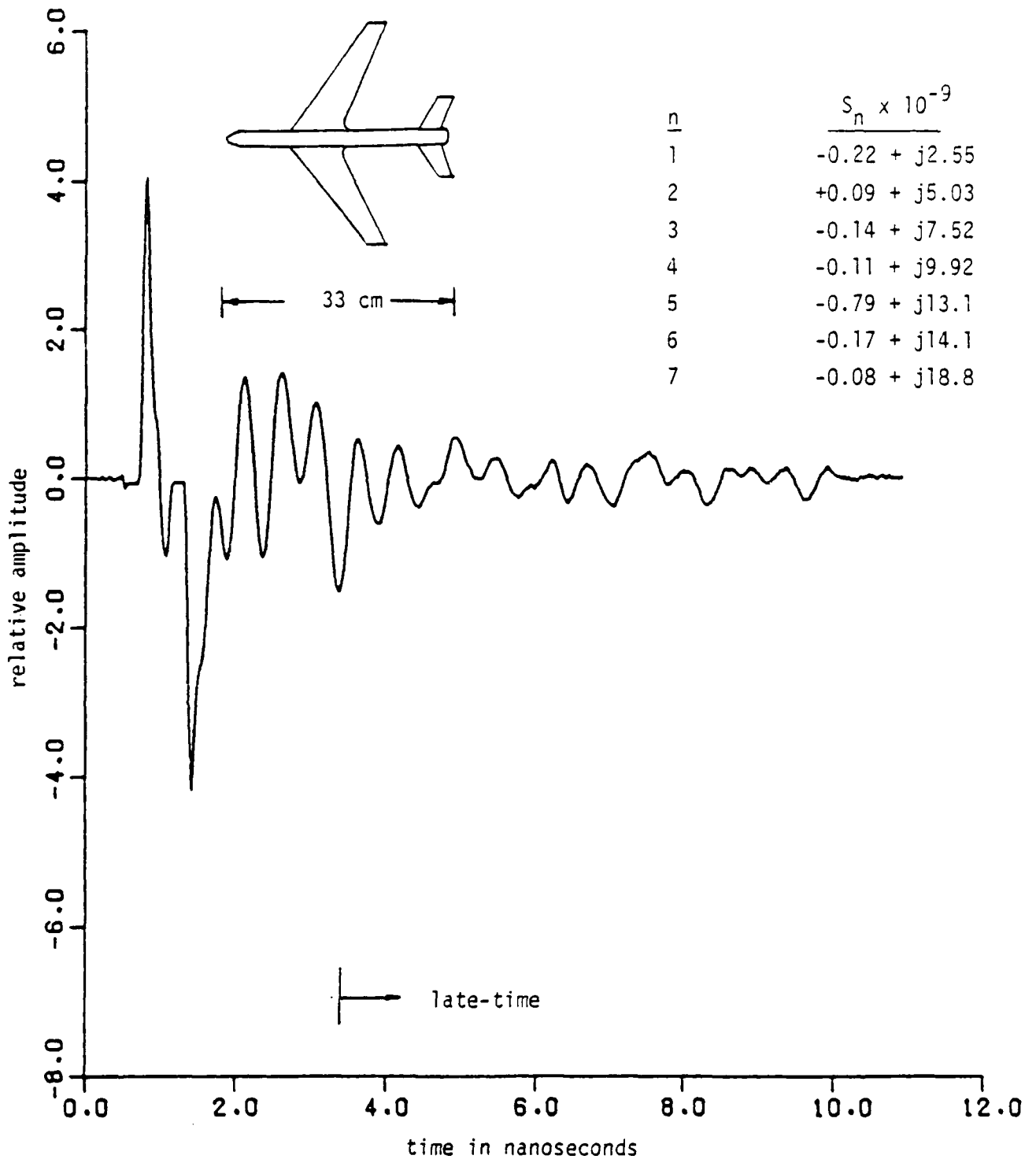


Figure 11 Measured response of a Boeing 707 aircraft model and seven dominant natural frequencies.

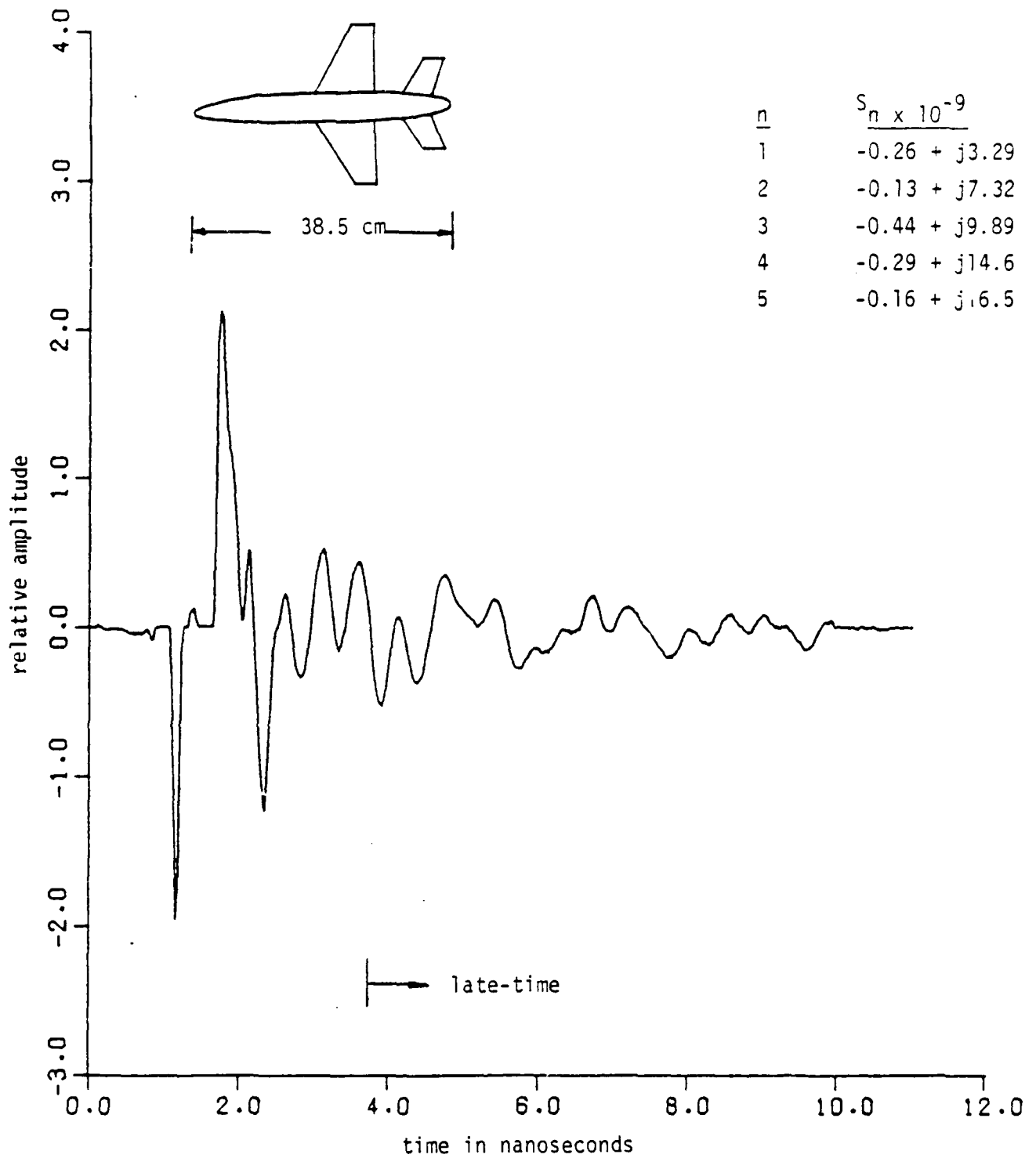


Figure 12 Measured response of a McDonnell Douglas F-18 aircraft model and five dominant natural frequencies.

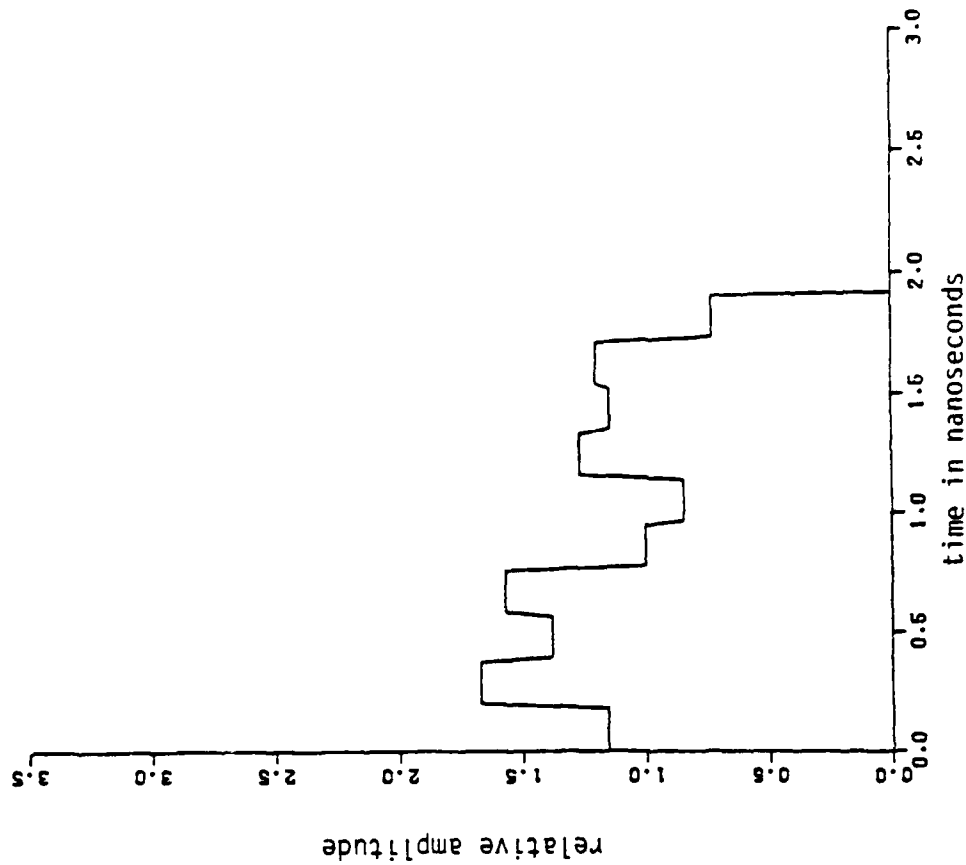


Figure 14 Natural E-pulse constructed to eliminate the five dominant modes in the F-18 measured response.

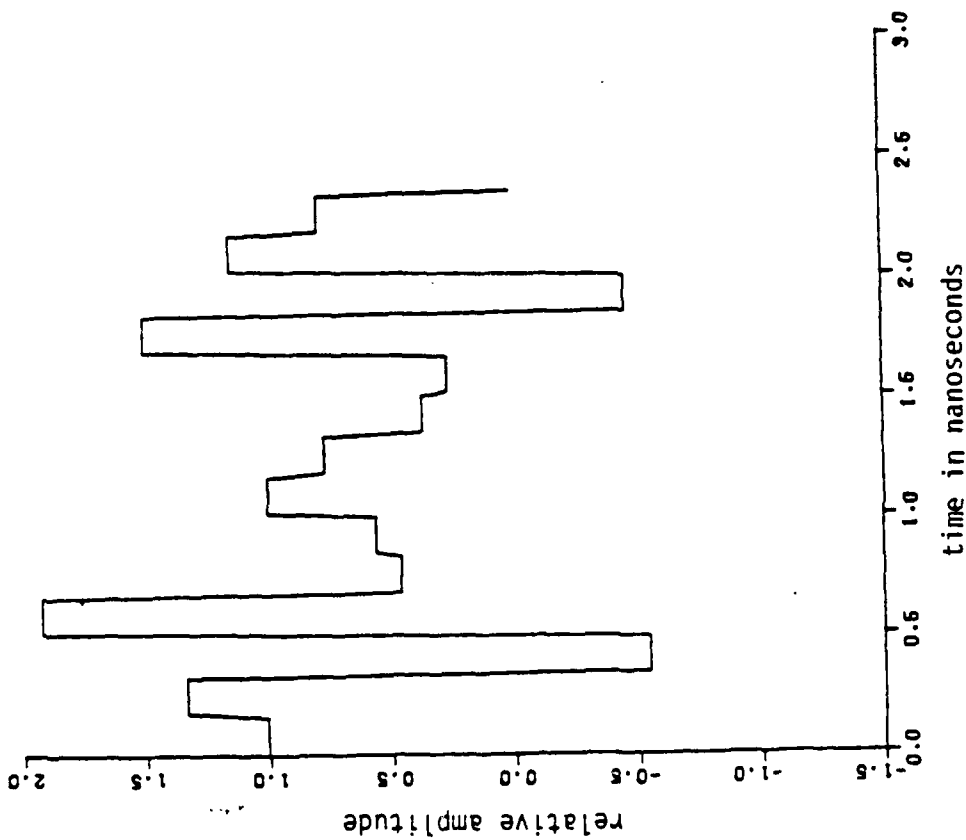


Figure 13 Natural E-pulse constructed to eliminate the seven dominant modes in the 707 measured response.

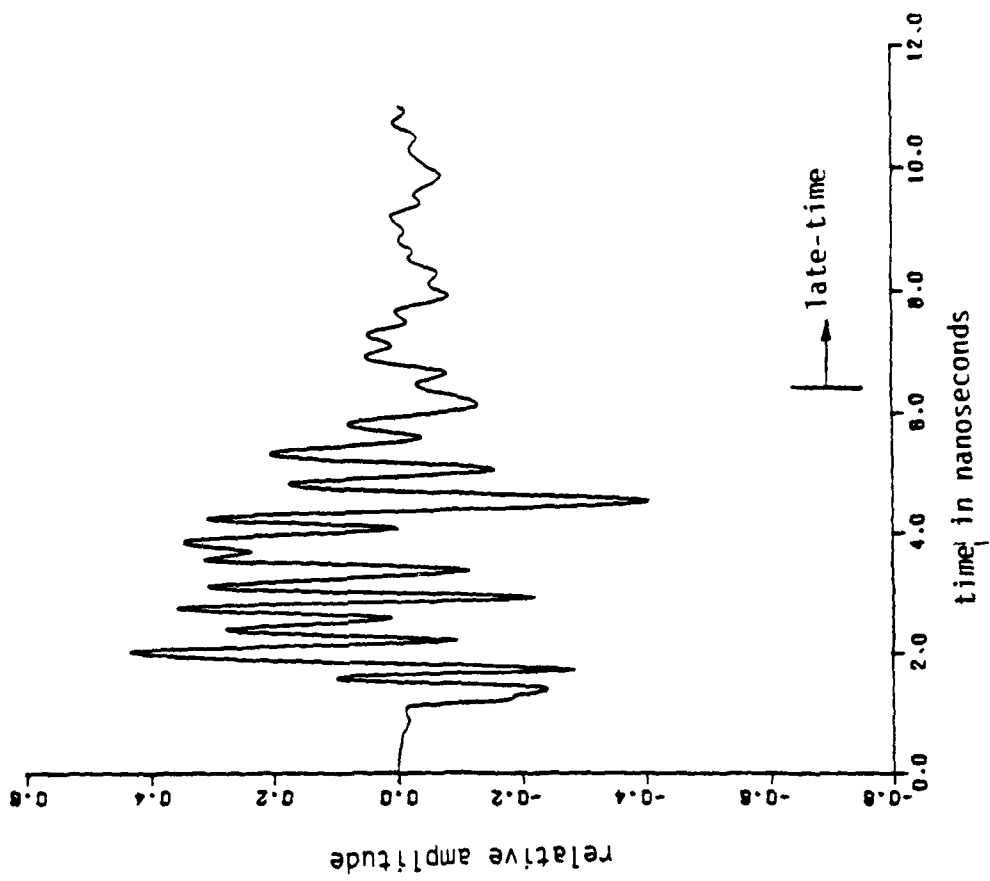


Figure 16 Convolution of the 707 E-pulse with the F-18 measured response.

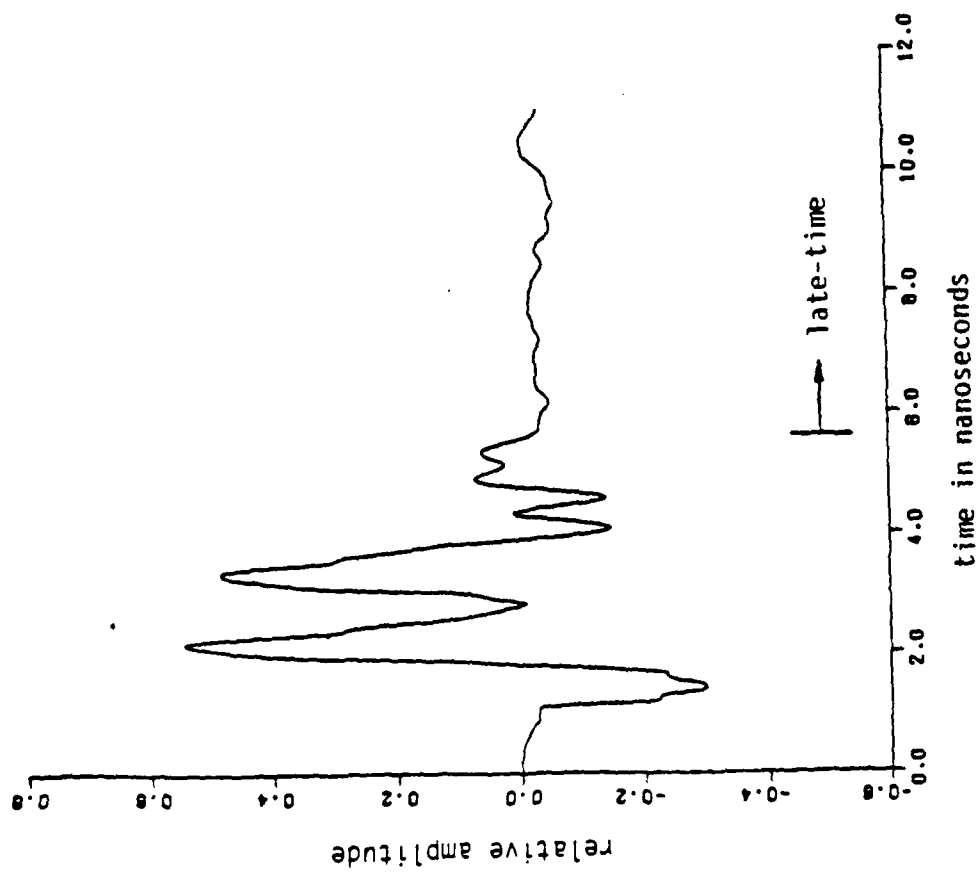


Figure 15 Convolution of the F-18 E-pulse with the F-18 measured response showing "extinguished" late-time region.

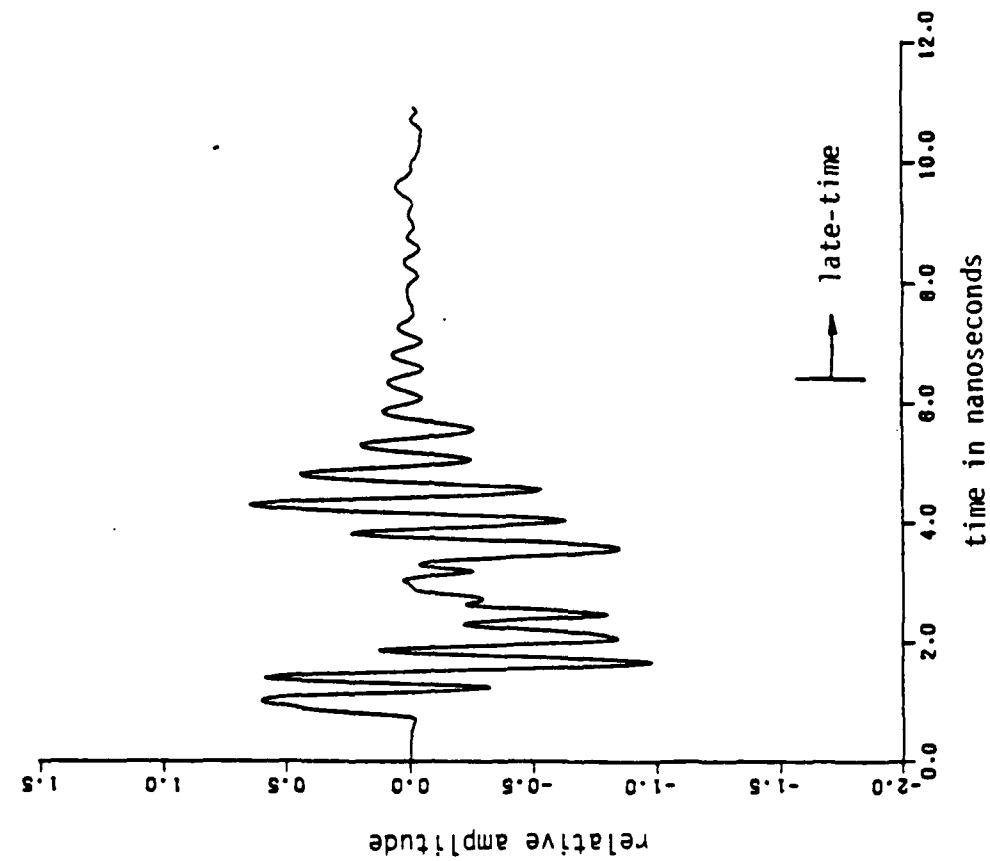


Figure 17 Convolution of the 707 E-pulse with the 707 measured response showing "extinguished" late-time region.

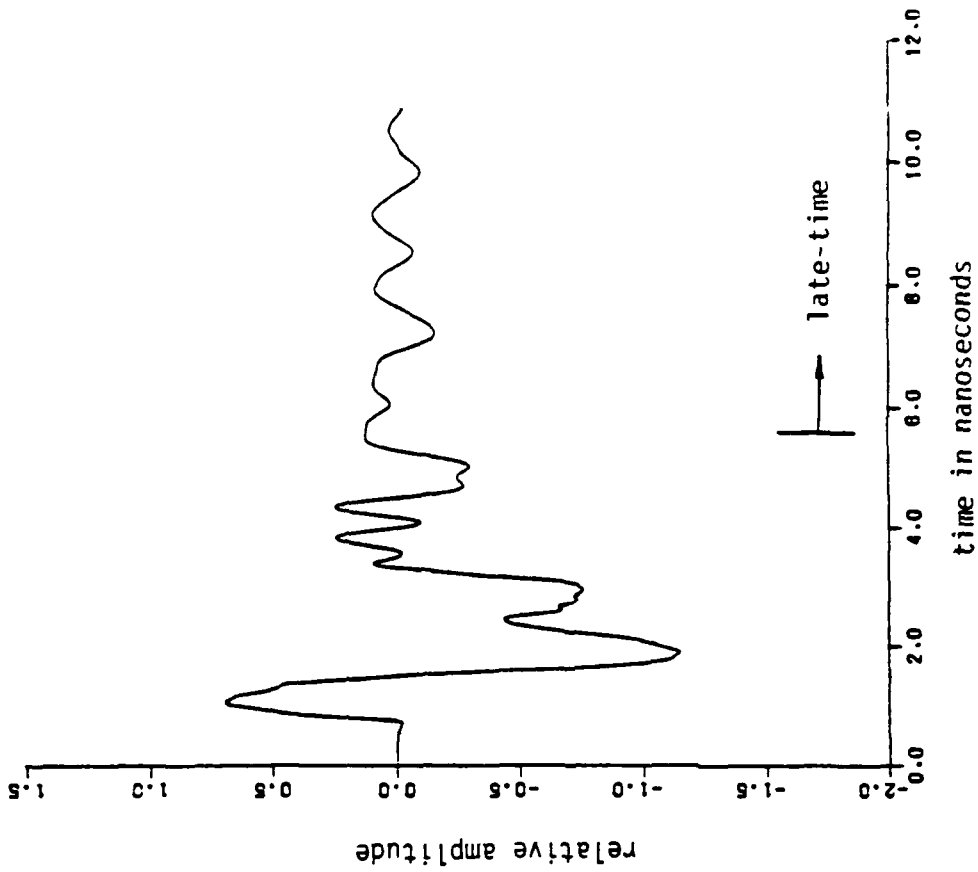


Figure 18 Convolution of the F-18 E-pulse with the 707 measured response.

2.3 FREQUENCY DOMAIN E-PULSE SYNTHESIS AND TARGET DISCRIMINATION

ABSTRACT

A frequency domain approach to the E-pulse radar target discrimination scheme is introduced. This approach is shown to allow easier interpretation of E-pulse convolutions via the E-pulse spectrum, and leads to a simplified calculation of pulse basis function amplitudes in the E-pulse expansion. Experimental evidence obtained using aircraft models verifies the single-mode discrimination scheme, as well as the aspect-independent nature of the E-pulse technique. This leads to an integrated technique for target discrimination combining the E-pulse with single mode extraction waveforms.

I. INTRODUCTION

The time-domain scattered field response of a conducting target has been observed to be composed of an early-time forced period, when the excitation field is interacting with the scatterer, followed immediately by a late-time period during which the target oscillates freely [1], [2]. The late-time portion can be decomposed into a finite sum of damped sinusoids (excited by an incident field waveform of finite usable bandwidth), oscillating at frequencies determined purely by target geometry. The natural resonance behavior of the late-time portion of the scattered field response can be utilized to provide an aspect-independent means for radar target discrimination [3-7].

An extinction pulse (E-pulse) is defined as a finite duration waveform which, upon interaction with a particular target, eliminates a pre-selected portion of the target's natural mode spectrum. By basing E-pulse synthesis on the target natural frequencies, the E-pulse waveform is made aspect-independent.

Discrimination is accomplished by convolving an E-pulse waveform with the measured late-time scattered field response of a target. If the scattered field is from the anticipated target, the convolved response will be composed of an easily interpreted portion of the expected natural mode spectrum. If the target is different from that expected, a portion of its dissimilar natural mode spectrum will be extracted, resulting in an unexpected convolved response.

This paper will consider the construction of two types of E-pulse waveforms. The first is designed to eliminate the entire finite expected natural mode spectrum of the target, and the second to extract just a single mode.

Both time and frequency domain analyses will be used to develop a set of defining E-pulse equations. The frequency domain approach will be shown to be of significant value not only for providing a much more convenient way of viewing E-pulse discrimination, but also for constructing certain E-pulse waveforms.

Lastly, experimental results using aircraft models will be presented, demonstrating single mode discrimination and verifying the aspect independence of the E-pulse technique.

II. TIME DOMAIN SYNTHESIS

Assume that the measured time domain scattered field response waveform of a conducting radar target can be written during the late-time period as a finite sum of damped sinusoids

$$r(t) = \sum_{n=1}^N a_n e^{\sigma_n t} \cos(\omega_n t + \phi_n) \quad t > T_\ell \quad (1)$$

where a_n and ϕ_n are the aspect dependent amplitude and phase of the n 'th mode, T_ℓ describes the beginning of late-time, and only N modes are assumed to be excited by the incident field waveform. Then, the convolution of an E-pulse waveform $e(t)$ with the measured response waveform becomes

$$c(t) = e(t) * r(t) = \int_0^{T_e} e(t') r(t-t') dt'$$

$$= \sum_{n=1}^N a_n e^{\sigma_n t} \left[A_n \cos(\omega_n t + \phi_n) + B_n \sin(\omega_n t + \phi_n) \right] \quad t > T_L = T_\ell + T_e \quad (2)$$

where

$$\begin{Bmatrix} A_n \\ B_n \end{Bmatrix} = \int_0^{T_e} e(t') e^{-\gamma_n t'} \begin{Bmatrix} \cos \omega_n t' \\ \sin \omega_n t' \end{Bmatrix} dt' \quad (3)$$

and T_e is the finite duration of $e(t)$.

Two interesting waveforms are now considered. Constructing $e(t)$ to result in $c(t)=0, t>T_L$, requires

$$A_n = B_n = 0 \quad 1 \leq n \leq N \quad (4)$$

This approach was considered in [3]. In addition, $e(t)$ can also be constructed so that $c(t)$ is composed of just a single mode. In this case $e(t)$ is termed a "single mode extraction signal," as discussed in [5-7]. If the specific value of the phase constant of $c(t)$ is unimportant, $e(t)$ can be synthesized by demanding

$$A_n = B_n = 0 \quad 1 \leq n \leq N, \quad n \neq m \quad (5)$$

to excite the m 'th natural mode. On the other hand, requiring

$$\begin{aligned} A_n = B_n = 0 & \quad 1 \leq n \leq N, \quad n \neq m \\ A_m = 0 & \end{aligned} \quad (6)$$

results in

$$c(t) = c_s(t) = a_m e^{\sigma_m t} B_m \sin(\omega_m t + \phi_m) \quad (7)$$

and requiring

$$\begin{aligned} A_n = B_n = 0 & \quad 1 \leq n \leq N, \quad n \neq m \\ B_m = 0 & \end{aligned} \quad (8)$$

yields

$$c(t) = c_c(t) = a_m e^{\sigma_m t} A_m \cos(\omega_m t + \phi_m) \quad (9)$$

The E-pulse resulting from (5) is termed a "sin/cos" single mode extraction

waveform, since $c(t)$ contains both sine and cosine components. Similarly, (6) results in a "sine" and (8) a "cosine" single mode extraction waveform. With the proper normalization of $e(t)$ (giving $A_m = B_m$), the convolved waveforms (7) and (9) can be combined to yield plots of the m 'th mode frequencies versus time, via

$$\omega_m t + \phi_m = \tan^{-1} \frac{c_s(t)}{c_c(t)} \quad (10)$$

$$\sigma_m t + \log |a_m A_m| = \frac{1}{2} \log [c_c^2(t) + c_s^2(t)]$$

III. FREQUENCY DOMAIN SYNTHESIS

The convolution of the E-pulse waveform with the measured response waveform can also be written in the form

$$c(t) = \sum_{n=1}^N a_n |E(s_n)| e^{\sigma_n t} \cos(\omega_n t + \psi_n) \quad t > T_L \quad (11)$$

where

$$E(s) = \mathcal{L} \{ e(t) \} = \int_0^T e(t) e^{-st} dt \quad (12)$$

is the Laplace transform of the E-pulse waveform, and

$$\psi_n = \phi_n + \tan^{-1} \left(-\frac{E_{in}}{E_{rn}} \right) \quad (13)$$

where

$$E_{in} = \text{Im} \left\{ E(s_n) \right\} \quad E_{rn} = \text{Re} \left\{ E(s_n) \right\} \quad (14)$$

Now, $c(t)=0$ for $t>T_L$ requires

$$E_{in} = E_{rn} = 0 \quad 1 \leq n \leq N \quad (15)$$

or, equivalently,

$$E(s_n) = E(s_n^*) = 0 \quad 1 \leq n \leq N \quad (16)$$

In addition, a sin/cos m 'th mode extraction waveform can be synthesized via

$$E(s_n) = E(s_n^*) = 0 \quad 1 \leq n \leq N, \quad n \neq m \quad (17)$$

while a sine m 'th mode extraction waveform requires

$$E(s_n) = E(s_n^*) = 0 \quad 1 \leq n \leq N, \quad n \neq m \quad (18)$$

$$E(s_m) = -E(s_m^*)$$

and a cosine m 'th mode extraction waveform necessitates

$$E(s_n) = E(s_n^*) = 0 \quad 1 \leq n \leq N, \quad n \neq m \quad (19)$$

$$E(s_m) = E(s_m^*)$$

It is easily shown that the frequency domain and time domain requirements for synthesizing an E-pulse are identical. By expanding the exponential in (12), one can show that (17), (18), and (19) are equivalent to (5), (6), and (8), respectively.

A significant benefit of using a frequency domain approach comes via the increased intuition allowed by equation (11). When an E-pulse waveform is convolved with the measured response of an unexpected target, the amplitudes of the resulting natural mode components are determined by evaluating the magnitude of the spectrum of $e(t)$ at the natural frequencies of the target (a result of the Cauchy residue theorem). Thus, the E-pulse spectrum becomes the key tool in predicting the success of E-pulse discrimination.

IV. E-PULSE SYNTHESIS USING FREQUENCY DOMAIN APPROACH

To implement the E-pulse requirements, it becomes necessary to represent the waveform mathematically. Let $e(t)$ be composed of two components

$$e(t) = e^f(t) + e^e(t) \quad (20)$$

Here $e^f(t)$ is a forcing component which excites the target, and $e^e(t)$ is an extinction component which extinguishes the response due to $e^f(t)$. The forcing component is chosen freely, while the extinction component is determined by first expanding in a set of basis functions

$$e^e(t) = \sum_{m=1}^M \alpha_m f_m(t) \quad (21)$$

and then employing the appropriate E-pulse conditions from section III. For an E-pulse designed to extinguish all of the modes of the measured response, using (16) results in the matrix equation

$$\begin{bmatrix} F_1(s_1) & F_2(s_1) & \dots & F_M(s_1) \\ \vdots & \vdots & & \vdots \\ F_1(s_N) & F_2(s_N) & \dots & F_M(s_N) \\ F_1(s_{1^*}) & F_2(s_{1^*}) & \dots & F_M(s_{1^*}) \\ \vdots & \vdots & & \vdots \\ F_1(s_{N^*}) & F_2(s_{N^*}) & \dots & F_M(s_{N^*}) \end{bmatrix} \begin{bmatrix} \alpha_1 \\ \alpha_2 \\ \vdots \\ \alpha_M \end{bmatrix} = \begin{bmatrix} -E^f(s_1) \\ \vdots \\ -E^f(s_N) \\ -E^f(s_{1^*}) \\ \vdots \\ -E^f(s_{N^*}) \end{bmatrix} \quad (22)$$

where

$$\begin{aligned} F_m(s) &= \mathcal{L} \{ f_m(t) \} \\ E^f(s) &= \mathcal{L} \{ e^f(t) \} \end{aligned} \quad (23)$$

and $M=2N$ is chosen to make the matrix square. Similar equations can be constructed to accommodate the requirements given by (17), (18) or (19).

As in [3], two types of E-pulses can be easily identified. When $e^f(t) \neq 0$, the forcing vector on the right hand side of (22) is nonzero, and solutions for the basis function amplitudes exist for any choice of E-pulse duration, T_e , which does not cause the matrix to be singular. In contrast, when $e^f(t) = 0$ the matrix equation becomes homogeneous, and solutions for $e^e(t)$ exist only for specific durations T_e , which are calculated by solving for the zeroes of the determinantal equation. The former type of E-pulse is termed "forced" and the latter "natural." Since a natural E-pulse has no forcing component, it is viewed as extinguishing its own excited response.

The frequency domain approach makes it possible to visualize an improved E-pulse waveform whose spectrum has been shaped to accentuate the response of a known target. For example, by using damped sinusoids or Fourier cosines as basis functions in the E-pulse expansion, it is possible to concentrate the energy of the E-pulse near pre-chosen frequencies, and enhance the single mode response of a particular target [4].

V. CALCULATION OF PULSE BASIS FUNCTION AMPLITUDES

A very useful application of the frequency domain approach results from using subsectional basis functions in (21). Let

$$f_m(t) = \begin{cases} g(t - [m-1]\Delta) & (m-1)\Delta \leq t \leq m\Delta \\ 0 & \text{elsewhere} \end{cases} \quad (24)$$

$$t_m = (-1)^m P_{(2N-1) - (m-1)} \quad (29)$$

where P_{n-i} is the sum of the products $n-i$ at a time, without repetitions, of the quantities $z_1, z_1^*, z_2, \dots, z_N^*$.

Note that $g(t)$ does not appear in this analysis, and thus the resulting pulse amplitudes are independent of the individual pulse shapes. However, when discriminating between different targets, $g(t)$ manifests itself through the term $F_1(s)$.

VI. EXPERIMENTAL RESULTS

This section will address two important topics. First, discrimination between two similar aircraft models will be demonstrated using single mode extraction waveforms. Second, the aspect independence of the E-pulse technique will be confirmed using the same two models.

The measured near field responses of simplified McDonnell Douglas F-18 and Boeing 707 aircraft models have been published previously [3]. The models are constructed of aluminum, and are shown in Fig. 1. The dominant natural frequencies have been extracted from the late-time portions of the responses using a continuation method [10]. With these, pulse function based natural sine and cosine single mode extraction waveforms of minimum duration can be constructed using equations (18) and (19) together with (24) to extract the first and fourth modes of the 707. The first mode waveforms are shown in Figure 2. Discrimination between the F-18 and the 707 can be accomplished by convolving the E-pulse waveforms with each of the measured aircraft responses. If the E-pulses are convolved with the expected (707) response, the result should be either a pure first or fourth mode damped sinusoid. If the E-pulses are convolved with the unexpected (F-18) response, the result will be an

unrecognizable conglomeration of the modes of the unexpected target.

Figures 3-6 show the results of convolving the 707 E-pulses with both the 707 and F-18 responses. These frequency plots are obtained from the actual convolved waveforms by using equation (10). The dotted lines represent the slopes of the expected first or fourth mode frequencies. It is seen that the frequency plots for the expected target (Figs 3 and 4) parallel the expected frequency lines in the late-time, while those for the unexpected target (Figs 5 and 6) do not. Thus, the 707 and the F-18 are easily discriminated.

It is also quite important to verify experimentally the aspect independence of the E-pulse technique. To accomplish this, measurements have been made of the near field pulse response of the 707 and F-18 models with the fuselage axes aligned at various angles with respect to the transmitting/receiving antenna configuration. Two natural rectangular pulse based E-pulses of minimum duration, one designed to eliminate all of the modes detected in the 707 responses and one designed to eliminate all the modes in the F-18 responses, are then constructed according to equations (28) and (29).

Convolution of the 707 and F-18 E-pulses with each of the measured aircraft responses yields the results shown in Figs 7-10. It is apparent from Fig. 7 that convolving the F-18 E-pulse with the measured F-18 response gives a waveform with negligible amplitude in the late-time, regardless of the aspect angle. Similar results are obtained in Figure 8 when the 707 E-pulse is convolved with the 707 measured response. In contrast, Figs. 9 and 10 reveal that when the 707 E-pulse is convolved with any F-18 response, or when the F-18 E-pulse is convolved with any 707 response, the late-time portion of the resulting waveform has significant amplitude. Thus, discrimination between the two aircraft models is possible regardless of the target aspect.

The experimental results suggest the feasibility of an E-pulse target

discrimination scheme which utilizes both a waveform designed to eliminate all the modes of a target and a set of waveforms designed to extract various individual target modes. This technique integrates the single mode extraction concept and the usual E-pulse technique into a scheme which has a greater potential for accurate target discrimination decisions.

VII. CONCLUSIONS

The E-pulse radar target discrimination concept has been expanded upon, incorporating single mode extraction waveforms into an integrated technique. Both time and frequency domain analyses have been included, and their equivalence demonstrated. The frequency domain viewpoint is helpful for interpreting E-pulse discrimination, and it has been applied to pulse basis function amplitude calculation.

Experimental results obtained using aircraft models have demonstrated the validity of radar target discrimination based on single mode extraction waveforms. Most importantly, experimental evidence has also shown the E-pulse technique to be successful regardless of target aspect angle. This aspect-independence of the E-pulse concept is fundamental for its application to practical situations.

References

1. Pearson, L.W., "A Note on the Representation of Scattered Fields as a Singularity Expansion," IEEE Trans. Ant. Prop., Vol. AP-32, pp. 520-524, May 1984.
2. Felsen, L.B., "Comments on Early Time SEM," IEEE Trans. Ant. Prop., Vol. AP-33, pp. 118-119, January 1985.
3. Rothwell, E., Nyquist, D.P., Chen, K.M., and Drachman, B., "Radar Target Discrimination Using the Extinction-Pulse Technique," IEEE Trans. Ant. Prop., Vol. AP-33, pp. 929-937, September 1985.
4. Rothwell, E., "Radar Target Discrimination Using the Extinction-Pulse Technique," Doctoral Dissertation, Michigan State University, June 1985.
5. Chen, K.M., Nyquist, D., Rothwell, E., Webb, L., and Drachman, B., "Radar Target Discrimination by Convolution of Radar Return with Extinction-pulses and Single-Mode Extraction Signals, to appear in IEEE Trans. Ant. Prop., Spring 1986.
6. Chen, K.M., and Westmoreland, D., "Radar Waveform Synthesis for Exciting Single-Mode Backscatters from a Sphere and Application for Target Discrimination," Radio Science, Vol. 17, pp. 574-588, June 1982.
7. Chen, K.M., Nyquist, D.P., Westmoreland, D., Chuang, C.I., and Drachman, B., "Radar Waveform Synthesis for Single-Mode Scattering by a Thin Cylinder and Application for Target Discrimination," IEEE Trans. Ant. Prop., Vol. AP-30, pp. 867-880, September 1982.
8. Hanus, P.H., *Theory of Determinants*, Ginn and Co., Boston, 1886.
9. Muir, T., *A Treatise on the Theory of Determinants*, Dover, N.Y., 1960.
10. Drachman, B., and Rothwell, E., "A Continuation Method for Identification of the Natural Frequencies of an Object Using a Measured Response," IEEE Trans. Ant. Prop., Vol. AP-33, pp. 445-450, April 1985.



Fig. 1. Aluminum aircraft models of Boeing 707 (left) and McDonnell-Douglas F-18 used in the experiment. Note that the models are not to the same scale, but rather are of similar physical size.

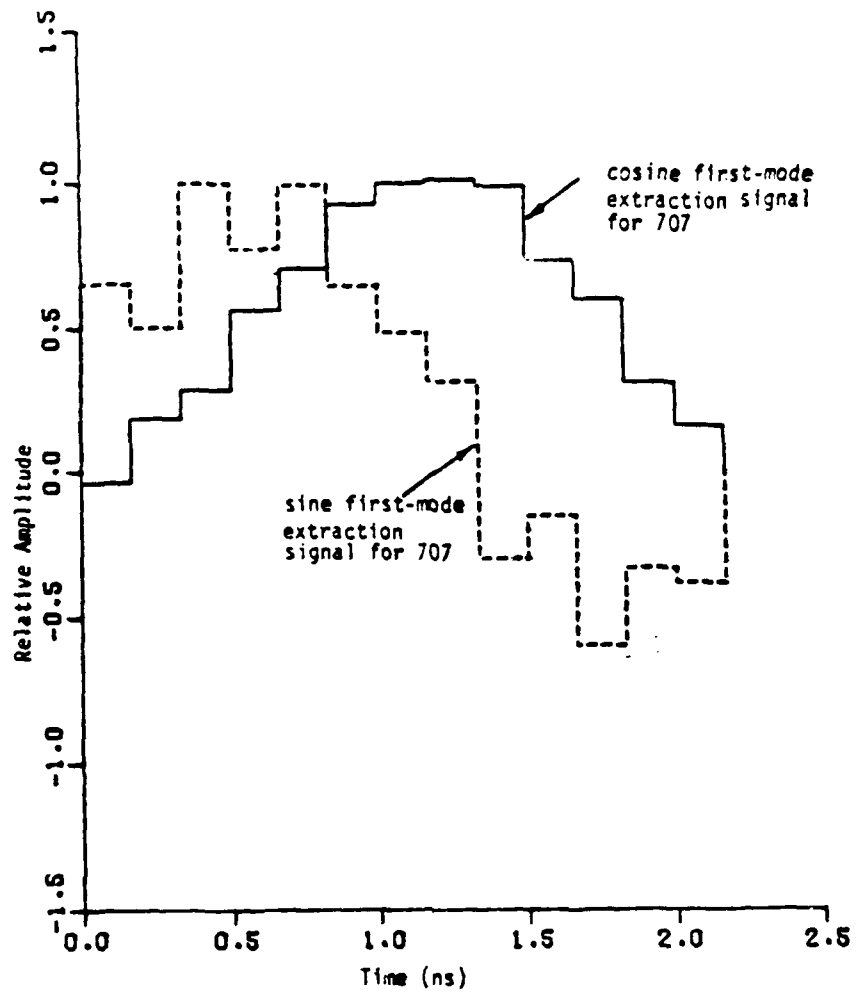


Fig. 2. Natural rectangular pulse function based first mode extraction waveforms for the Boeing 707 aircraft model.

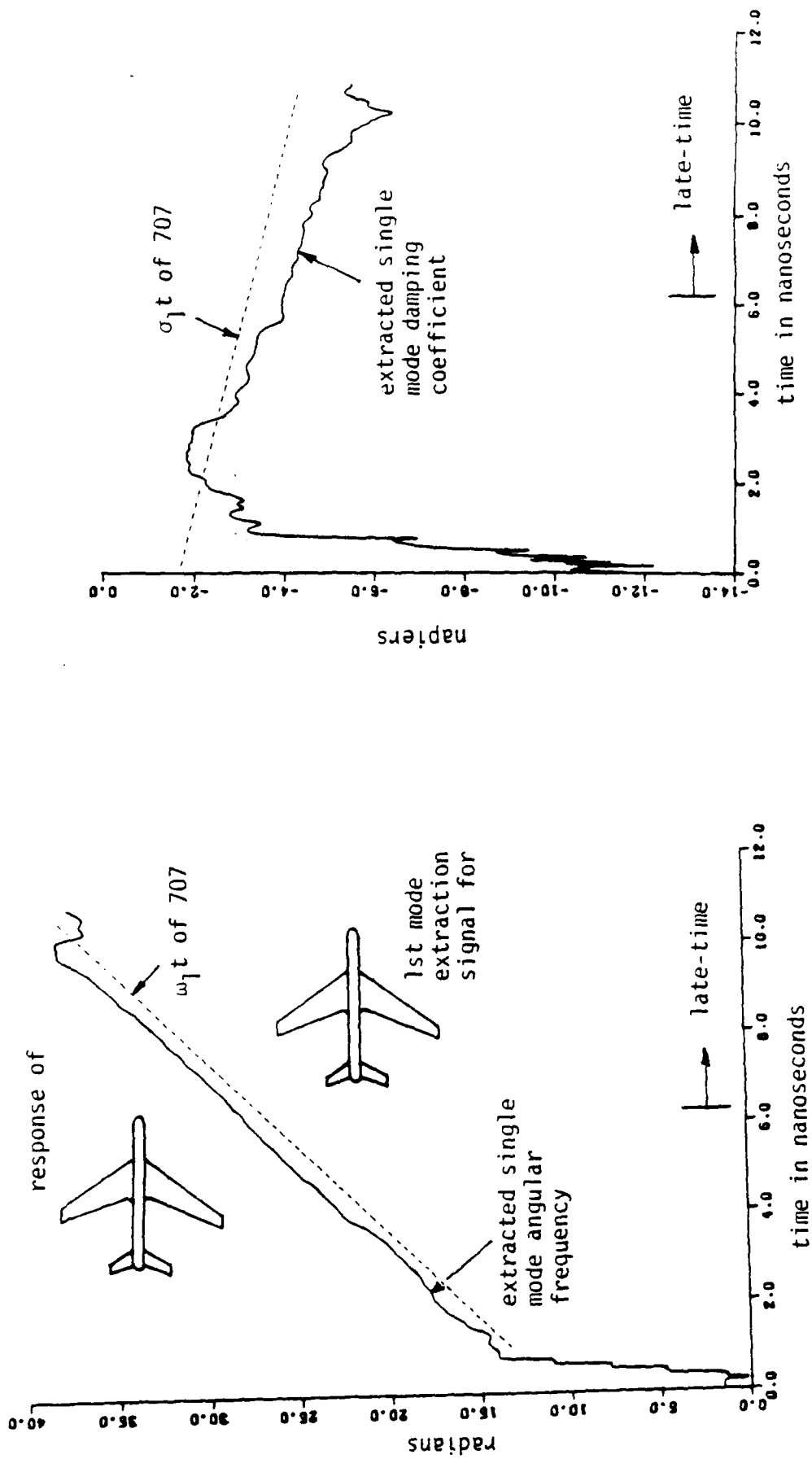


Fig. 3. Single mode angular frequency and damping coefficient extracted from the convolved outputs of the first mode extraction signals for the 707 target and the 707 measured response.

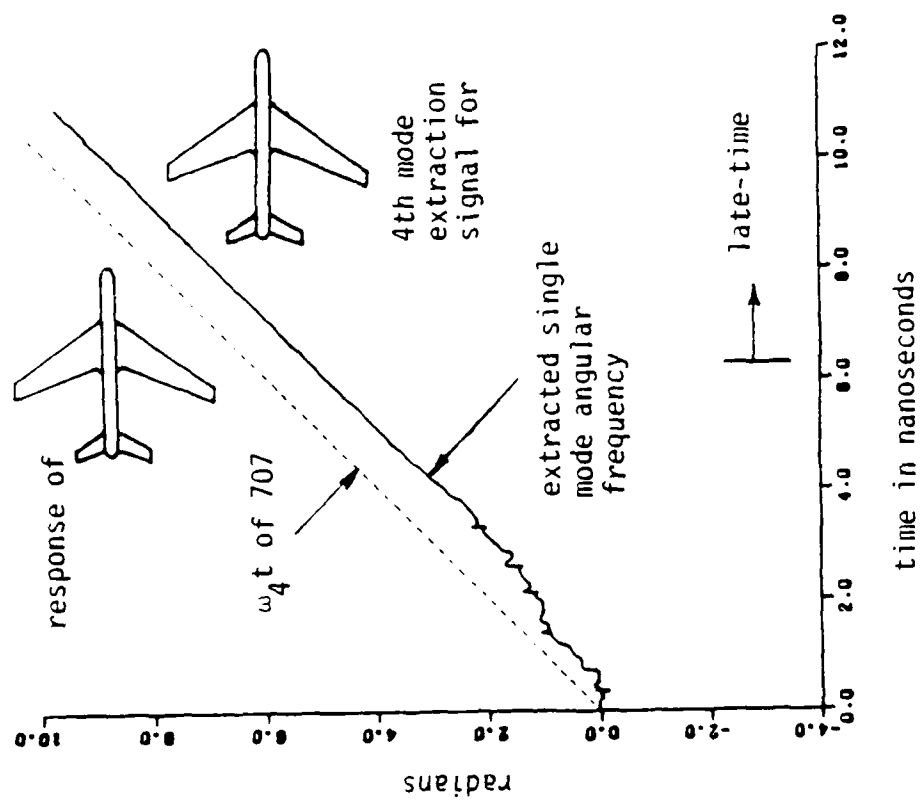
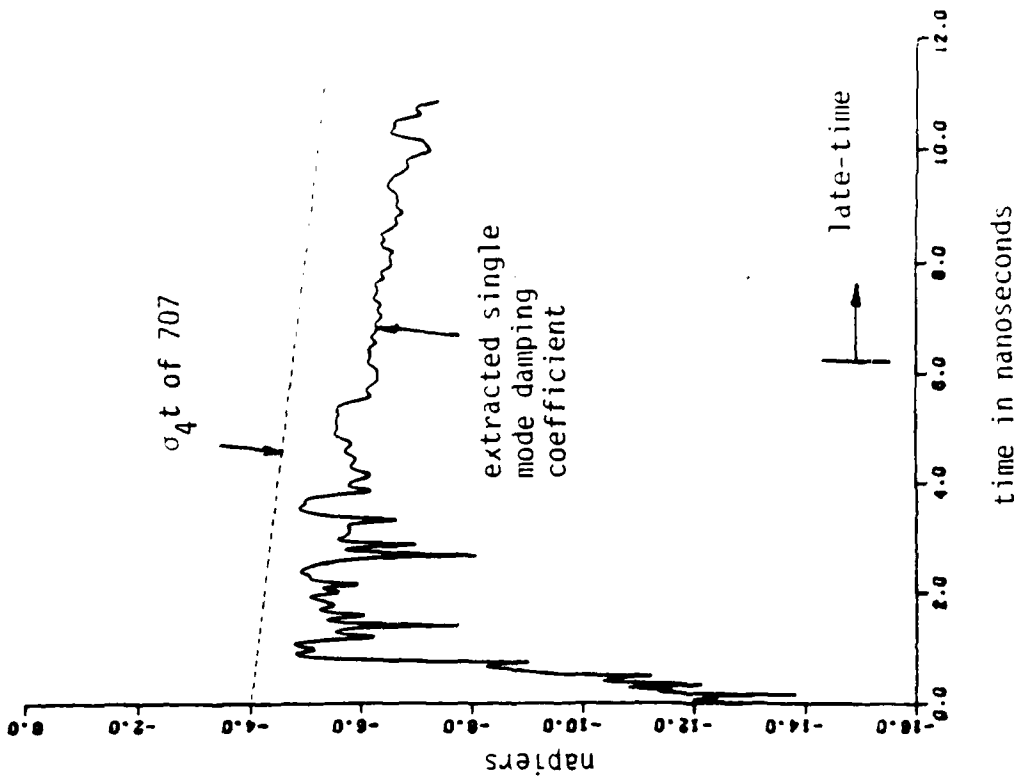


Fig. 4. Single mode angular frequency and damping coefficient extracted from the convolved outputs of the fourth mode extraction signals for the 707 target and the 707 measured response.

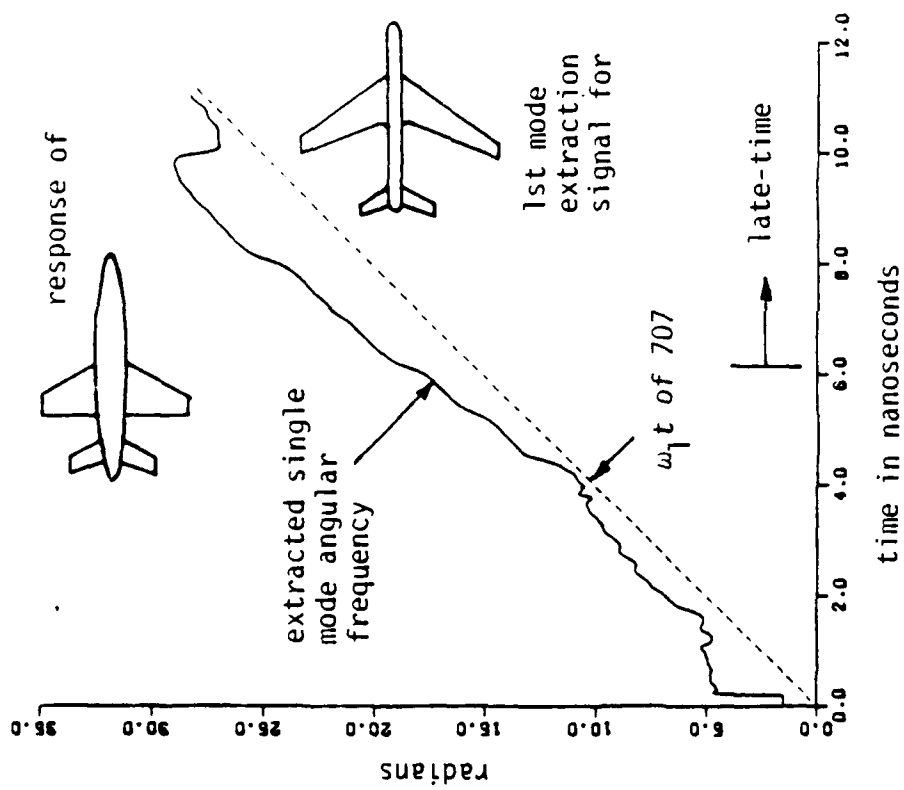
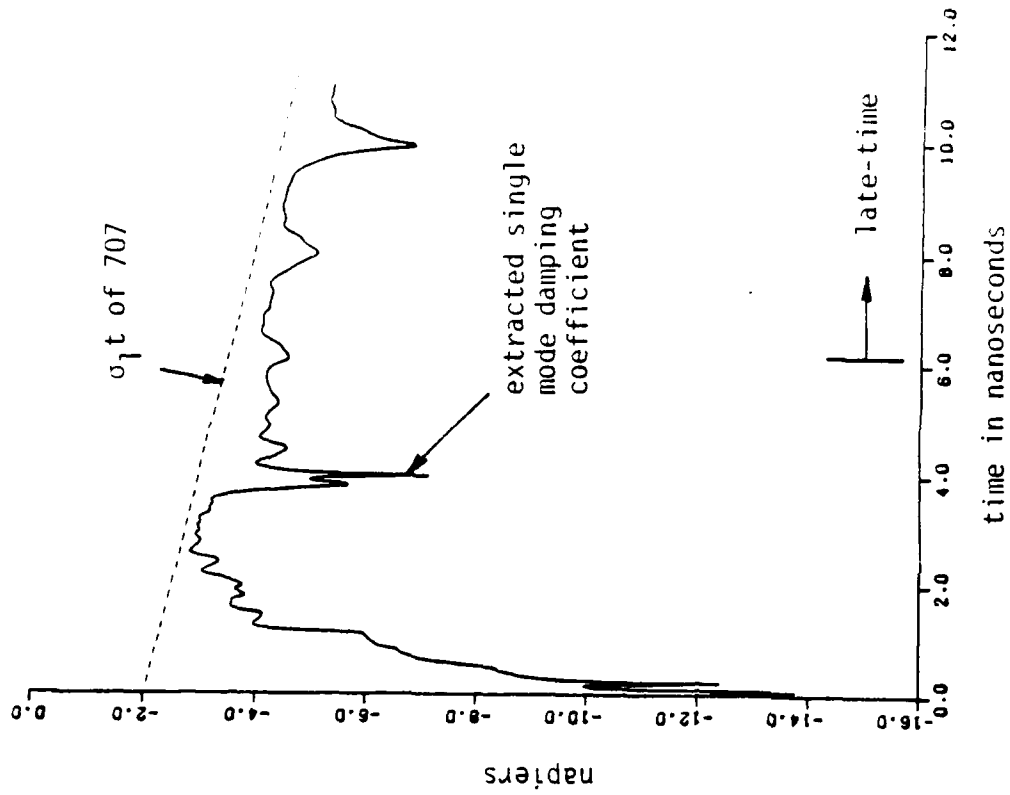


Fig. 5. Single mode angular frequency and damping coefficient extracted from the convolved outputs of the first mode extraction signals for the 707 target and the F-18 measured response.

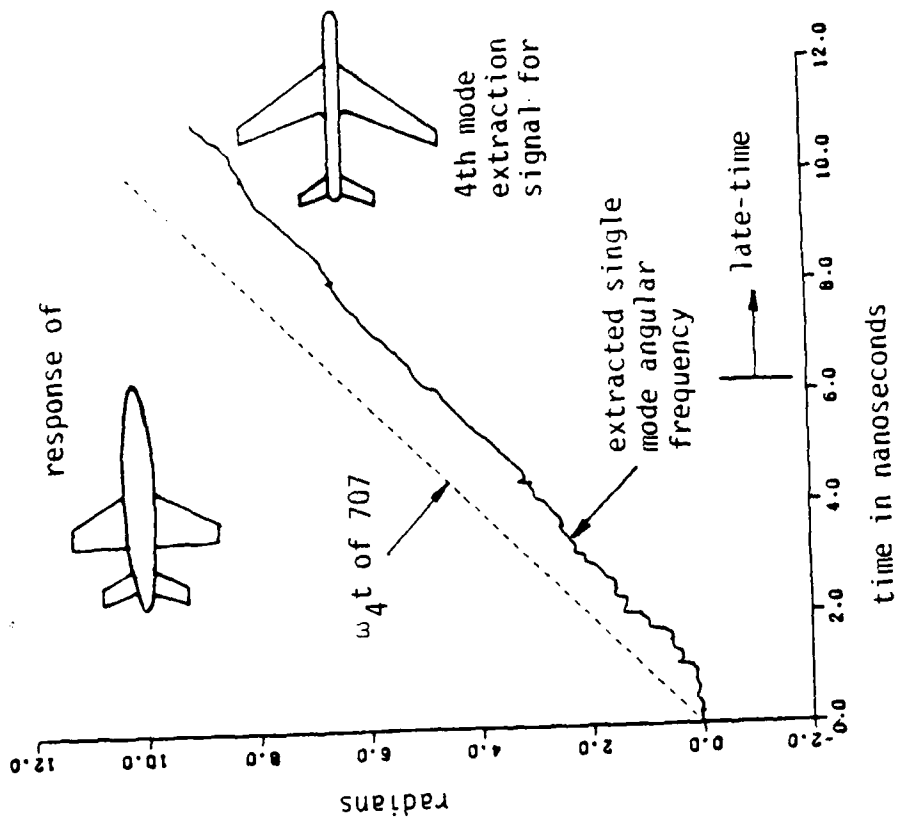
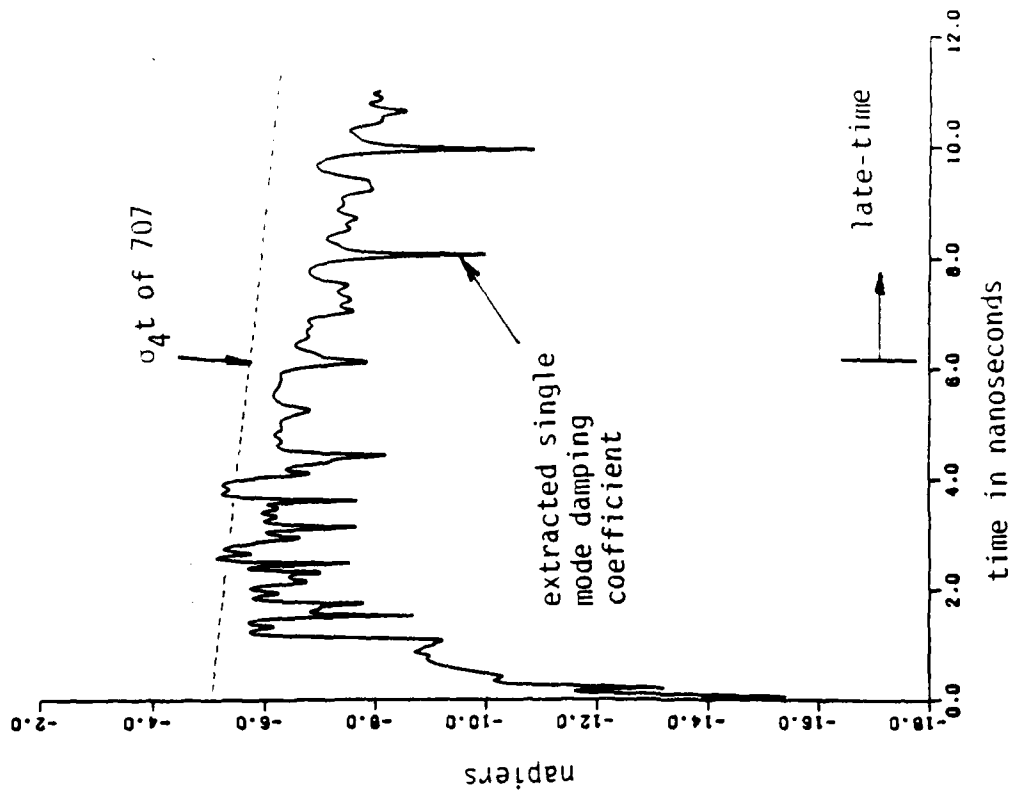


Fig. 6. Single mode angular frequency and damping coefficient extracted from the convolved outputs of the fourth mode extraction signals for the 707 target and the F-18 measured response.

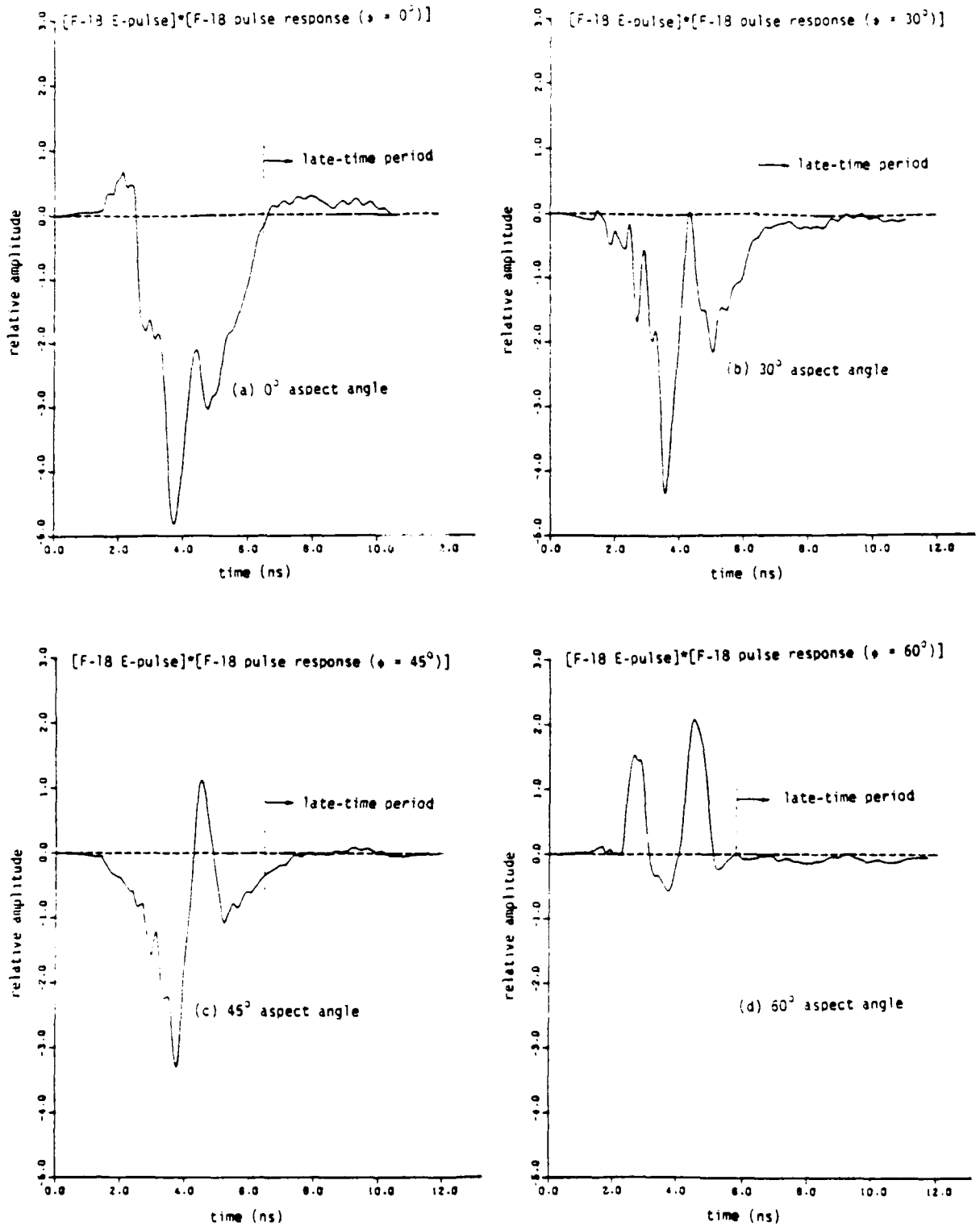


Fig. 7 Convolved outputs of F-18 E-pulse and pulse responses of F-18 model measured at (a) 0° aspect angle, (b) 30° aspect angle, (c) 45° aspect angle, (d) 60° aspect angle.

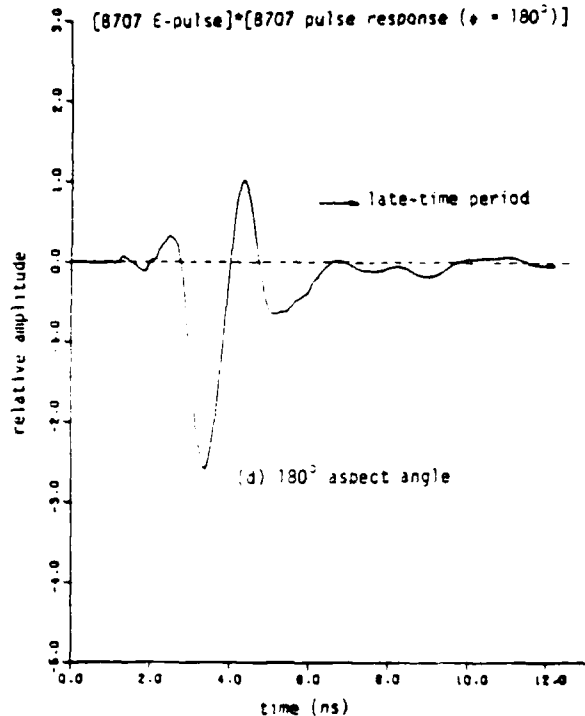
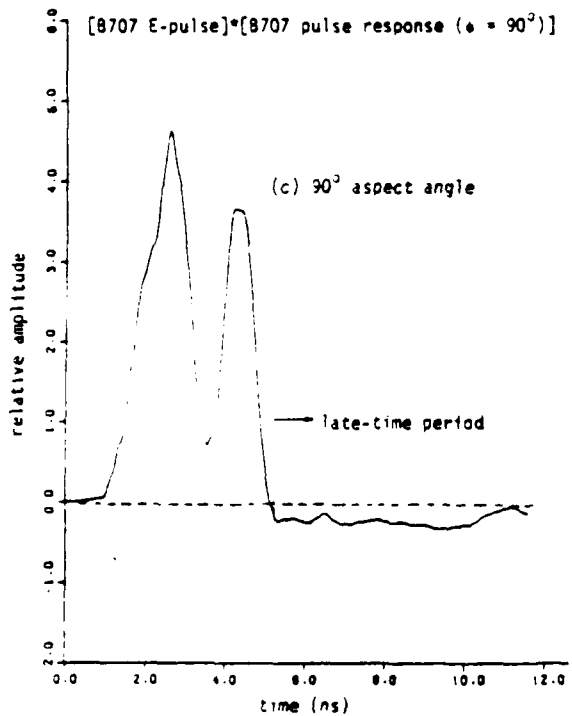
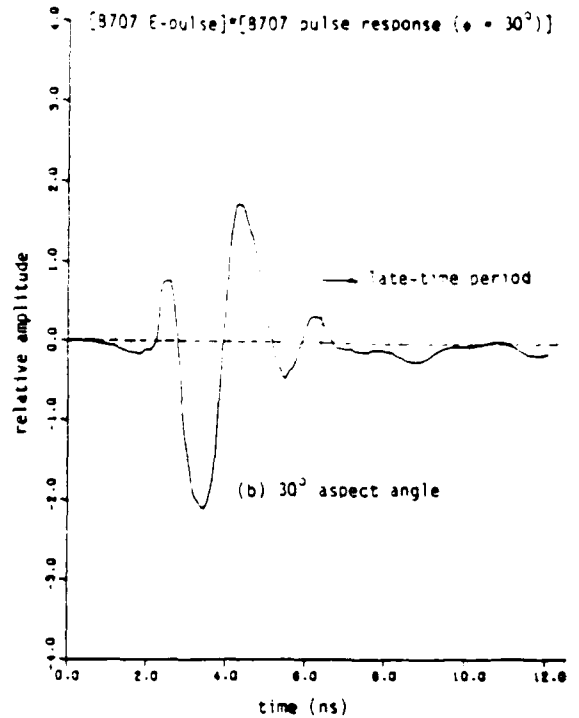
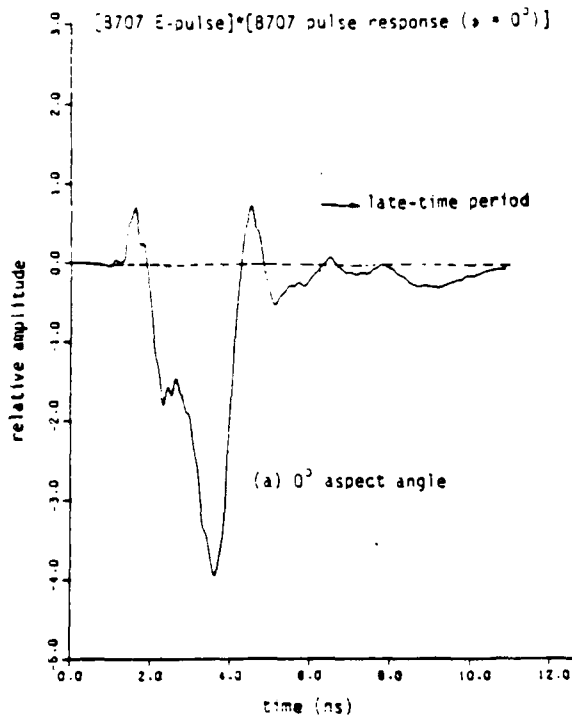


Fig. 8. Convolved outputs of B707 E-pulse and pulse responses of B707 model measured at (a) 0° aspect angle, (b) 30° aspect angle, (c) 90° aspect angle, (d) 180° aspect angle.

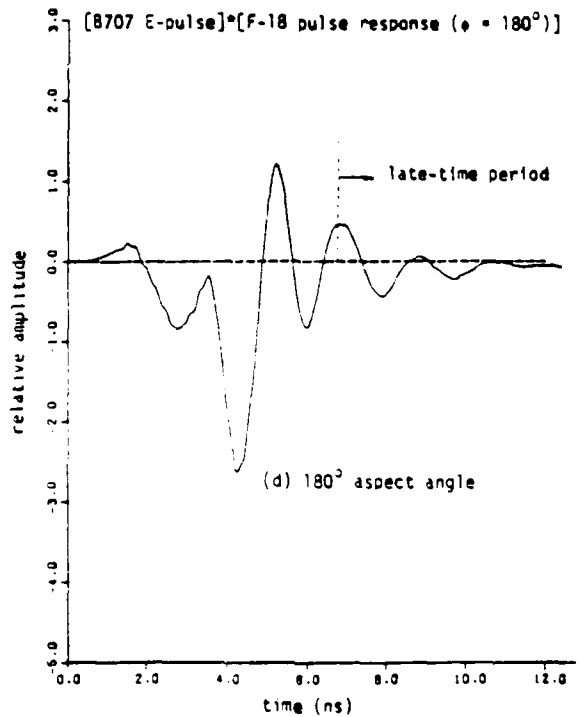
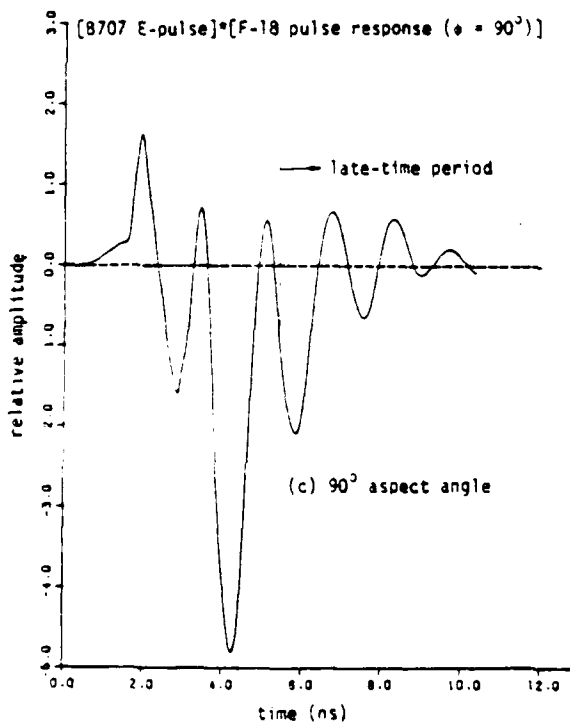
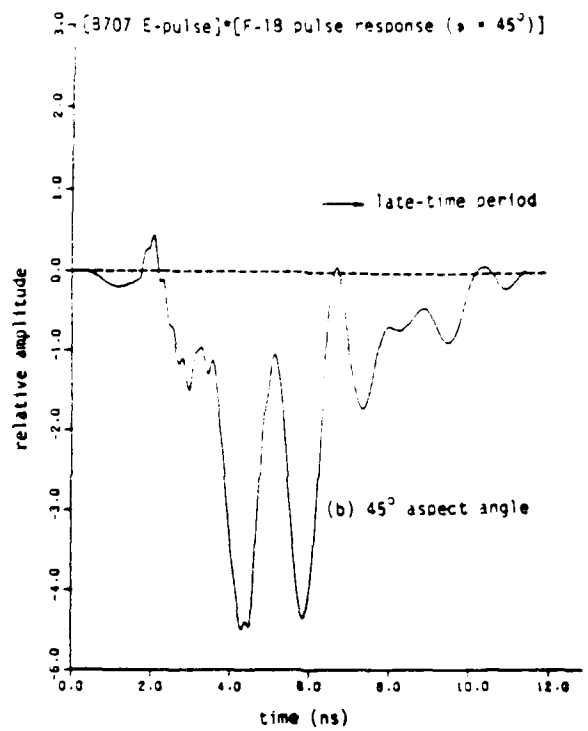
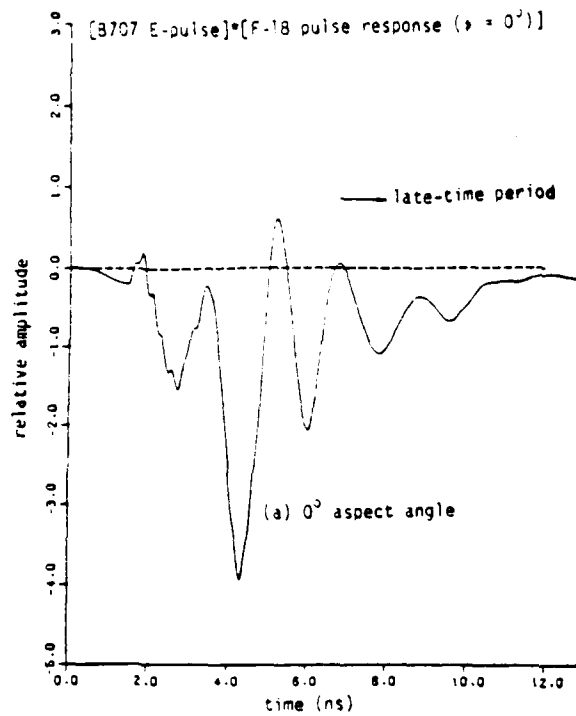


Fig. 9 Convolved outputs of B707 E-pulse and pulse responses of F-18 model measured at (a) 0° aspect angle, (b) 45° aspect angle, (c) 90° aspect angle, (d) 180° aspect angle.

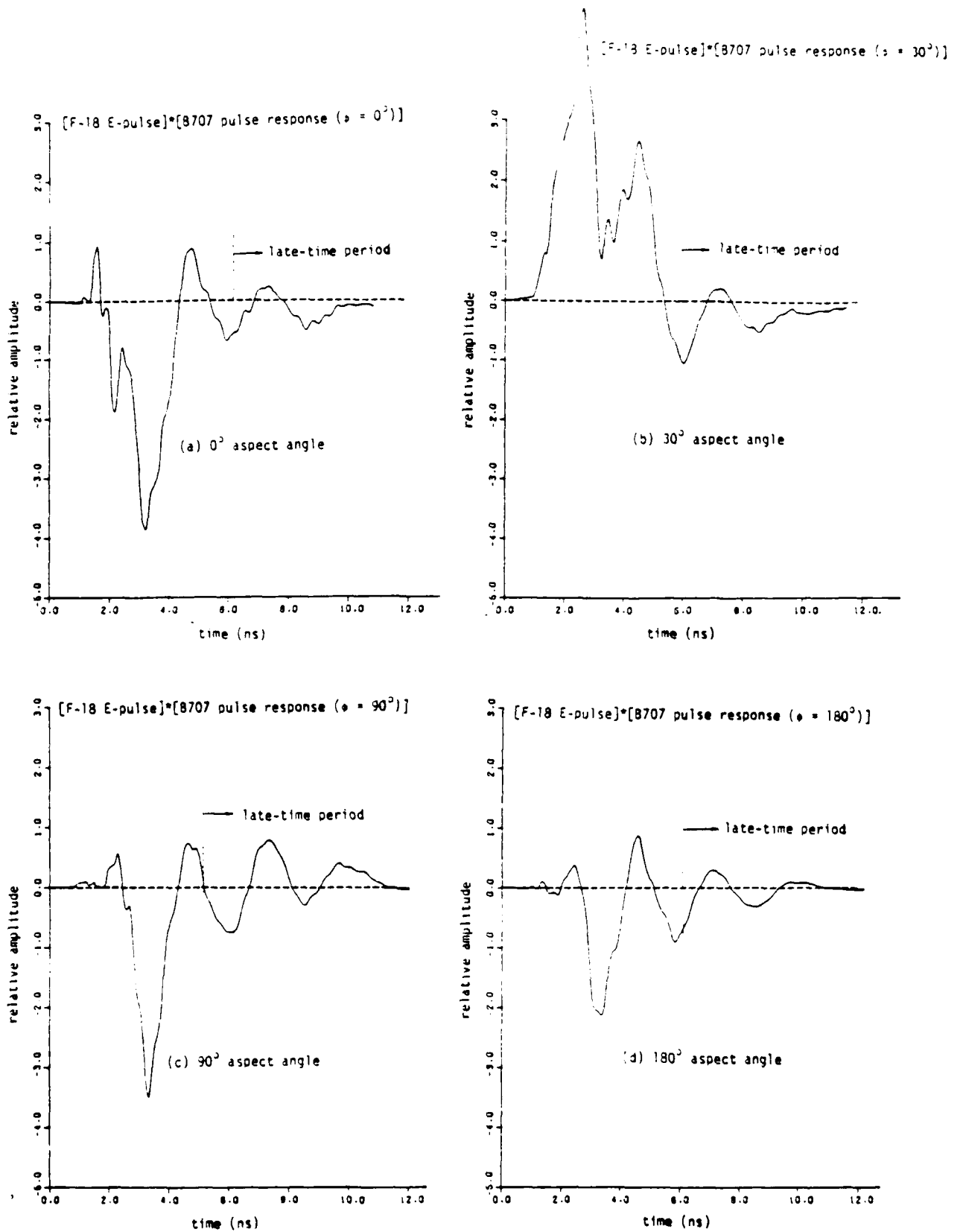


Fig. 10 Convolved outputs of F-18 E-pulse and pulse responses of B707 model measured at (a) 0° aspect angle, (b) 30° aspect angle, (c) 90° aspect angle, (d) 180° aspect angle.

2.4 EXTRACTION OF THE NATURAL FREQUENCIES OF A RADAR TARGET FROM A MEASURED RESPONSE USING E-PULSE TECHNIQUE

ABSTRACT

A new scheme is introduced for extracting the natural resonance frequencies of a radar target from a measured response. The method is based on the E-pulse technique and is shown to be relatively insensitive to random noise and to estimates of modal content. Verification of the technique is accomplished by comparing the natural frequencies extracted from the measured responses of a thin cylinder and a circular loop with those obtained from theory. The applicability of the technique to low-Q targets is also demonstrated, using the measured response of a scale model aircraft.

I. INTRODUCTION

Many recent radar target discrimination schemes have utilized the late-time natural oscillation behavior of conducting targets [1-5]. These techniques are based upon the assumption that the late-time scattered field response of the target obeys the natural mode representation

$$E^S(t) = \sum_{n=1}^N a_n e^{\sigma_n t} \cos(\omega_n t + \phi_n) \quad t > T_L \quad (1)$$

where $s_n = \sigma_n + j\omega_n$ is the aspect independent natural frequency of the n'th target mode, a_n and ϕ_n are the aspect and excitation dependent amplitude and phase of the n'th target mode, T_L describes the beginning of the late-time period, and the number of modes in the response, N , is determined by the finite frequency content of the waveform exciting the target.

Since the natural frequencies of the target are aspect independent, they form an ideal set of discriminants. Employing this set requires the knowledge of the natural frequencies of a wide variety of targets. As a theoretical determination of the natural frequencies of a complex target is impractical, it becomes necessary to develop a scheme for extracting the frequencies from a measurement of the response of the target.

A typical approach might use Prony's method [6,7]. Although this technique is simple and efficient, it has been found to be overly sensitive to random noise and to the number of modes assumed to be present in the measured response. A nonlinear least squares curve-fitting scheme can overcome these drawbacks, but requires a time consuming minimization involving $4N$ variables [8].

In this paper an alternative scheme is proposed, utilizing E-pulse

waveforms. It will be shown that this approach also overcomes the drawbacks of Prony's method, but is more efficient than nonlinear curve-fitting. The scheme was first introduced in [12] and [15], and is based on the frequency domain E-pulse concept first discussed in [14].

II. THE E-PULSE TECHNIQUE

An extinction-pulse (E-pulse) $e(t)$ is defined as a waveform of finite duration T_e which extinguishes $E^S(t)$ in the late-time [1]. That is, convolution of $e(t)$ and $E^S(t)$ yields the null result

$$c(t) = e(t) * E^S(t) = \int_0^{T_e} e(t') E^S(t-t') dt' = 0 \quad t > T_L + T_e \quad (2)$$

Using the natural mode representation for $E^S(t)$ allows (2) to be written as

$$c(t) = \sum_{n=1}^N |E(s_n)| a_n e^{\sigma_n t} \cos(\omega_n t + \psi_n) = 0 \quad t > T_L + T_e \quad (3)$$

where ψ_n is a new phase factor and $E(s)$ is the Laplace transform of $e(t)$

$$E(s) = \mathcal{L}\{e(t)\} = \int_0^{T_e} e(t) e^{-st} dt \quad (4)$$

If the natural frequencies of a target are known, an E-pulse for that target can be synthesized by demanding

$$E(s_n) = E(s_n^*) = 0 \quad 1 \leq n \leq N \quad (5)$$

and the convolution (3) will yield zero regardless of the aspect angle of the target for which $E^S(t)$ is measured.

Conversely, if the natural frequencies of a target are unknown, they can be extracted from the measured $E^S(t)$ by solving the integral equation given by (2). This equation can either be solved directly for the complex frequencies

used to construct $e(t)$ or for $e(t)$ itself. If $e(t)$ is determined, the complex frequencies eliminated by $e(t)$ can be found by locating the roots to [12]

$$E(s) = 0 \quad (6)$$

An E-pulse waveform can be represented as an expansion over a set of basis functions $\{f_k(t)\}$

$$e(t) = \sum_{k=1}^K \alpha_k f_k(t) \quad (7)$$

where α_k are the basis function amplitudes. Then, the requirements (5) result in a matrix equation for the real amplitude parameters α_k . Choosing $K=2N$ results in a homogeneous equation which has solutions only at discrete values of T_e .

The difficulty associated with locating all the roots of (6) can be overcome by choosing subsectional basis functions in the E-pulse expansion

$$f_k(t) = \begin{cases} g(t - [k-1]\Delta) & (k-1)\Delta \leq t \leq k\Delta \\ 0 & \text{elsewhere} \end{cases} \quad (8)$$

resulting in the E-pulse shown in figure 1. Here $g(t)$ is any Laplace-transformable function. The E-pulse spectrum is then easily calculated as

$$E(s) = F_1(s) e^{s\Delta} \sum_{k=1}^K \alpha_k e^{-sk\Delta} \quad (9)$$

where $F_1(s)$ is the Laplace transform of the first basis function. Now the roots to $E(s)$ are easily found by solving the polynomial equation

$$\sum_{k=1}^K \alpha_k z^k = 0 \quad (10)$$

where

$$z = e^{-s\Delta} \quad (11)$$

This set of functions also allows a simple calculation of duration T_e when synthesizing E-pulses. It has been shown [9] that the solutions to the homogeneous matrix equation demanded by (5) are

$$\Delta = \frac{p \pi}{\omega_k} \quad 1 \leq k \leq N, \quad p = 1, 2, 3, \dots \quad (12)$$

III. SOLUTIONS TO THE INTEGRAL EQUATION

Solutions to the integral equation (2) have been obtained using two different methods. The first approach is to minimize

$$c^2(t) = [e(t) * E^S(t)]^2 \quad (13)$$

over the range of t corresponding to the late-time period of the convolution, $t > T_L + T_e$. This can be done either with respect to the complex frequencies used to construct the E-pulse via (5), or with respect to the basis function amplitudes used to construct $e(t)$ via (7). If minimization is done with respect to the complex frequencies, then the estimated values of the natural frequencies contained in $E^S(t)$ are available directly at the minimum point. If minimization is done with respect to the basis function amplitudes, then estimates of the natural frequencies in $E^S(t)$ are obtained by solving (6) or (10) using the values of α_k obtained at the minimum point. The latter minimization is computationally less intensive, since a new E-pulse need not be created at each step in the minimization, but it requires a normalization scheme to prevent the trivial solution $\alpha_k = 0$.

The integral equation can also be solved by using the method of moments [10]. The E-pulse is expanded as in (7) and moments are taken with a set of weighing functions $\left\{ w_m(t) \right\}$

$$\left\langle w_m(t), \sum_{k=1}^K \alpha_k \int_0^{T_e} f_k(t') E^S(t-t') dt' \right\rangle = 0 \quad m=1, 2, \dots, M \quad (14)$$

where the brackets $\langle \rangle$ indicate the inner product

$$\langle f(t), g(t) \rangle = \int f(t)g(t)dt \quad (15)$$

Choosing $K=M=2N$ to reflect the number of modes believed to be in $E^S(t)$ results in a homogeneous matrix equation for the basis function amplitudes, a solution to which is possible only at discrete values of T_e which cause the determinant of the matrix of coefficients to vanish. By choosing subsectional basis functions (8) an estimate for the natural frequencies in $E^S(t)$ is found by solving (10).

With either of the two approaches, the amplitudes and phases of the natural modes comprising $E^S(t)$ can be found as a last step by using linear least squares.

IV. DISCUSSION OF THE METHODS

The major benefit of each of the two E-pulse methods is that they overcome the sensitivity of Prony's method to noise and to estimates of modal content. Although the minimization approach requires a computationally time consuming multi-variable minimization procedure, because the amplitudes and phases are not involved the total number of parameters utilized is only $2N$, compared to $4N$ for nonlinear curve-fitting, and only half the number of initial guesses are needed for starting the minimization. On the other hand, the moment method approach is extremely efficient; no minimization scheme is required, only a search for the single parameter T_e .

The insensitivity of these two approaches to the number of modes estimated to be present in $E^S(t)$ leads to a particularly useful scheme. Extraction of the frequencies in $E^S(t)$ may begin by assuming a small number of modes (usually one) to be present. For the methods requiring minimization, the frequencies extracted with a small number of modes assumed present prove

to be very good initial guesses for the case when more modes are assumed present. For the moment method, because of the relationship (12), the value of T_e obtained allows an excellent estimate of the T_e to expect with more modes allowed.

The reasons for the success of the E-pulse method in the presence of random noise can be identified by investigating the relationship between Prony's method and the moment method approach to the E-pulse technique. By choosing impulses for both expansion and weighting functions in (14) and taking $K=M+1$, an inhomogeneous matrix equation results. The matrix can be solved directly for α_k and the natural frequencies contained in $E^S(t)$ estimated by solving (10). Such an approach is found to be identical in all respects to Prony's method.

Because of the discrete nature of the convolution integral, each of the matrix entries and the right hand side vector elements are merely a single sampled value of the measured waveform. Thus, Prony's method is very sensitive to noise contamination of $E^S(t)$ and so is an inherently ill-conditioned algorithm (see [16]). The moment method approach can be viewed as a generalization of the basic Prony's method, where preprocessing of the measured data is naturally introduced. The preprocessing step can be incorporated in two places, individually or simultaneously, each of which works to reduce the noise sensitivity of the technique. First, by utilizing expansion functions which together span the E-pulse duration T_e (such as rectangular pulses), the convolution integral in (14) performs a moving window type smoothing of the measured data. Second, by using weighting functions which together span the late-time region of the convolution, the inner product integral (15) introduces additional smoothing. Although the numerical

examples presented below utilize impulse functions for weighting, preliminary results using rectangular pulses indicate an additional reduction in noise sensitivity.

The result of preprocessing the measured data is matrix elements which are each a function of a large portion of the measured data. Consequently, solutions are less sensitive to the perturbation of individual sampled values of $E^S(t)$, and so the E-pulse technique is a better conditioned algorithm. Further noise reduction capabilities can be introduced by using basis functions that individually span T_e (such as Fourier cosines) and/or weighting functions that individually span the late-time of the convolution, involving even more of the measured data in each matrix element. However, choosing basis functions which are not subsectional complicates the search for zeroes of the E-pulse spectrum, since (10) can no longer be used.

One last distinction between Prony's method and the E-pulse techniques is the manner in which the E-pulse duration T_e is selected. Whereas in Prony's method T_e is determined solely by the sampling interval (so that discrete convolution may be performed), in the E-pulse technique T_e is linked directly to the natural frequencies contained in the measured response.

When minimizing with respect to the natural frequencies, the duration of the E-pulse convolved with the data is chosen to be the smallest allowed by (12). Note that this is given by

$$(T_e)_{\min} = 2N \frac{\pi}{\omega_h} \quad (16)$$

where ω_h is the largest value of ω present among the natural frequencies in the response. This choice results in the largest amount of the late-time convolved response used in minimizing $c^2(t)$. As the frequencies change during the minimization process the duration will change as well, but it is

always related through (16).

When minimizing with respect to the basis function amplitudes, the E-pulse duration is allowed to be a free variable. However, at each step the basis function amplitudes represent an E-pulse which eliminates a certain set of natural frequencies, and the duration is tied to those frequencies via (12).

In employing the moment method, the E-pulse duration is the only free parameter. When a zero of the determinantal equation is located, it will again be tied to the natural frequencies eliminated by the E-pulse through (12). As before, it is prudent to search for the smallest value of T_e which satisfies the determinantal equation since this results in the longest late-time portion of the convolution.

As a last note, the E-pulse technique as a whole should not be considered just a generalization of Prony's method. For instance, the minimization with respect to natural frequencies approach completely avoids the second step in Prony's method — solving a polynomial equation for the natural frequencies (which itself can be an ill-conditioned problem.) In the moment method approach, a different choice of basis functions requires finding not the roots of a polynomial, but those of a sum of different functions altogether.

V. EXAMPLES

As a simple numerical example, Figure 2 shows the theoretical impulse response of a thin cylinder oriented at 30° with respect to the incident field, constructed using the first eight natural frequencies of the cylinder [11]. An attempt will be made to extract these frequencies from the response using the E-pulse techniques.

To simulate a practical situation, this waveform is sampled at 500

points. The convolution indicated in (2) is then carried out by interpolating linearly between sampled points, and analytically integrating the product of the linear curve and the mathematical representation of the basis functions from (8). To keep the integrals simple, rectangular pulse basis functions are used throughout.

The minimization schemes utilize standard Newton's method and thus require initial guesses. For minimization with respect to the complex frequencies, initial guesses for σ_n and ω_n are required. These can often be obtained from the Fourier spectrum of $E^S(t)$ via the FFT. For minimization with respect to the basis function amplitudes, initial guesses are required for α_k . Anticipating these values is difficult, since intuition is lacking. However, a good guess for the amplitudes can be obtained by constructing at the first step an E-pulse based on guesses for σ_n and ω_n .

The number of basis functions chosen in the E-pulse expansion reflects the number of modes expected -- two functions for each mode. If a DC component is present in $E^S(t)$ as an artifact of the measurement system, it can be effectively eliminated by utilizing an additional basis function [9].

To demonstrate the insensitivity of the E-pulse techniques to the number of modes assumed present in $E^S(t)$, an attempt will be made to extract four of the eight frequencies used to construct Figure 2. Figure 3 shows the results of using the moment method with impulse weighting functions, and minimization with respect to the complex frequencies. Obviously, the first four modes have been extracted with very good precision, even though the number of modes present has been drastically underestimated.

To demonstrate the insensitivity of the E-pulse techniques to the presence of random noise, an attempt will be made to extract the frequencies from a noisy version Figure 2. The amplitude of the added noise is chosen to

be 10% of the maximum value of the waveform. Figure 4 shows the results of using the same moment method and minimization approaches, and the results are seen to be quite adequate. Note that the values of ω_n obtained are usually much better than the values of σ_n . As a direct comparison, Figure 3d of [8] shows the natural frequencies extracted from the noisy response using Prony's method. It is apparent that utilizing the E-pulse concept provides a decrease in the noise sensitivity of the extracted natural frequencies.

As a more practical example, Figure 5 shows the measured surface current response of a thin cylinder to a nanosecond pulse excitation field (see [1] for a detailed description of the experiment). The measurement system has sampled this response at a total of 240 points. Figure 6 shows the results of extracting the five dominant natural frequencies using minimization with respect to the complex frequencies. Rectangular pulse basis functions have been used again, and sampled point convolution performed as described above. The comparison of the extracted frequencies to those given by theory is excellent.

As a second practical example, Figure 7 shows the measured late-time scattered field response of a thin wire circular loop to a nanosecond pulse excitation field. The measurement system has sampled this waveform at 1024 points. Figure 8 shows the result of using minimization with respect to the complex frequencies to extract the six dominant natural frequencies. Also shown in Figure 8 are the theoretical values calculated using a Fourier series type solution [13]. Again, the frequencies extracted from the measured waveform compare quite well with the theoretical values.

Lastly, it is important to demonstrate that the E-pulse technique will work successfully for low-Q type targets. Figure 11 of [1] shows the measured nanosecond pulse scattered field response of a Boeing 707 aircraft model,

sampled at 400 points. Although no theory is available for predicting the natural frequencies of this structure, they have been extracted from the measured response using a nonlinear least squares technique [8]. Figure 9 shows the six dominant natural frequencies extracted using the least squares approach, and also those extracted using minimization of the late-time convolved response with respect to the complex frequencies (again, using rectangular pulse expansion functions). The agreement between the results obtained by these radically different methods is very good, verifying the usefulness of the E-pulse technique for low-Q structures.

VI. CONCLUSIONS

Two new approaches to extracting the natural frequencies of a radar target have been presented. They are based on the E-pulse technique, and have been shown to be relatively insensitive to random noise and to the number of modes assumed present in the measured response. They have also been shown to work in practical situations, accurately reproducing the expected natural frequencies of a thin cylinder and a circular loop from measured values of their transient responses. Lastly, the new methods have been used to verify the values of the natural frequencies of a low-Q aircraft model obtained using a different approach.

References

- [1] E.J. Rothwell, D.P. Nyquist, K.M. Chen, and B. Drachman, "Radar target discrimination using the extinction-pulse technique," IEEE Transactions on Antennas and Propagation, vol. AP-33, pp. 929-937, September 1985.
- [2] C. Chuang and D. Moffatt, "Natural resonances of radar targets via Prony's method and target discrimination," IEEE Transactions on Aerospace and Electronic Systems, vol. AES-12, pp. 583-589, September 1976.
- [3] A. Berni, "Target identification by natural resonance estimation," IEEE Transactions on Aerospace and Electronic systems, vol. AES-11, pp. 147-154, March 1975.
- [4] J. Auton, et. al., "On the practicality of resonance-based identification of scatterers," presented at the IEEE/AP-S Symposium and National Radio Science Meeting, Boston, MA, June 1984.
- [5] E. Miller, "A study of target identification using electromagnetic poles," Lawrence Livermore Laboratory, Livermore, CA, Report UCRL-52685 (1979).
- [6] M. Van Blaricum and R. Mittra, "A technique for extracting the poles and residues of a system directly from its transient response," IEEE Transactions on Antennas and Propagation, vol. AP-23, pp. 777-781, November 1975.
- [7] A. Poggio, et. al., "Evaluation of a processing technique for transient data," IEEE Transactions on Antennas and Propagation, vol. AP-26, pp. 165-173, January 1978.
- [8] B. Drachman and E. Rothwell, "A continuation method for identification of the natural frequencies of an object using a measured response," IEEE Transactions on Antennas and Propagation, vol. AP-33, pp. 445-450, April 1985.
- [9] E. Rothwell, K.M. Chen, D.P. Nyquist, "Frequency domain E-pulse synthesis and target discrimination," IEEE Transactions on Antennas and Propagation, to appear.
- [10] R.F. Harrington, Field Computation by Moment Methods, Macmillan, New York, 1968.
- [11] Chen, K.M., et.al., "Radar waveform synthesis for single-mode scattering by a thin cylinder and application for target discrimination," IEEE Transactions on Antennas and Propagation, vol. AP-30, pp. 867-880, September 1982.

- [12] E. Rothwell, "Radar target discrimination using the extinction-pulse technique," Doctoral Dissertation, Michigan State University, 1985.
- [13] R.F. Blackburn and D.R. Wilton, "Analysis and synthesis of impedance-loaded loop antenna using the singularity expansion method," IEEE Transactions on Antennas and Propagation, vol. AP-26, pp. 136-140, January 1978.
- [14] E.J. Rothwell, K.M. Chen, D.P. Nyquist, N. Gharsallah, and B. Drachman, "Frequency domain E-pulse synthesis and target discrimination," presented at the North American Radio Science Meeting and International IEEE/AP-S Symposium, Vancouver, B.C., June 17-21, 1985.
- [15] E.J. Rothwell, D.P. Nyquist, K.M. Chen, and W.M. Sun, "Identification of the natural frequencies of a target from a measured response using E-pulse techniques," presented at the National Radio Science Meeting, University of Colorado, Boulder, CO, January 13-16, 1986.
- [16] F.B. Hildebrand, Introduction to Numerical Analysis, McGraw-Hill, New York, 1956.

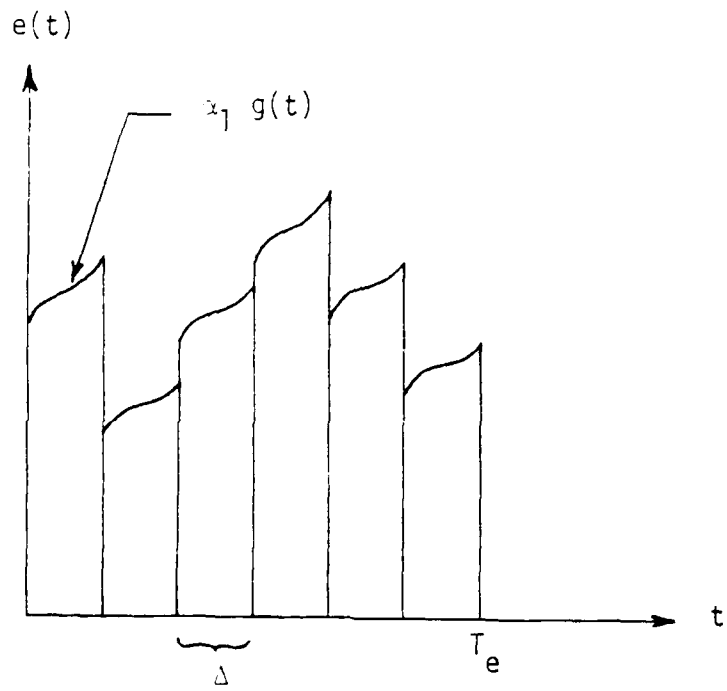


Figure 1. E-pulse waveform constructed using subsectional basis functions.

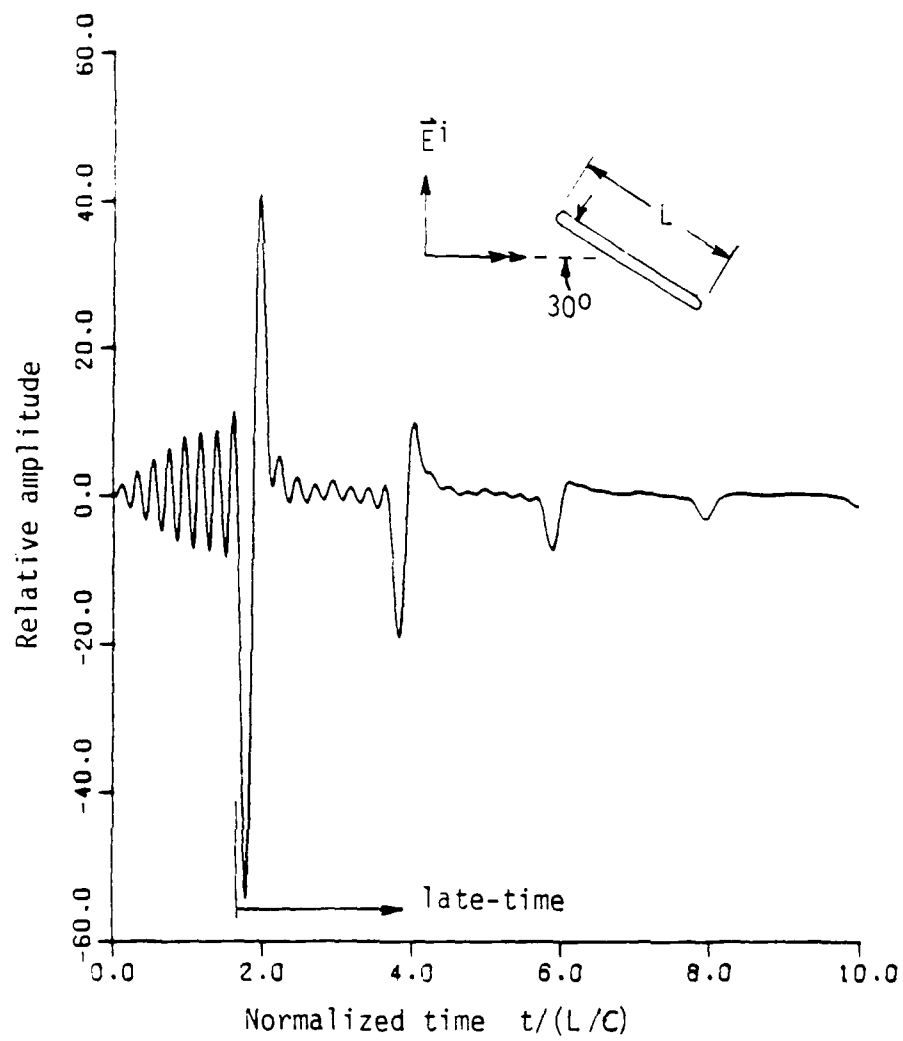


Figure 2. Eight mode 30° thin cylinder impulse response.

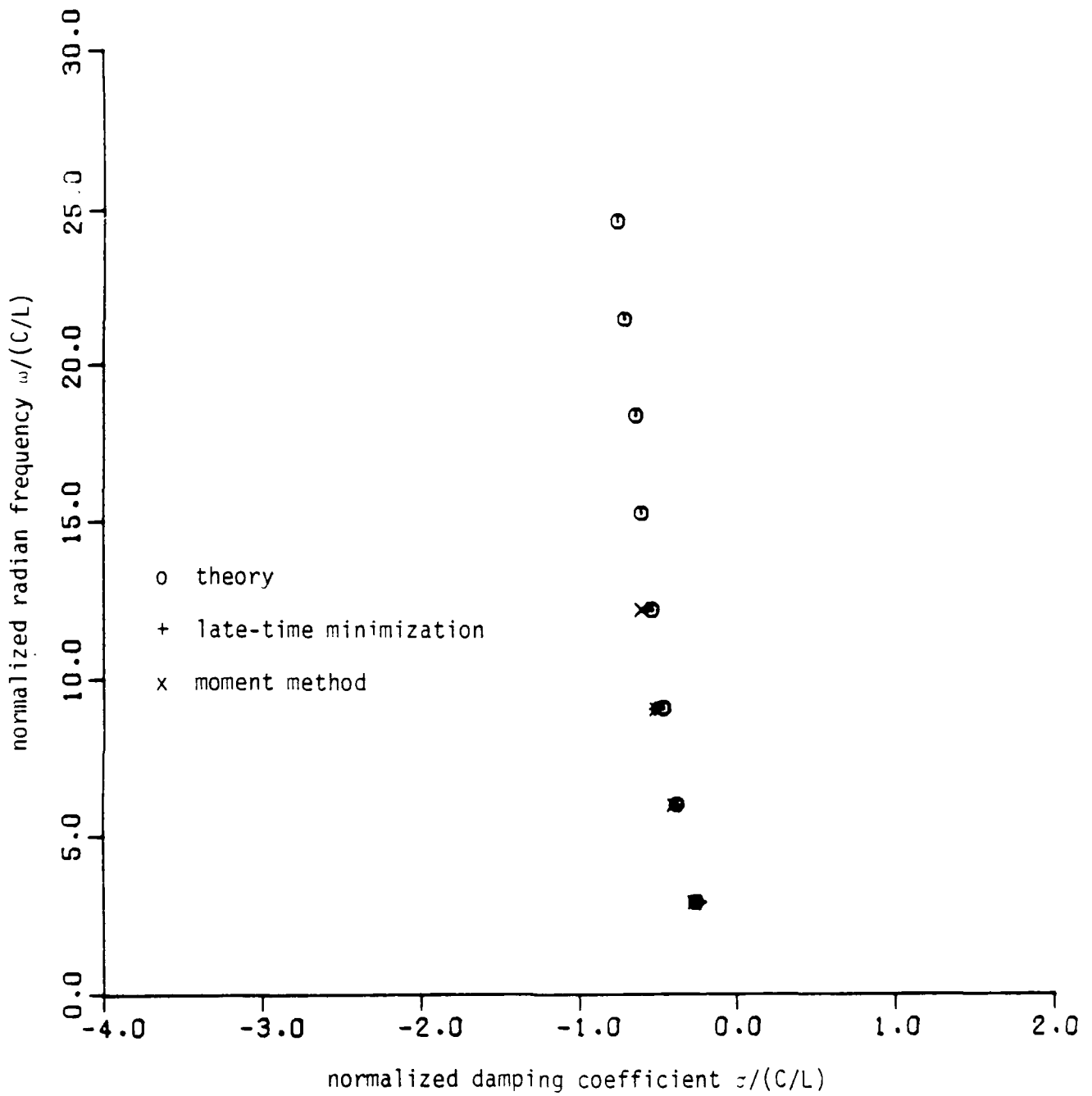


Fig. 3. Natural frequencies extracted from thin cylinder impulse response, four modes assumed present.

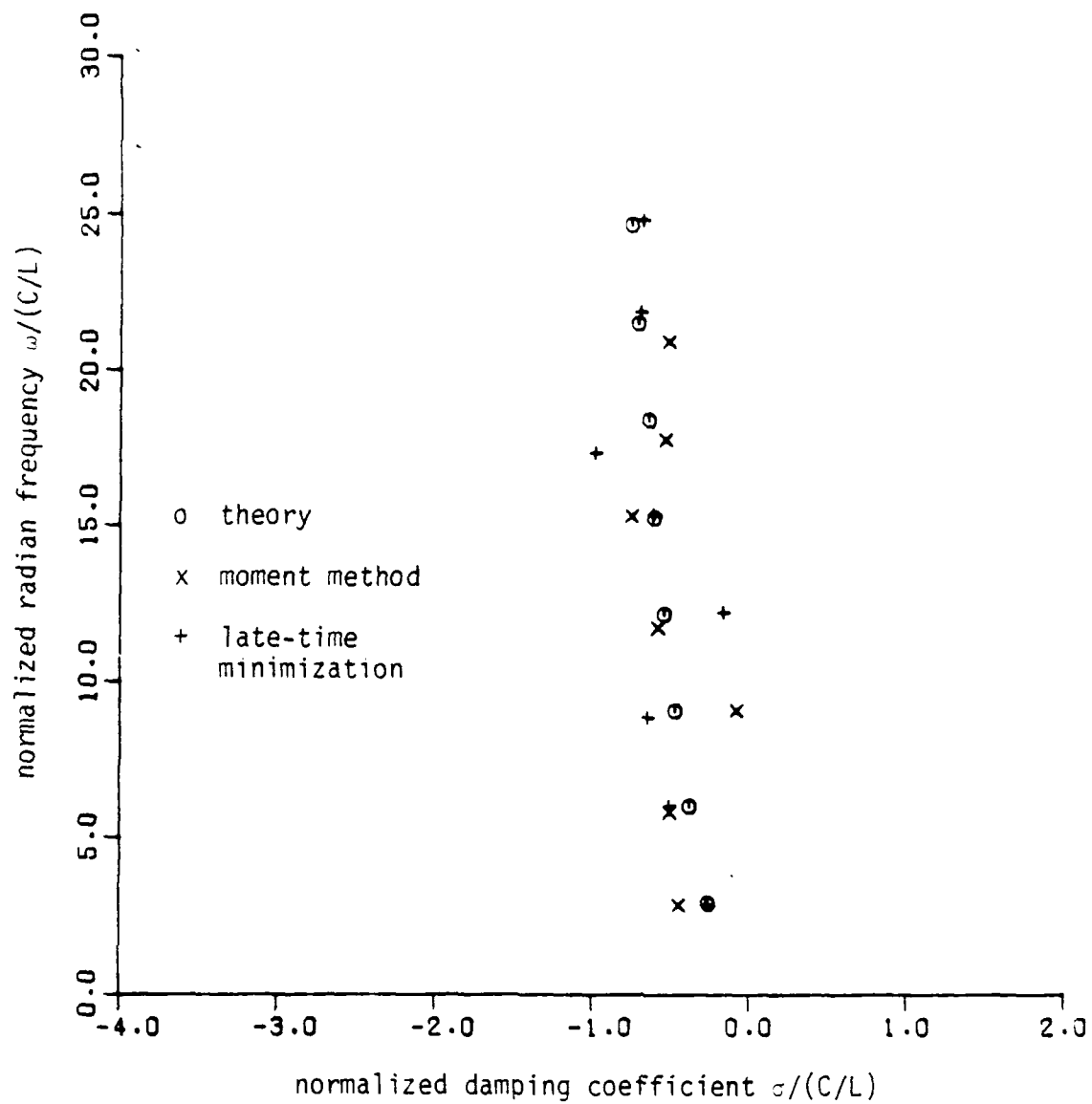


Fig. 4. Natural frequencies extracted from noisy thin cylinder impulse response.

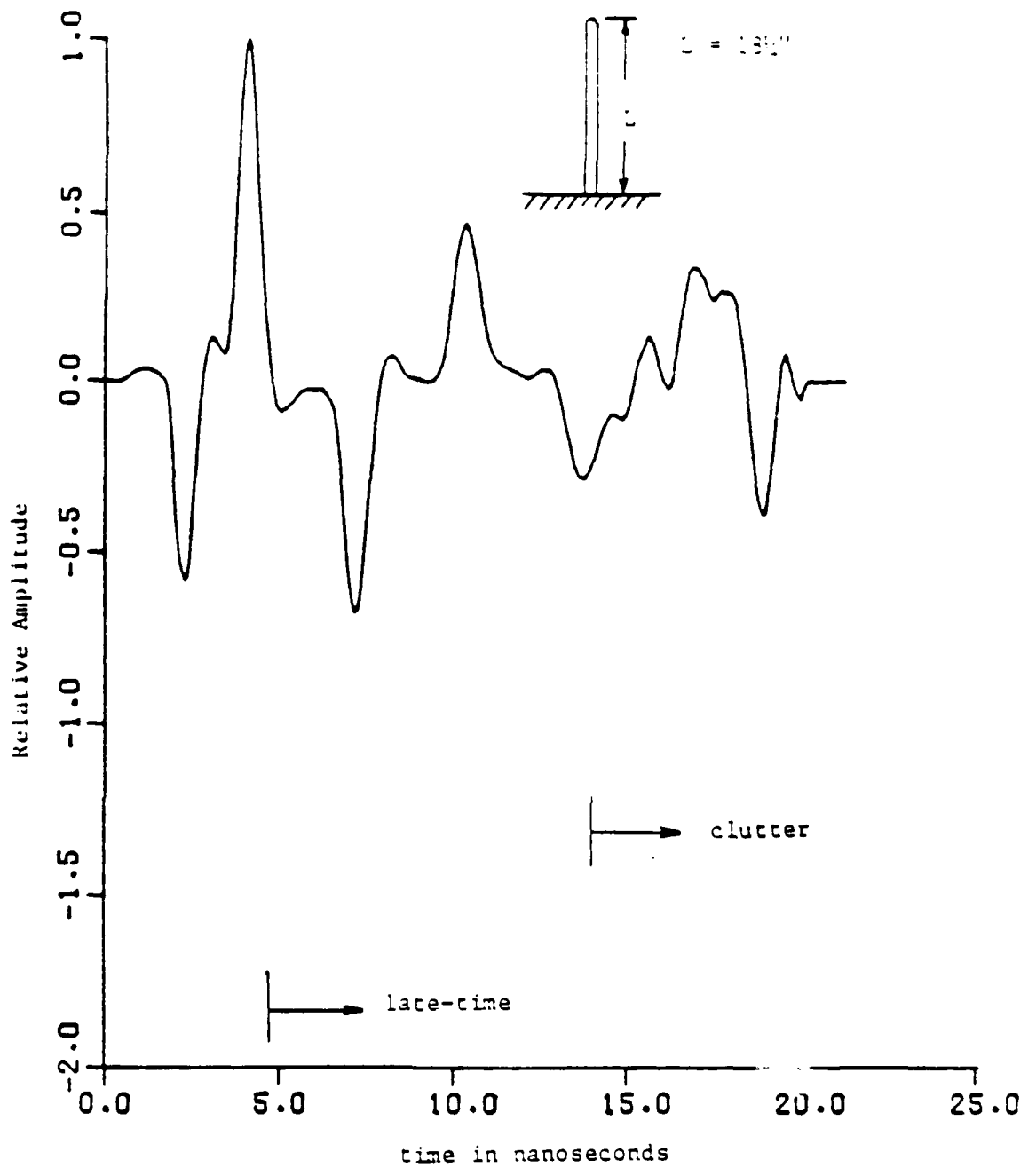


Figure 5. Measured surface current response of a thin cylinder of length 18.25 inches placed perpendicular to the ground screen.

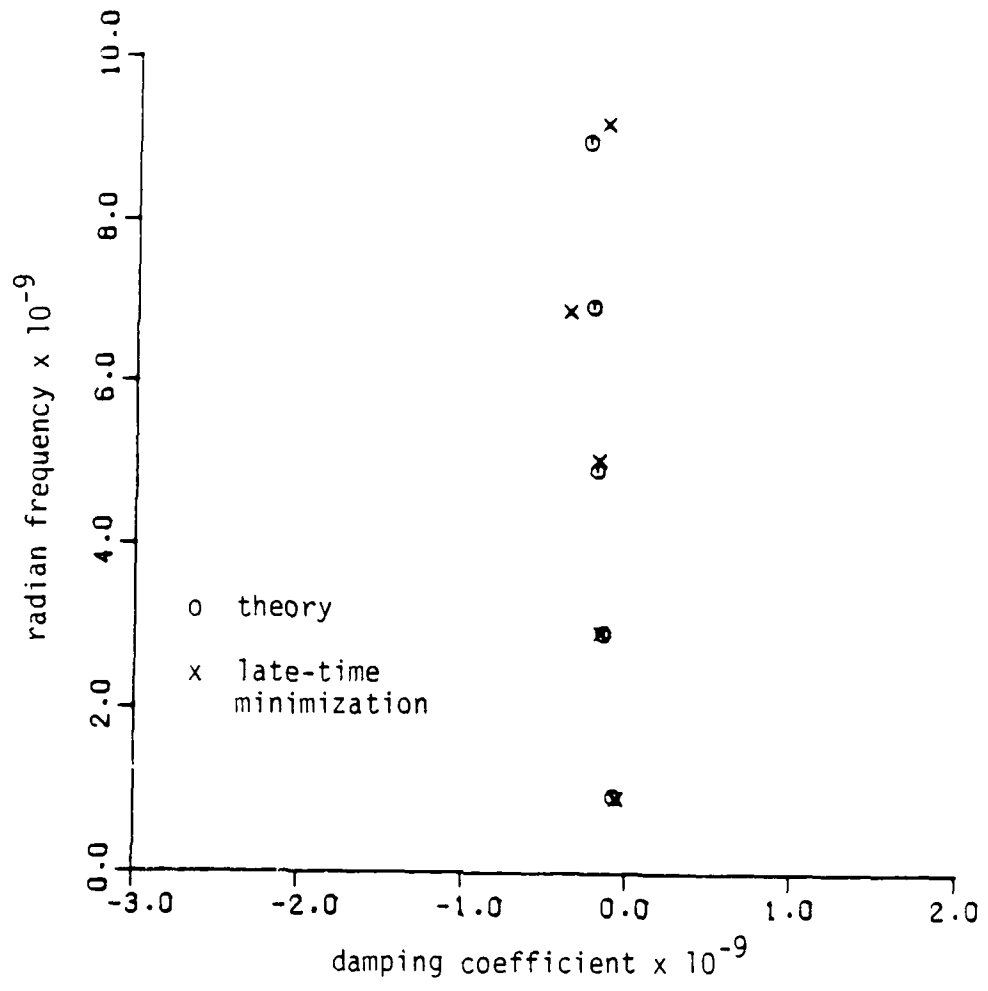


Fig. 6. Natural frequencies extracted from surface current response of 18 1/4" thin cylinder.

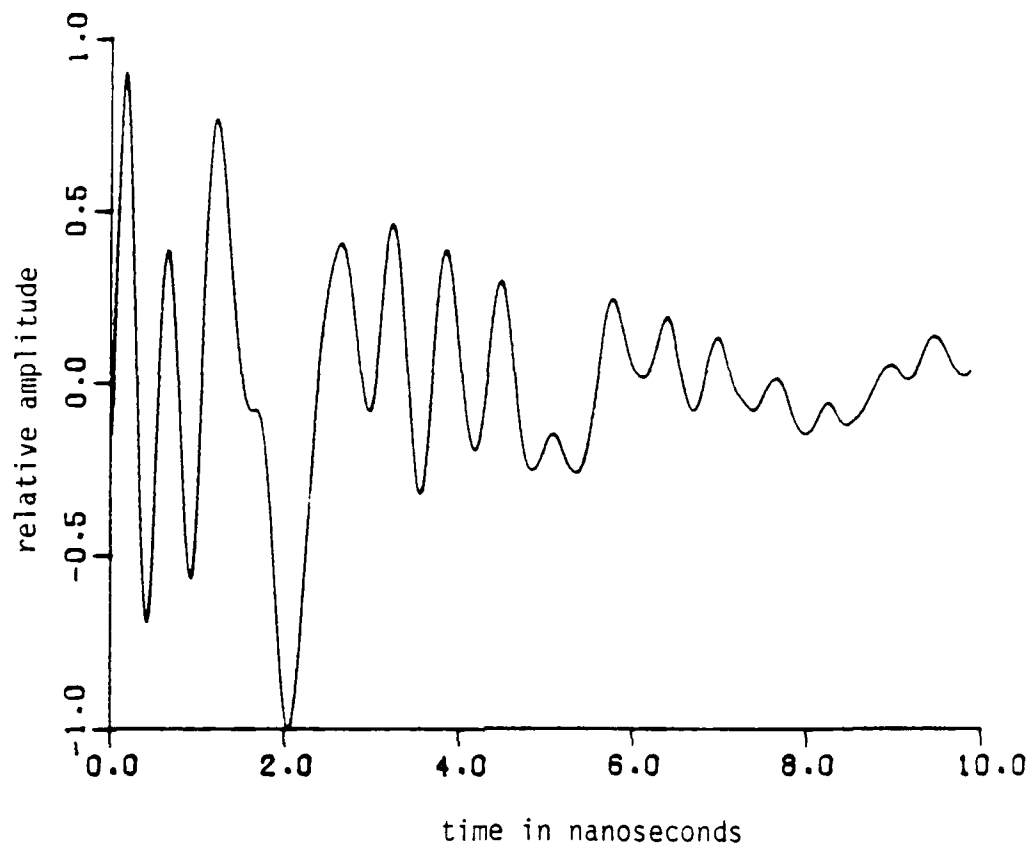


Figure 7. Late-time measured scattered field response of thin wire circular loop. Mean radius of loop = 11.5 cm, wire radius = 0.32 cm.

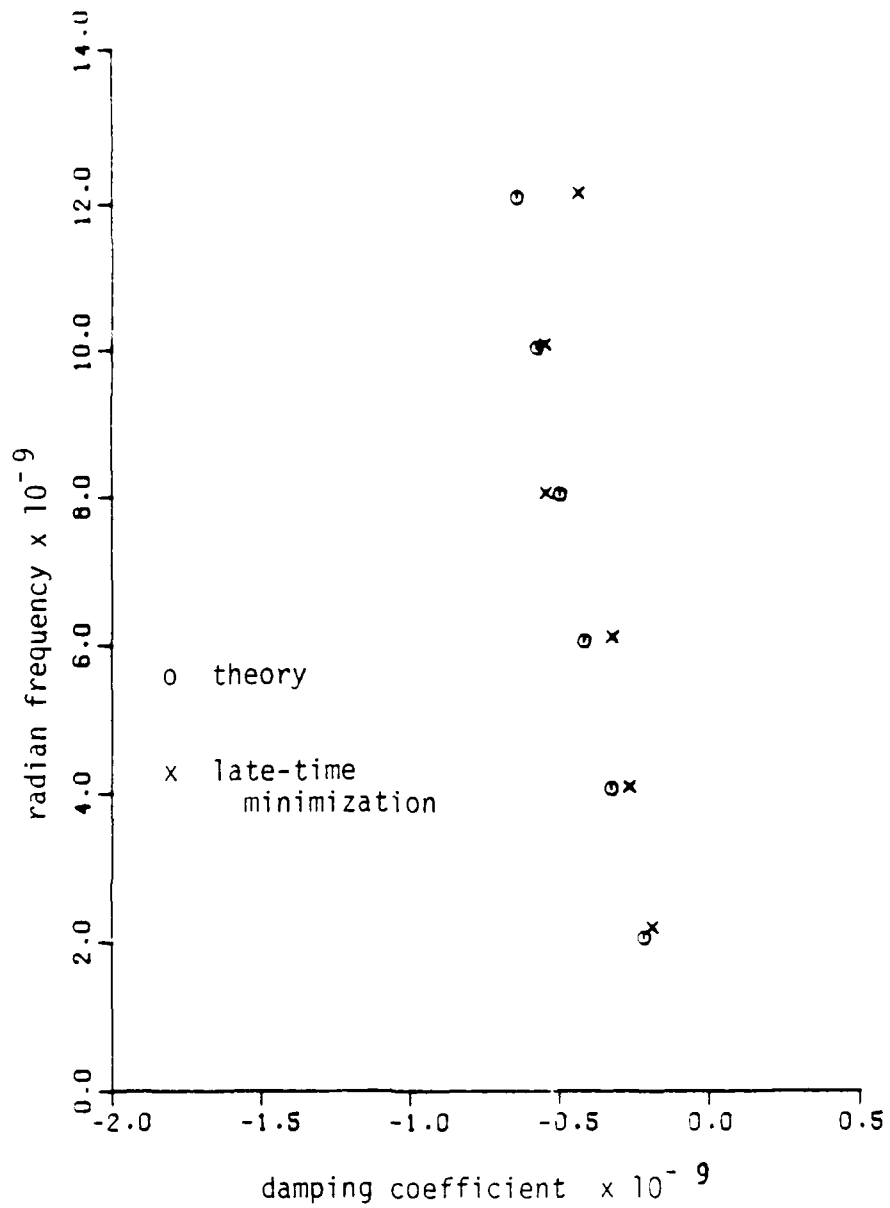


Figure 8. Natural frequencies extracted from measured response of thin wire circular loop.

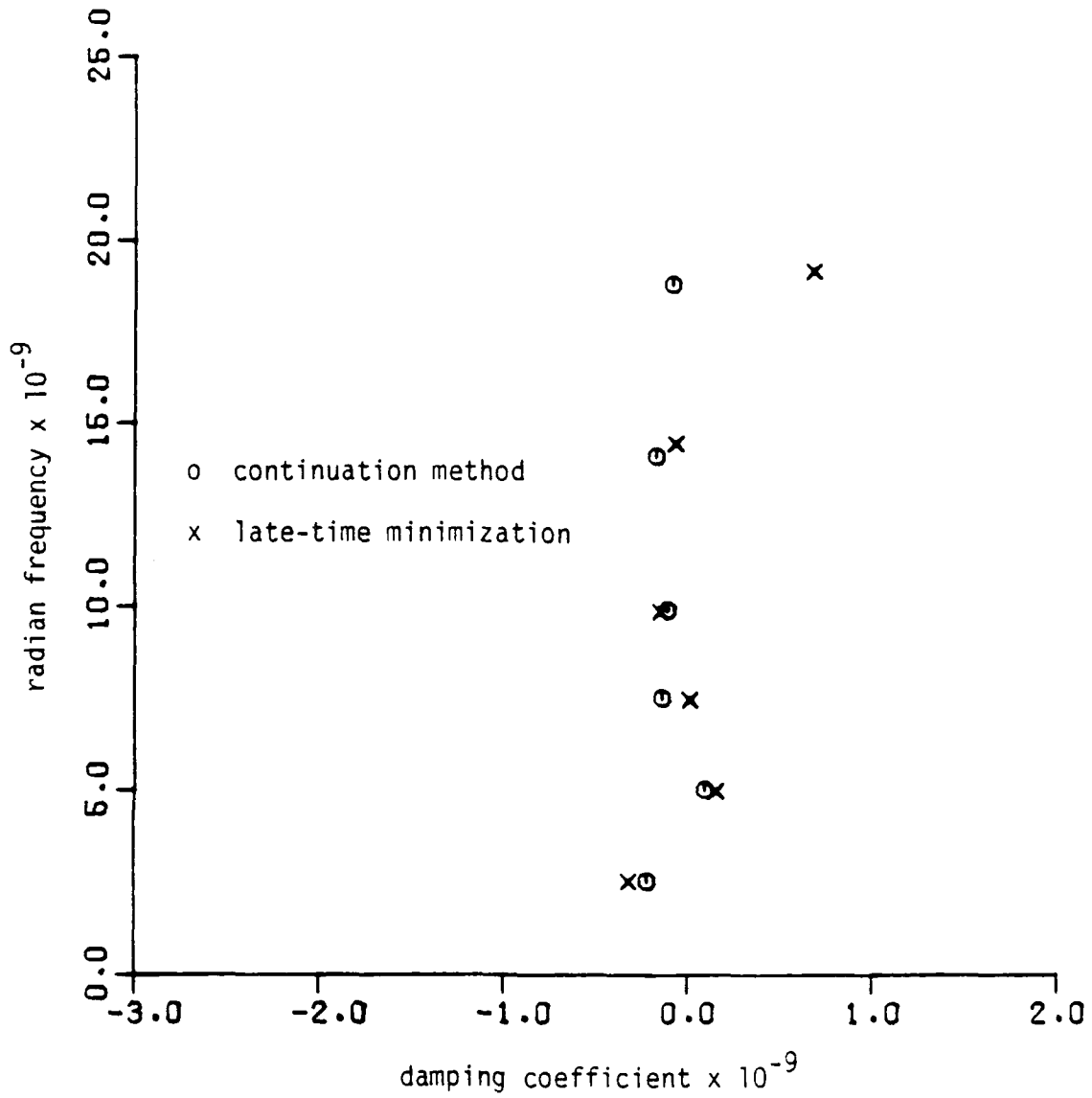


Fig. 9. Natural frequencies extracted from measured response of 707 aircraft model.

2.5 NOISE-INSENSITIVITY OF E-PULSE TECHNIQUE FOR TARGET DISCRIMINATION

To prove the noise insensitivity of our scheme, we have created very noisy radar responses of complex targets by intentionally adding a large random noise to the measured radar responses of the targets. These noisy responses were then used to convolve with the discriminant signals, the E-pulse and the single-mode extraction signals, of the targets. We have found that the discriminant signals of the targets are very powerful and effective in rejecting a large random noise and are capable of discriminating between the right and the wrong targets from very noisy radar responses. The following figures will demonstrate this finding.

Figure 1 shows the pulse response (the response excited by an incident Gaussian pulse) of B707 model measured at 90° aspect angle without adding an extra random noise. Figure 2 is the convolved output of the pulse response of Fig. 1 with the E-pulse of B707 model. As expected, a very small output was obtained in the late-time period of the convolved output. This indicates that the pulse response of Fig. 1 came from the right target of B707 model. Next, a very noisy pulse response was created by intentionally adding a large random noise (created by a computer) to the measured pulse response of B707 model shown in Fig. 1. This random noise amounted to 30% of the maximum amplitude of the measured response of Fig. 1. The created noisy pulse response is shown in Fig. 3. When this noisy pulse response of Fig. 3 was convolved with the E-pulse of B707 model, a very satisfactory convolved output was obtained, as shown in Fig. 4. This convolved output resembles that of Fig. 2; the early-time response stayed nearly unchanged and, more importantly, the late-time response still remained small. This indicates that the E-pulse of B707 model was capable of identifying that the noisy pulse response of Fig. 4 belonged to B707 model.

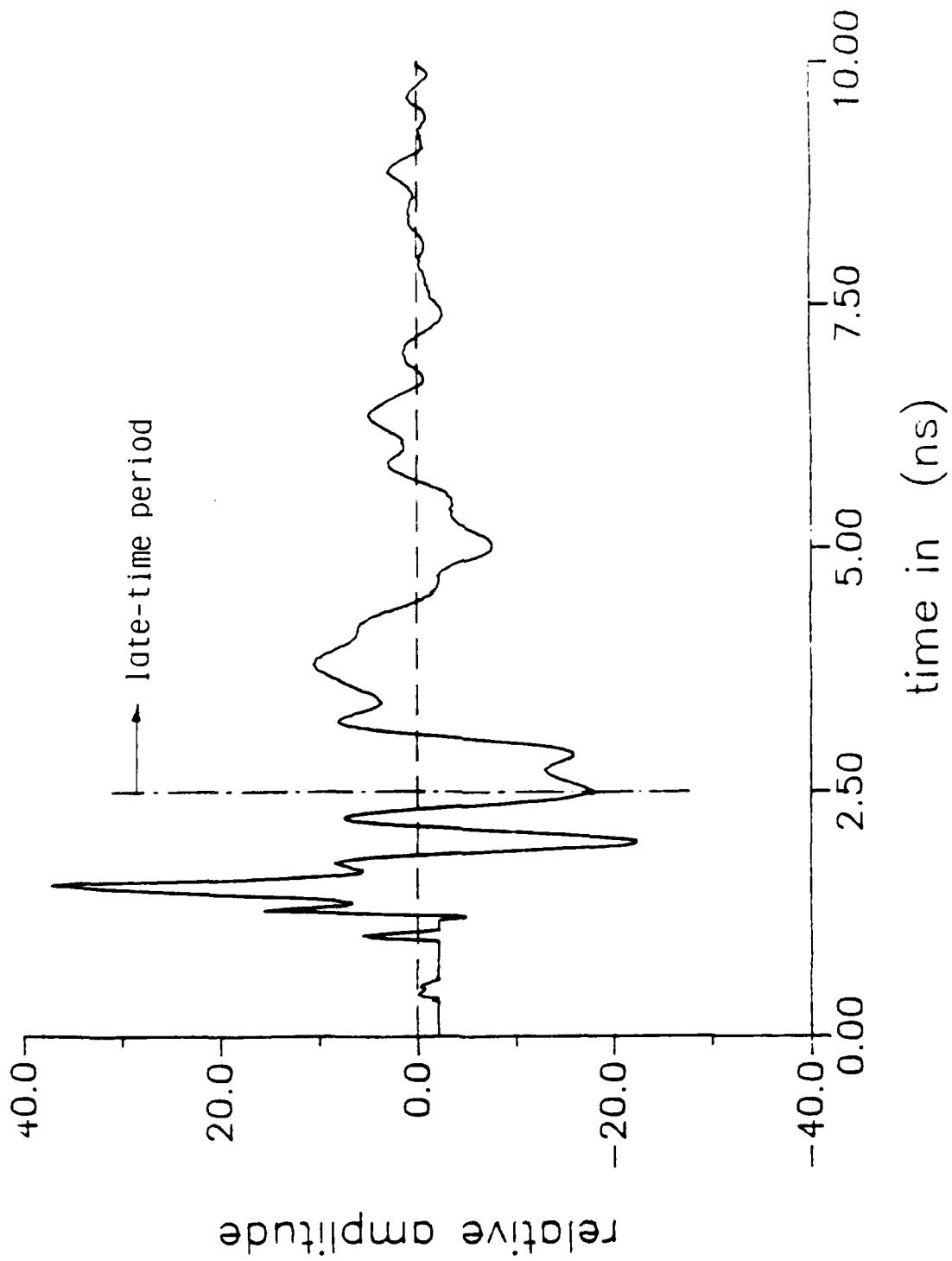


Figure 1. Pulse response of B707 model measured at 90° aspect angle without an extra noise added.

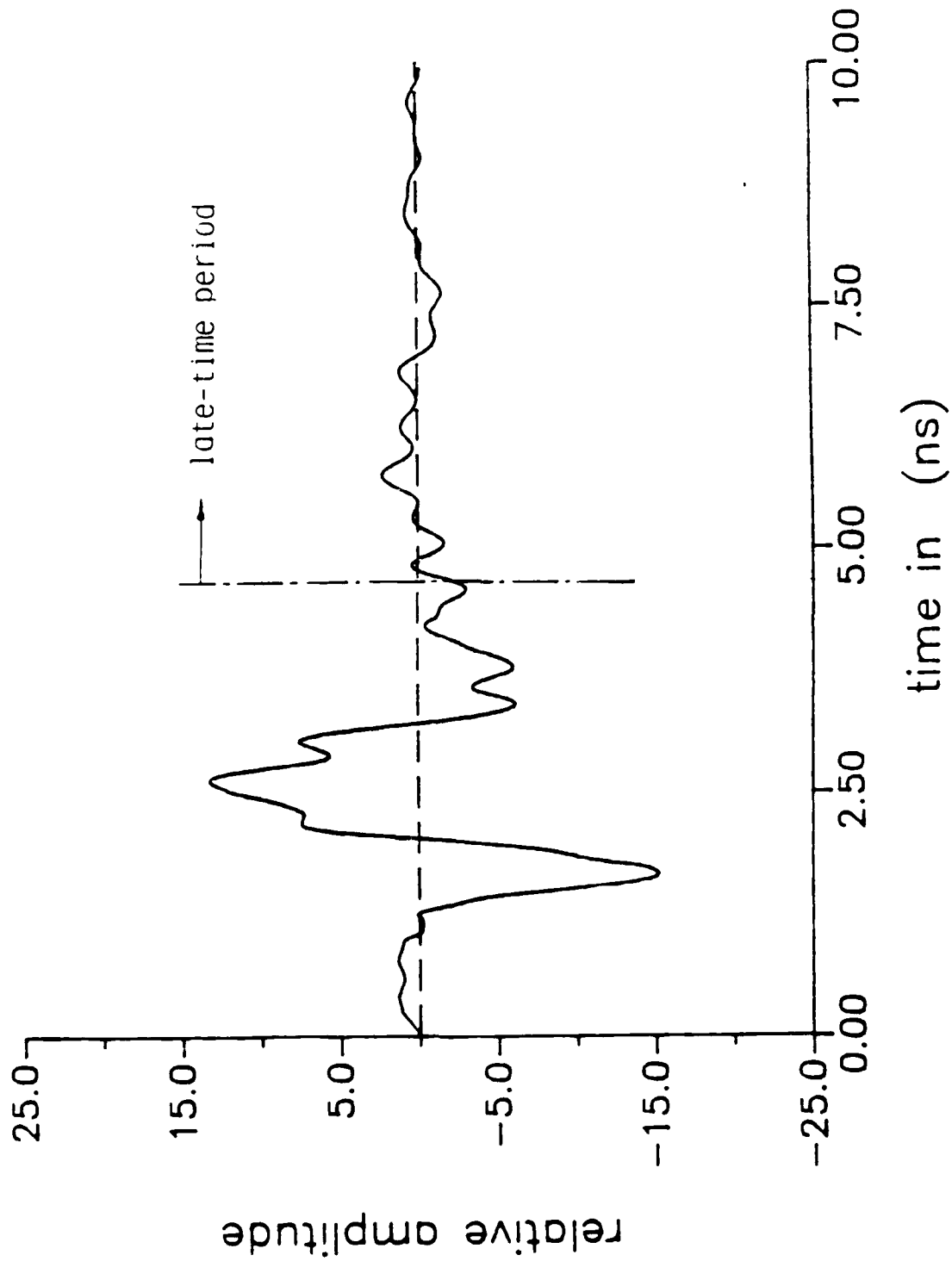


Figure 2. Convolved output of the E-pulse of B707 model with the pulse response of B707 model measured at 90° aspect without an extra noise added. A very small late-time response was obtained.

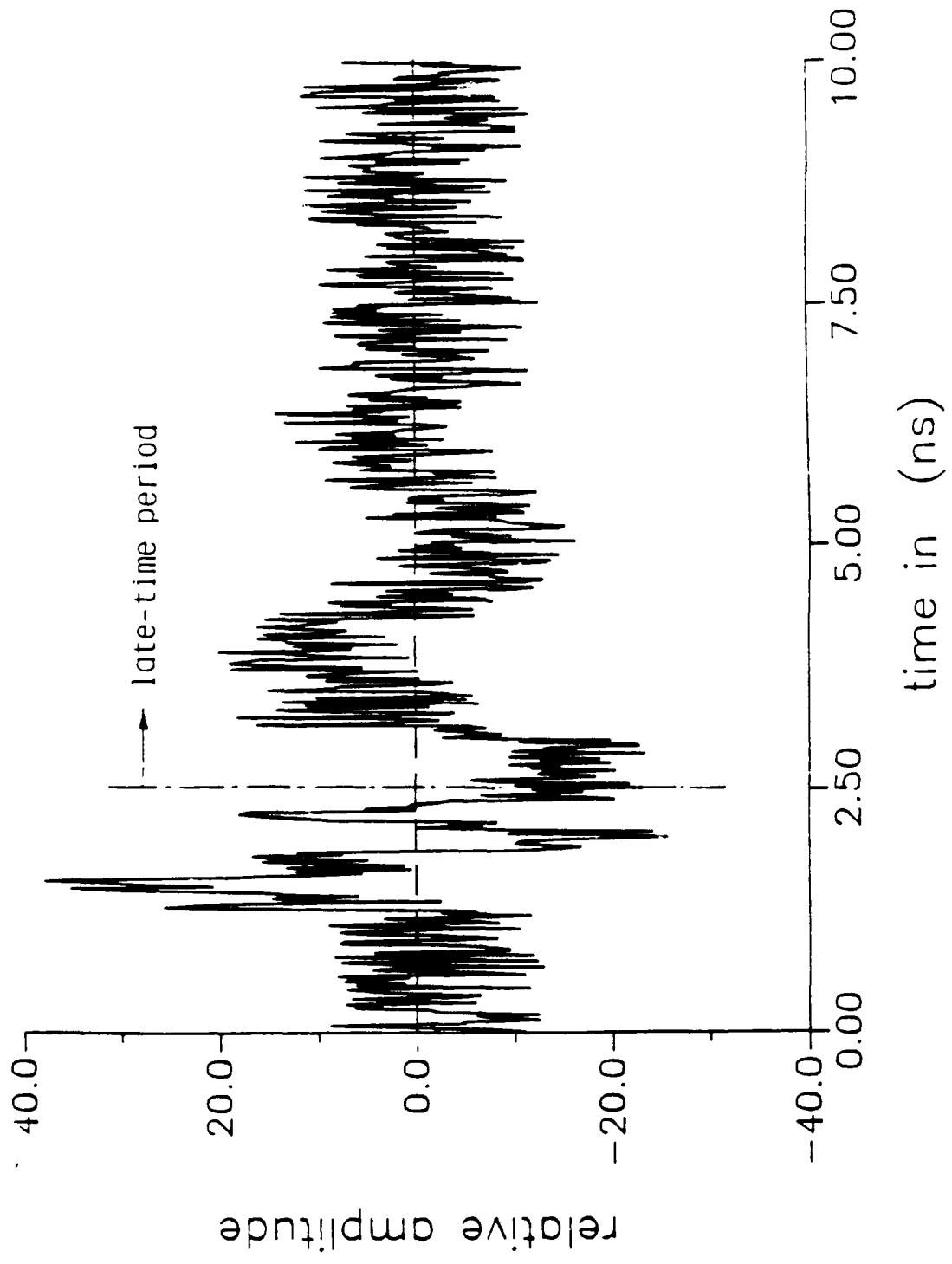


Figure 3. Pulse response of B707 model measured at 90° aspect angle with an extra random noise (30% of the maximum waveform amplitude) added.

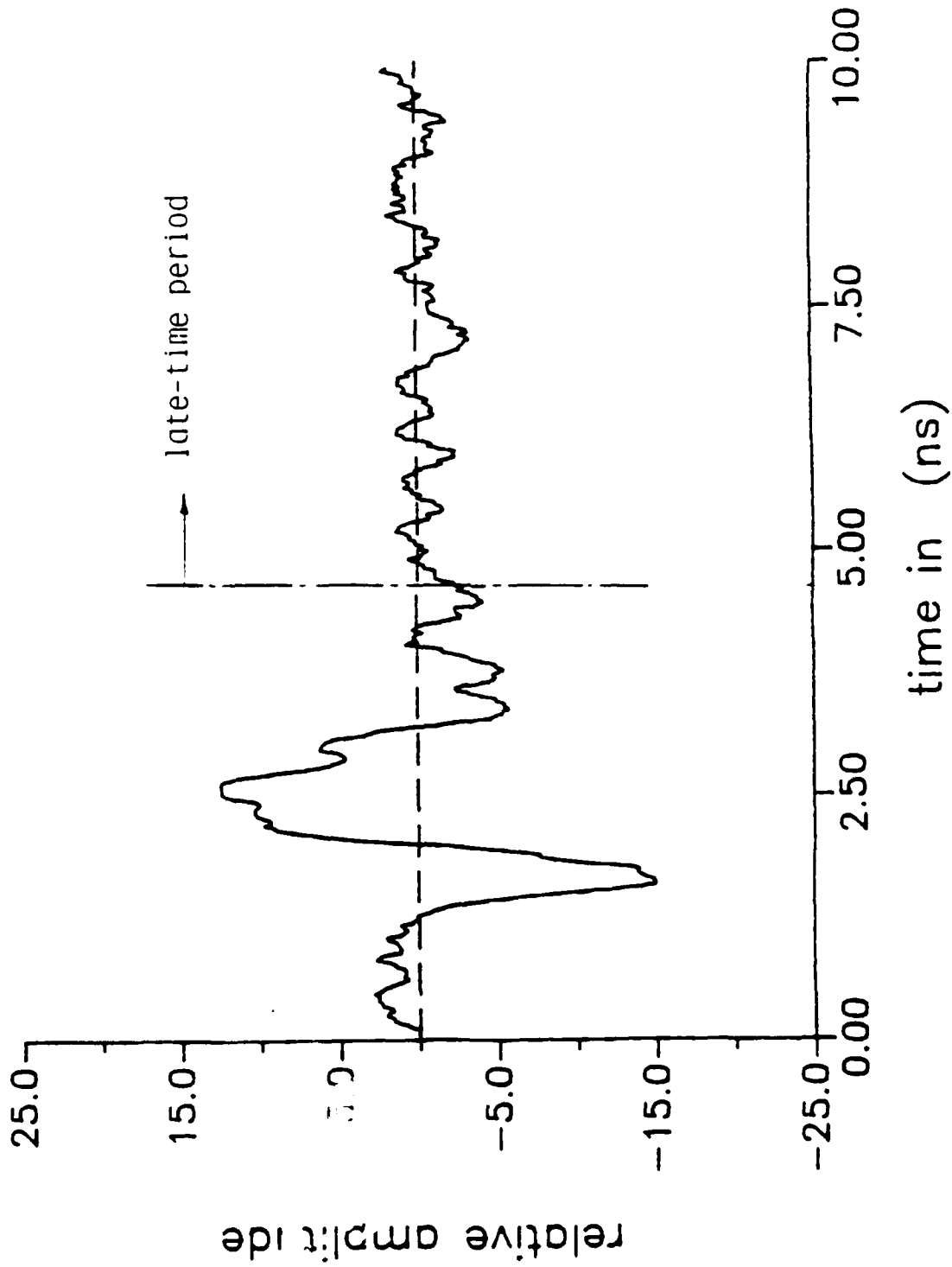


Figure 4. Convolved output of the E-pulse of B707 model with the pulse response of B707 model measured at 90° aspect angle with an extra random noise (30% maximum amplitude) added. The late-time response was still very small.

Next, we tried to discriminate a wrong target, a F-18 model, with the E-pulse of B707 model using noisy pulse responses of the wrong target. Figure 5 is the pulse response of F-18 model measured at 90° aspect angle without adding a random noise. When the response of Fig. 5 was convolved with the E-pulse of B707, the convolved output is shown in Fig. 6. In Fig. 6, it is seen that a large late-time response was obtained. This indicates that the response of Fig. 5 came from a wrong target other than B707 model. Next, a very noisy pulse response of F-18 model was created by intentionally adding a large random noise, 30% of the maximum amplitude of the response of Fig. 5, to the measured response of Fig. 5. This noisy pulse response of F-18 model is shown in Fig. 7. The noisy pulse response of Fig. 7 was then used to convolve with the E-pulse of B707, and the convolved output is shown in Fig. 8. The convolved output of Fig. 8, as compared with the result of Fig. 6, shows a relatively unchanged early-time response followed by a still large and somewhat noisy late-time response. This large late-time response is sufficient to indicate that the noisy pulse response of Fig. 7 belonged to a wrong target other than B707 model.

We have also convolved noisy pulse responses of complex targets with single-mode extraction signals of the targets. Similar results as those described in Figs. 1 to 8 were obtained; the single-mode extraction signals of a complex target are capable of discriminating between the right target and wrong targets based on very noisy pulse responses of the targets.

Based on this study, we can conclude that our target discrimination scheme of using the E-pulse and single-mode extraction signals is very noise insensitive.

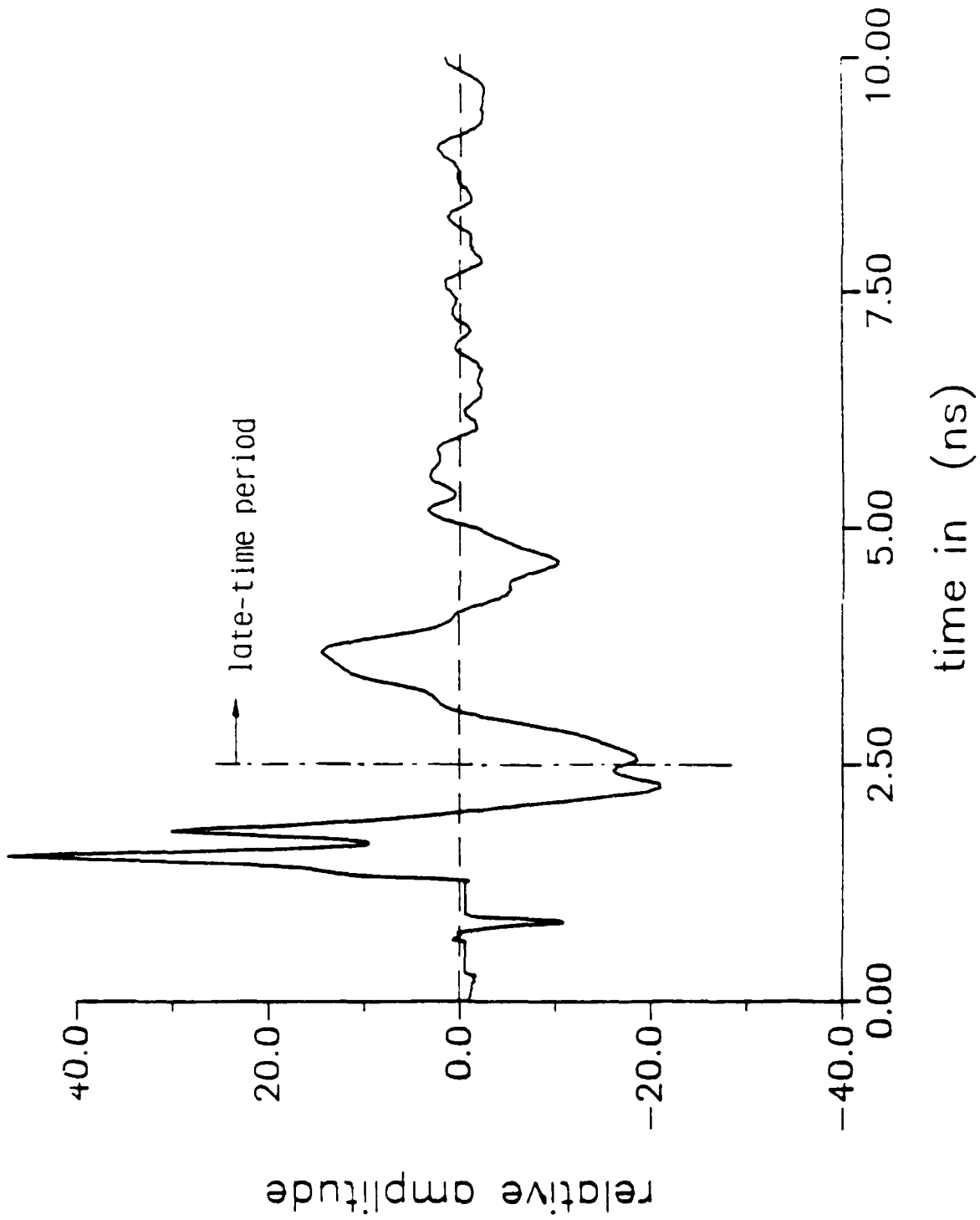


Figure 5. Pulse response of F-18 model measured at 90° aspect angle without an extra noise added.

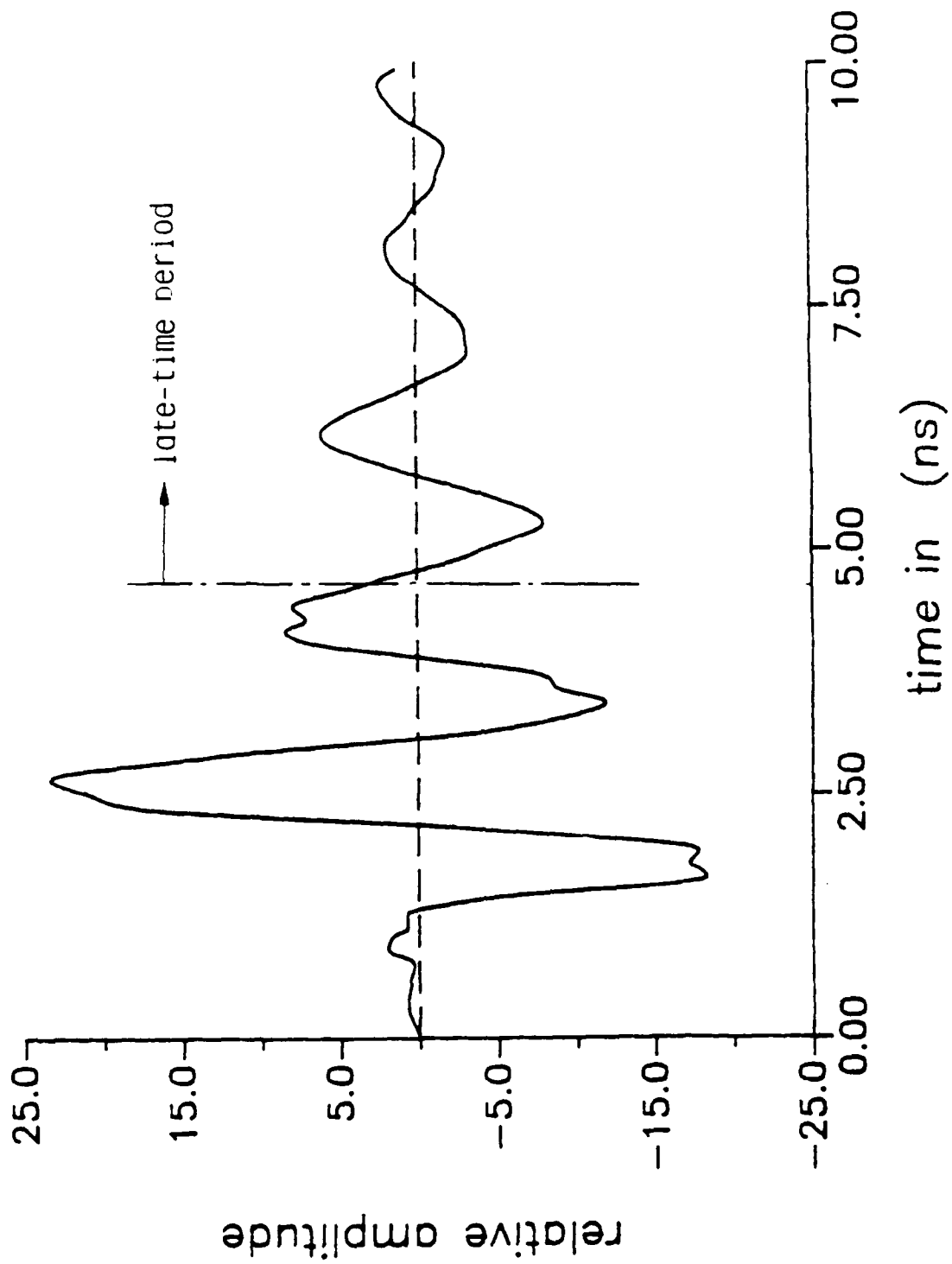


Figure 6. Convolved output of the E-pulse of B707 model with the pulse response of F-18 model measured at 90° aspect angle without an extra noise added. A large late-time response was obtained.

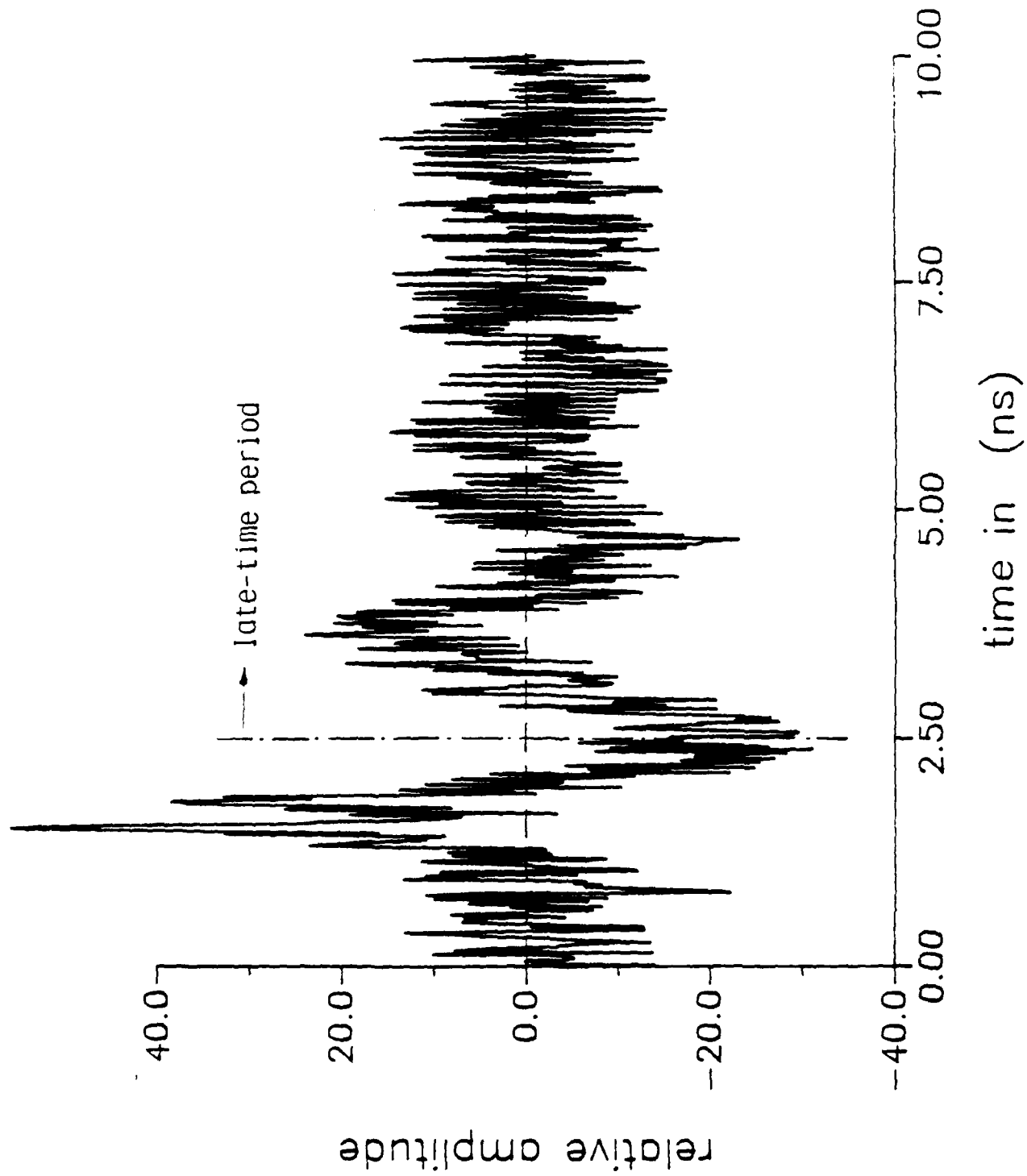


Figure 7. Pulse response of F-18 model measured at 90° aspect angle with an extra random noise (30% of the maximum waveform amplitude) added.

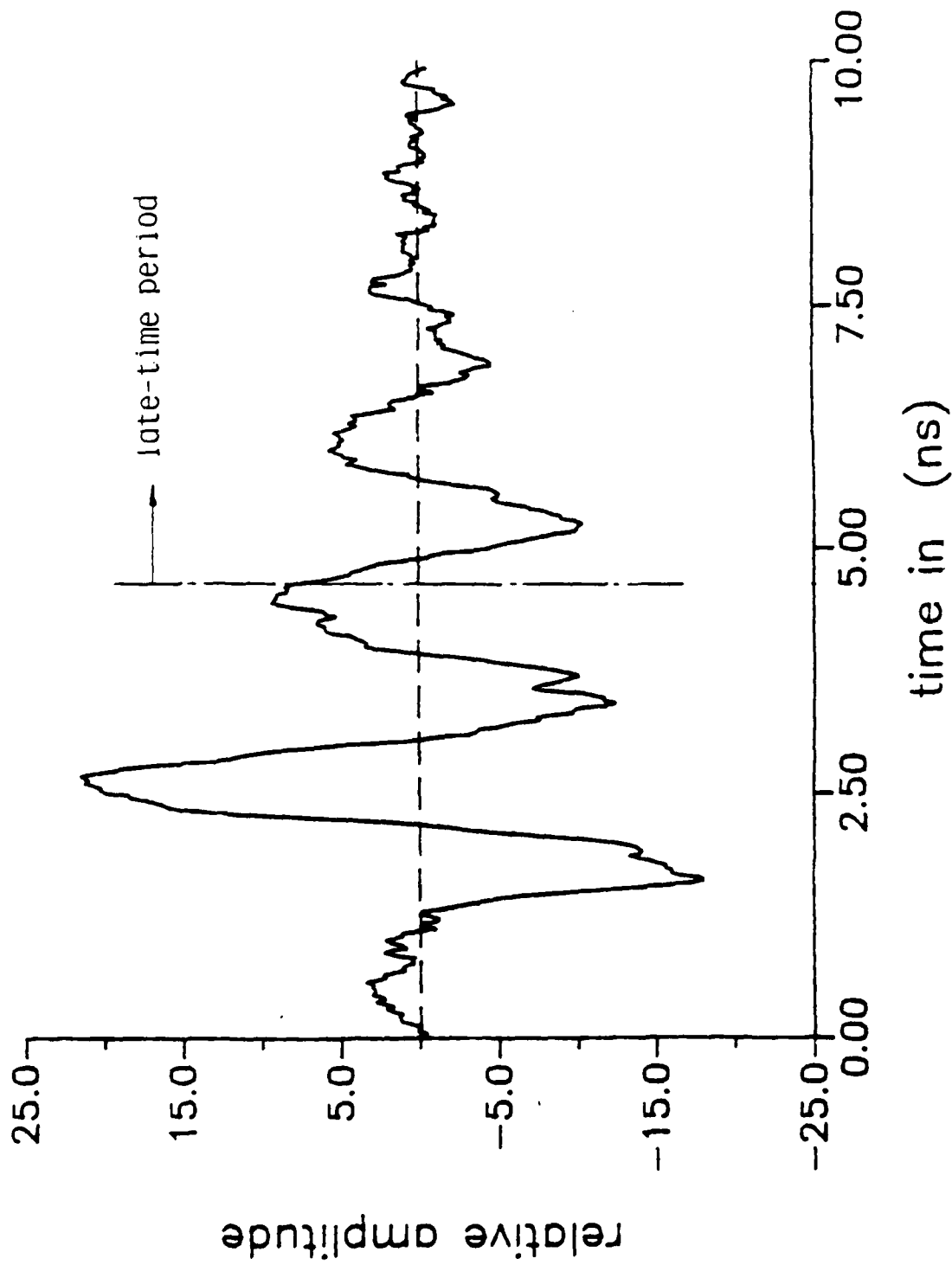


Figure 8. Convolved output of the E-pulse of B707 model with the nulse response of F-18 model measured at 90° aspect angle with an extra random noise (30% maximum amplitude) added. The late-time response remained large.

2.6 DETERMINATION OF THE IMPULSE RESPONSE OF A COMPLEX TARGET THROUGH A DECONVOLUTION

When a target is illuminated by an electromagnetic impulse, the impulse response of the target measured by a receiving system is usually entirely distorted due to non-ideal frequency characteristics of the system. Furthermore, the existence of a delta function in the response due to specular reflection from the target will exacerbate the problem. We have developed a method which is capable of recovering the actual impulse response of the target from real-time measured data.

(I) Mathematical background

The equation we are attempting to solve is

$$E \cdot H = R \tag{1}$$

where E and R are measured and H is to be solved for. When this is discretized, the set of equations for the values of E, H and R at discrete time intervals is

$$\begin{aligned} r_1 &= e_1 h_1 \\ r_2 &= e_1 h_2 + e_2 h_1 \\ r_3 &= e_1 h_3 + e_2 h_2 + e_3 h_1 \\ r_n &= e_1 h_n + \dots + e_n h_1 \end{aligned}$$

Or, in matrix form

$$\begin{bmatrix} e_1 & 0 & 0 & \dots & 0 \\ e_2 & e_1 & 0 & \dots & 0 \\ e_3 & & & & 0 \\ \vdots & & e_2 & e_1 & 0 \\ e_n & \dots & e_3 & e_2 & e_1 \end{bmatrix} \cdot \begin{bmatrix} h_1 \\ h_2 \\ h_3 \\ \vdots \\ h_n \end{bmatrix} = \begin{bmatrix} r_1 \\ r_2 \\ r_3 \\ \vdots \\ r_n \end{bmatrix}$$

$$\text{or, } E \cdot H = R \tag{2}$$

where E is now a matrix and H and R are vectors. Here, H represents the

impulse response of a target, E represents the system response of transmission and reception, and R represents measured data of the total response. Solving this is an ill-conditioned problem. Instead, we minimize the matrix equation

$$[E \cdot H - R]^2 + p \cdot [H]^2. \quad (3)$$

p is a parameter which can be varied to a suitable value to obtain the most information with the least noise. p = 0 corresponds to the original ill-conditioned problem. As p is increased, the equation becomes less ill-conditioned, and the results are smoother. If p is made too large, the results are too smooth and higher frequencies are lost. Minimizing the matrix equation, we obtain

$$E^t \cdot E \cdot H + p \cdot H = E^t \cdot R. \quad (4)$$

This equation is less ill-conditioned than the original one. The product $E^t \cdot E$, however, is twice as ill-conditioned as the original matrix E. We avoid forming this through singular value decomposition. This is a method of breaking a matrix E into three matrices U, V^t and S such that

$$E = U \cdot S \cdot V^t \quad (5)$$

with S diagonal. Also,

$$V^t = V^{-1}$$

and $U^t = U^{-1}$.

Correspondingly,

$$E^t = V \cdot S \cdot U^t \quad (5')$$

so $E^t \cdot E = V \cdot S \cdot U^t \cdot U \cdot S \cdot V^t = V \cdot S^2 \cdot V^t$

and our equation becomes

$$[V \cdot S^2 \cdot V^t + p \cdot I] \cdot H = V \cdot S \cdot U^t \cdot R. \quad (6)$$

$V^t \cdot V = I$, so

$$[S^2 + p \cdot I] \cdot V^t \cdot H = S \cdot U^t \cdot R. \quad (7)$$

This equation is then solved easily for H since $[S^2 + p \cdot I]$ is diagonal and

$$V^{-1} = V^t.$$

$$H = V \cdot (S^2 + p \cdot I)^{-1} S \cdot U^t \cdot R. \quad (8)$$

(II) Practical difficulties

When a data set representing a reasonably smooth impulse response is convolved with another data set representing a system response, a third set representing measured data is obtained. When the system response is deconvolved out, the impulse response is recreated, as it should be, with only small differences near the end of the data set due to data truncation.

If, however, the impulse response contains a delta function within it, represented by a single data point of value much larger than the surrounding data, reproduction of the impulse response is much more difficult.

The delta function creates an instability in the deconvolution process separate from the ill-conditioned nature of the problem. The source of the difficulty lies in the matrix equation we are minimizing,

$$\|E \cdot H - R\|^2 + p \cdot \|H\|^2. \quad (3)$$

The term $\|H\|^2$, for the H which we are attempting to discern contains the square of a delta function as one of its terms. When minimization is carried out, the solution will forego the target H, (which causes the first term in eq. (3) to be zero) since the second term would then be very large. Instead, another data set, H', will be obtained which doesn't have a delta function term and for which the second term will be reduced. Obviously, increasing the parameter p increases the instability, rather than lowering it out. Only as p approaches zero, does H' approach H as eq. (3) becomes equivalent to eq. (2).

If noise is added to the data set representing the measured response, we don't have the luxury of allowing p to approach zero. In order to obtain a reasonable approximation to the desired H, p must be a significantly large

number, or else the solution obtained will contain high frequency oscillations that overwhelm the desired solution. Thus, attempting to obtain an impulse response which contains a delta function in the presence of noise is difficult.

This situation is important in determining the impulse response of a radar target since a delta function exists in the response due to specular reflection from the target. This delta function response is there even though the transmitted pulse is band-limited.

To circumvent this difficulty, the delta function must be removed somehow. We can't simply subtract it because it is smeared out across the measured data. Instead, the measured data set is first convolved with a smooth pulse roughly gaussian in shape. This has the effect of smearing out the delta function that is implied in the measured data before attempting to deconvolve the impulse response out. The pulse is chosen thin enough that the desired features of the impulse response won't be altered much, but thick enough that deconvolution can be carried out reasonably well.

We applied this method to data simulating an impulse response containing a delta function. We created a data set that represented a smooth target impulse response, H , with a single point of large magnitude. We convolved H with a second set representing the known system transfer function, E , to get R . We then added random noise to R to get R' and attempted to regain the target impulse response by directly deconvolving E from R' . We didn't succeed— H' didn't resemble H for any values of the parameter p . We then convolved R' with a thin pulse to get R'' , and then deconvolved E from this. Upon doing so, we obtained a data set H'' which resembled our original H ,

except for some roundedness which is to be expected from convolution with the pulse.

(III) Experimental results

We applied this method to actual measured data. The experimental set-up consists of a transmitting antenna, a receiving probe and a target, all placed above a ground plane. The direct response of the probe to a pulse without a target present is measured. This serves as the reference response, $e(t) = E$. The target is positioned and the response of the probe to the scattered wave, $m(t) = M$, is then measured. Since the probe still responds to the direct wave, the direct response is subtracted off, leaving the pure scattered response, $r(t) = m(t) - e(t) = M - E = R$. We then use (8) via (5) and (5') to obtain H such that, as near as possible, $E H = R$.

An example is given here. In this example, the target was a 6" thin cylinder, and its scattered field was measured by three different probes with the lengths of 2", 3" and 4 1/2". When we extracted the impulse responses without regularizing the scattered responses, we obtained three different responses, shown in figure 1, with the 4 1/2" response looking especially bad. We also extracted the impulse response after convolving the scattered responses with a smooth pulse, shown in figure 2. The results for the three cases were improved, with the three looking much more similar to one another, even the 4 1/2" case.

3. Future Plans

The following topics will receive major attention in the future.

- (1) The noise-insensitivity of our scheme.

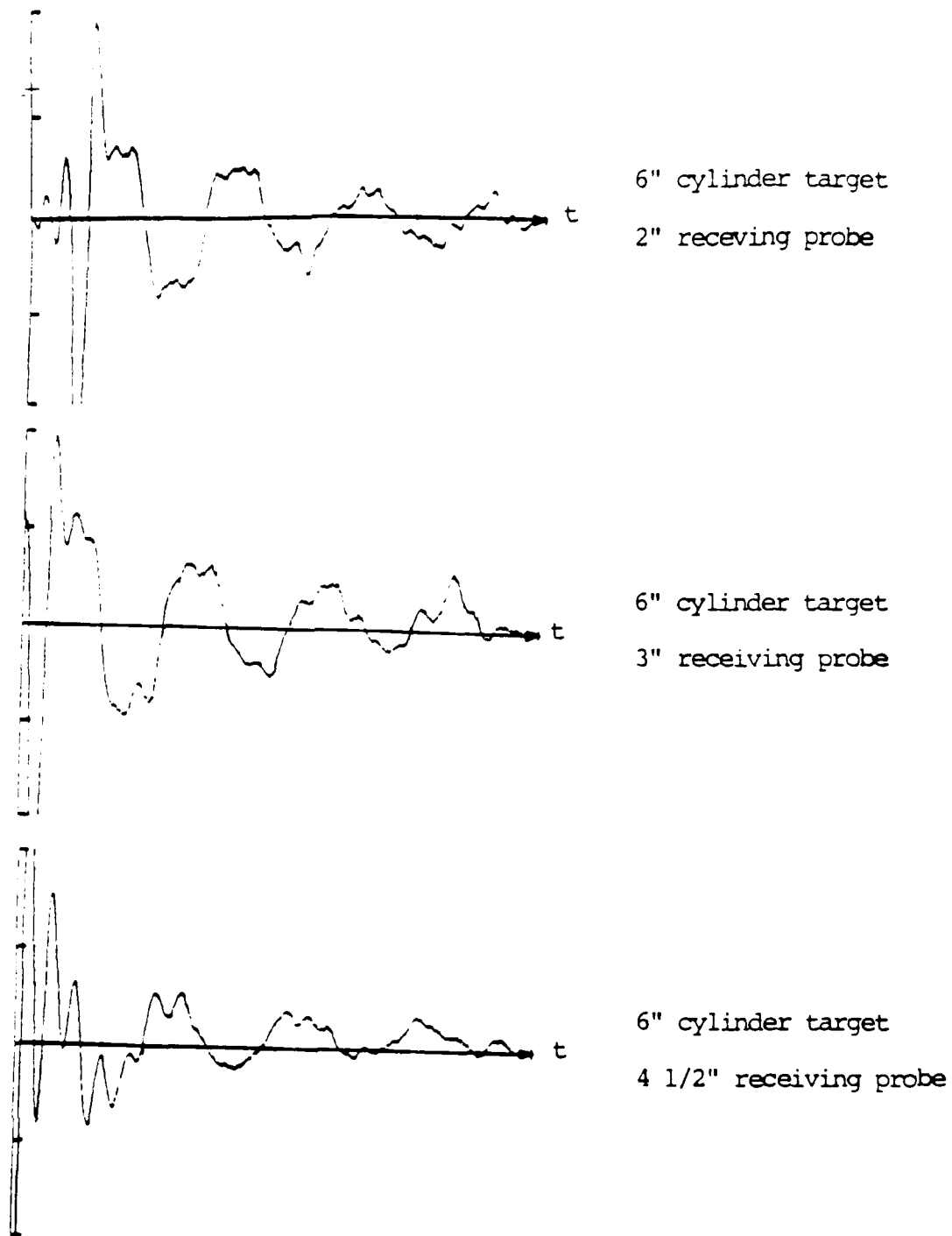


Fig. 1. The impulse responses of a 6" thin cylinder extracted from its scattered fields measured by three different receiving probes with lengths of 2", 3" and 4 1/2". The scattered fields were not regularized by convolving with a smooth pulse before deconvolution. The extracted impulse responses of the target were found to be dependent on the sizes of the receiving probes.

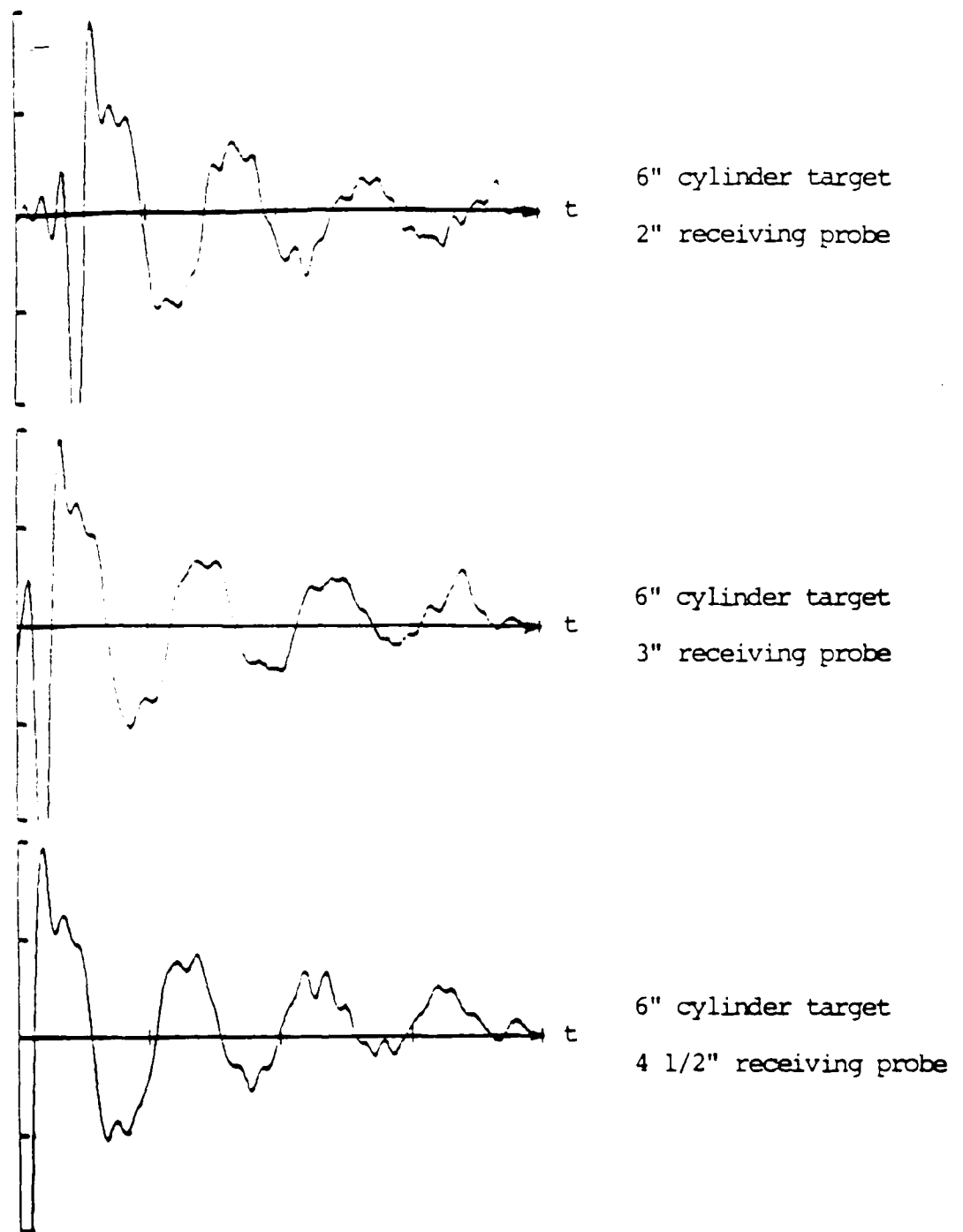


Fig. 2. The impulse responses of a 6" thin cylinder extracted from its scattered fields measured by three different receiving probes with lengths of 2", 3" and 4 1/2". The scattered fields were regularized by convolving with a smooth pulse before deconvolution. The extracted impulse responses of the target were found to be quite independent of the sizes of the receiving probes.

3. PUBLICATION

During 1986, the following papers reporting the results of the present research program have been published.

- (1) K.M. Chen, D.P. Nyquist, E. Rothwell, L. Webb and B. Drachman, "Radar target discrimination by convolution of radar return with Extinction-pulses and single-mode extraction signals," IEEE Trans. on Antennas and Propagation, Vol. Ap-34, No. 7, 896-904, July 1986.
- (2) K.M. Chen, D.P. Nyquist, E. Rothwell, W.M. Sun, N. Gharsallah and B. Drachman, "Aspect-independent target discrimination using discriminant signals," presented at 1986 National Radio Science Meeting, University of Colorado, Boulder, Colorado, Jan. 13-17, 1986.
- (3) E. Rothwell, D.P. Nyquist, K.M. Chen and N. Gharsallah, "Theoretical and experimental determination of the natural frequencies of a thin wire elliptical loop," presented at 1986 National Radio Science Meeting, University of Colorado, Boulder, Colorado, Jan. 13-17, 1986.
- (4) E. Rothwell, D.P. Nyquist, K.M. Chen and W.M. Sun, "Identification of the natural frequencies of a target from a measured response using E-pulse techniques," presented at 1986 National Radio Science Meeting, University of Colorado, Boulder, Colorado, Jan. 13-17, 1986.
- (5) K.M. Chen, D.P. Nyquist, E. Rothwell, W.M. Sun, N. Gharsallah, M. Blischke and B. Drachman, "Discrimination of complex radar targets with E-pulse and single-mode extraction signals," presented at 1986 National Radio Science Meeting, Philadelphia, Pennsylvania, June 9-13, 1986.
- (6) E. Rothwell, K.M. Chen, D.P. Nyquist, W.M. Sun and B. Drachman, "Recent developments in the extraction of radar target natural resonance frequencies from a measured response," presented at 1986 International IEEE AP/S Symposium, Philadelphia, Pennsylvania, June 9-13, 1986.
- (7) W.M. Sun, E. Rothwell, K.M. Chen, D.P. Nyquist, "Extraction of the natural frequencies of a complex radar target from measurements of its response," presented at 1986 National Radio Science Meeting, Philadelphia, Pennsylvania, June 9-13, 1986.
- (8) N. Gharsallah, E. Rothwell, D.P. Nyquist and K.M. Chen, "Extraction of target natural frequencies from measured transient surface charge of current waveforms," presented at 1986 National Radio Science Meeting, Philadelphia, Pennsylvania, June 9-13, 1986.
- (9) M. Blischke, E. Rothwell, B. Drachman, D.P. Nyquist and K.M. Chen, "Extraction of target impulse response by deconvolution of real-time measured data," presented at 1986 National Radio Science Meeting, Philadelphia, Pennsylvania, June 9-13, 1986.

4. PERSONNEL

The following persons have participated in the research program during the reporting period.

1. Kun-Mu Chen, Professor and Principal Investigator
2. Dennis P. Nyquist, Professor and Senior Investigator
3. Edward Rothwell, Assistant Professor and Senior Investigator
4. W.M. Sun, Graduate Assistant
5. Neila Gharsallah, Graduate Assistant
6. Michael Blischke, Graduate Assistant